



Università degli Studi di Ferrara

DOTTORATO DI RICERCA IN SCIENZE CHIMICHE E
FARMACEUTICHE

CICLO XXX

COORDINATORE Prof. Bignozzi Carlo Alberto

**Design, Synthesis and Biological activities of
Benzothiazole, Benzimidazole and
Imidazopyrimidine polyphenols as multifunctional
molecules against oxidative stress sustained
processes**

Settore Scientifico Disciplinare CHIM/08

Dottoranda

Djuidje Ernestine Nicaise

Tutore

Prof. Manfredini Stefano

Co-tutore

Dr. Baldisserotto Anna

Anni 2014/2017

Abstract

Reactive oxygen species regulate several essential physiological processes such as cell proliferation, differentiation, vascular tone, and inflammation. However, their higher concentrations can have deleterious effects on many molecules including protein, lipid, RNA and DNA which leads to cell destruction causing several diseases including Parkinson's diseases, inflammatory disease, cardiovascular, cancer, diabetes, Alzheimer's disease, cataracts, autism and aging. Most of these diseases involve more physiopathological indications. Nevertheless, different pharmacological strategies, including the use of multifunctional drugs, have been designed to prevent or restore redox imbalances and to treat complex diseases.

The present research project comes from the desire to synthesize multifunctional compounds with the capacity to prevent or treat multifactorial diseases such as cancer. For this purpose, isosteric modification was performed on 2-Phenyl-1H-benzimidazol-5-sulfonic acid (PBSA) and three sets of compounds were obtained: benzimidazole, benzothiazole and imidazopyrimidine derivatives. Synthesized compounds were evaluated for their UV-filter, antioxidant, antifungal and antiproliferative activities.

Photoprotective capacity was determined using spectrophotometric transmittance technique, regarding DPPH and FRAP were performed to determine antioxidant activity. Diffusion method in Sabouraud Dextrose Agar (SDA) was used to evaluate anti-dermatophyte activity, while for broth microdilution method in RPMI was used to investigate anti-candida activity. Finally, MTS assay were performed to determine antiproliferative activity.

For benzimidazole derivatives, compound **DE 35** was found to be a potential candidate in the development of multifunctional drugs, while for benzothiazole and imidazopyrimidine we respectively have **4g/4k** and **14g**. In addition, these sets of compounds might have possible application as a drug for the treatment of neoplastic diseases such as childhood leukemia, pancreatic cancer and melanoma.

Abbreviation

AcOEt: Ethylacetate

AIDS: Acquired Immunodeficiency Syndrome

APX: Ascorbate Peroxidase

CAT: Catalase

CPD: Cyclobutane Pyrimidine Dimers

DCM: Dichloromethane

DMSO: Dimethylsulfoxide

DNA: Deoxyribonucleic Acid;

DPDT: Disodium Dhenyl dibenzimidazole tetrasulfonate

DPPH: 2,2-Diphenyl-1-picryl Hydrazyl

EtO₂: Diethyl ether

EtOH: Ethanol

5FC: 5-Fluorocytosine

FDA: Food and Drug Administration

Fe₂O₃: Iron Oxide

FRAP: Ferric Reducing Antioxidant Power

GABA: *gamma*Amino Butyric acid

GPx: Glutathione Peroxidase

GR: Glutathione Reductase

GSH: Glutathione

HCl: Hydrochloric acid

HIV: Human Immunodeficiency Virus

H₃PO₄: Phosphoric acid

4-HNE: 4-Hydroxynonenal

MDA: Malondialdehyde

MED: Minimal Erythematous Dose

MeOH: Methanol

MOPS: 3-(N-morpholino)propanesulfonic acid

NADPH: Nicotinamide Adenine Dinucleotide Phosphate

NaOH: Sodium Hydroxide

PBSA: 2-Phenyl-1H-Benzimidazole-Sulfonic Acid

POCl₃: Phosphoryl Chloride

RNA: RiboNucleic Acid
RNS: Reactive Nitrogen Species
ROS: Reactive Oxigen Species
RPMI: Roswell Park Memorial Institute
SDA: Sabouraud Dextrose Agar
SOD: Superoxide Dismutase
SPF: Sun Protection Factor
RSS: Reactive Sulfur Species
TiO₂: Titanium Dioxide
TPTZ: 2,4,6-Tripyridyl-Triazine
UV: Ultraviolet
UVA-PF: Ultraviolet A Protection Factor
ZnO: Zinc oxide

Index

Introduction	5
I. Oxidative stress: Impact on human health.....	6
I.1. Free radicals.....	6
I.2. Oxidative damage to lipid, protein and DNA.....	7
I.3. Oxidative stress and human diseases.....	10
I.4. Antioxidants	11
I.4.1. Enzymatic antioxidants.....	11
I.4.2. Non-enzymatic antioxidants	12
II. Sunlight, skin damages and and ossidative stress	18
II.1. Generality of sunlight.....	18
II.2. Cutaneous physiology	19
II.2.1. Epidermis.....	19
II.2.2. Dermis	24
II.2.3. Hypodermis	24
II.3. Skin damages by UV irradiation	25
II.4. UV-photoprotection	28
II.4.1. Organic or chemical filters	29
I.4.2. Inorganic filter	30
III. Infectious diseases induce oxidative stress.....	31
III.1. Fungi	31
III.1.1. Fungal infection.....	34
III.1.2. Fungal infection and oxidative Stress	36
III.1.3. Antimycotic drug.....	36
III.2. Virus.....	39
III.2.1. Viral infection	41
III.2.2. Viral infections and oxidative Stress.....	42
IV. Focus on bioisosteric and isosteric concepts	43
IV.1. Bioisosteres in drug discovery.....	43

IV.2. Classification of bioisosterism.....	44
IV.2.1. Classical bioisosteres	44
IV.2.2. Non-classical bioisosteres	45
V. Aim of work.....	46
VI. Results and discussion	48
VI.1. Benzimidazole derivatives.....	49
VI.1.1. Chemistry	49
VI.1.2. Biological evaluations.....	51
VI.1.2.1. Photoprotective activity	51
VI.1.2.2. Antioxidant activity.....	54
VI.1.2.2.1. DPPH test.....	54
VI.1.2.2.2. FRAP Test.....	56
VI.1.2.3. Antifungal activity	58
VI.1.2.3.1. Anti-dermatophytes activity.....	58
VI.1.2.3.2. Antifungal activityon <i>Candida albicans</i>	60
VI.1.2.4. Antiviral activity	61
VI.1.2.5. Antiproliferative activity.....	63
VI.2. Benzothiazole derivatives	63
VI.2.1. Chemistry	63
VI.2.2. Biological evaluations.....	69
VI.2.2.1. Photoprotective activity	69
VI.2.2.1.1. <i>In vitro</i> studies of dilute solutions of target compounds by spectrophotometry.....	71
VI.2.2.1.2. In vitro sun protection factor of the Cosmetic formulation	75
VI.2.2.1.3. Photostability study by spectral analysis	76
VI.2.2.2. Antioxidant activity.....	77
VI.2.2.3. Antifungal activity	81
VI.2.2.3.1. Antidermatophyte activity.....	81
VI.2.2.3.2. Anti- <i>candida</i> Activity	83
VI.2.2.4. Antiviral activity	84
VI.2.2.5. Antiproliferative activity.....	87
VI.2.2.6. Benzothiazole derivatives block hERG potassium channels expressed in HEK293 cells	90

VI.3. Imidazopyrimidine derivatives	91
VI.3.1. Chemistry	91
VI.3.2. Biological Evaluation.....	92
VI.3.2.1. Photoprotection activity of purine derivatives	92
VI.3.2.2. Antioxidant activity.....	95
VI.3.2.3. Antifungal activity	96
VI.3.2.4. Antiproliferative activity.....	97
VII: Stability studies.....	99
VIII. Conclusion	100
IX. Experimental section.....	104
IX.1. General information.....	104
IX.2. Synthetic Procedures	104
IX.2.1. Synthesis of Benzimidazole derivatives.....	104
IX.2.2. Synthesis of Benzothiazole derivatives.....	107
IX.2.3. Synthesis of imidazopyrimidine derivatives	113
IX.3. Protocols for the evaluation of the biological activity.....	117
IX.3.1. Antioxidant Activity Assays	117
IX.3.1.1. Free radical Scavenging Activity on DPPH.....	117
IX.3.1.2. Ferric Reducing Antioxidant Power (FRAP) assay	117
IX.3.2. Photoprotection assay	118
IX.3.2.1. Evaluation of filtering parameters of compounds in solution.....	118
IX.3.2.2. <i>In vitro</i> evaluation of filtering parameters of cream formulation	118
IX.3.3. Study of photostability	119
IX.3.4. Stability study by HPLC analysis	120
IX.3.5. Antifungal activity	120
IX.3.5.1. Anti-dermatophytes activity.....	120
IX.3.5.1. Anti- <i>Candida albicans</i> activity.....	121
IX.3.6. Antiproliferative activity.....	122
IX.3.7. HERG expressed in HEK.....	123
X. References.....	125

Introduction

Living species are continuously and inevitably exposed to the attacks of oxidizing agents which damage the cellular components such as proteins, lipids, DNA. Oxidizing agents include free radicals that are produced by the cells themselves during normal metabolic processes or by external factors. Under normal physiological conditions, the body possesses endogenous defense systems that can enzymatic or nonenzymatic antioxidant. At moderate concentrations, reactive species have important effects on cellular redox signaling and defense mechanisms which induce and maintain the oncogenic phenotype of cancer cells [1], neutrophil function and shear-stress induced vasorelaxation. However, an excessive production of free radicals breaks the balance and induces the oxidative stress which is directly related to the development of various pathologies including photo-ageing, cancer, Parkinson's diseases, Alzheimer's, inflammatory diseases, cardiovascular diseases, diabetes, cataracts and autism. In addition, reactive species produced under conditions of oxidative stress can directly damage DNA thus causing mutagens. In the same way they can suppress apoptosis and promote proliferation, invasiveness and metastasis. Moreover, the most severe oxidative stress can cause cell death through necrosis [2].

The main external factors that lead to the formation of free radicals are: ultraviolet (UV) and X radiation, atmospheric pollutants, cigarette smoking, toxic chemicals, fungal, viral or bacterial infections and lifestyle. Moreover, several biochemical systems of the body are at the origin of the production of prooxidants. The instability of reactive species due to their extremely short life span (nano to milli second) makes it difficult to detect them in different biological system [3]. Indeed, the toxicity of the reactive oxygen species is not necessarily correlated with their reactivity, in many cases the less reactive species can be at the origin of a great toxicity because of their long half life that allows them to spread and cause damage over long distances to their production sites. Therefore, detoxification of reactive oxygen species is paramount to the survival of all aerobic life.

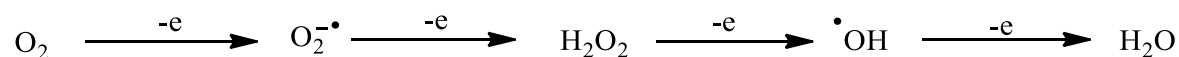
I. Oxidative stress: Impact on human health

I.1. Free radicals

Free radicals are atoms or molecules containing unpaired electron(s) in their outer orbit. This unpaired electron(s) are unstable and highly reactive. To achieve stability, free radicals react with surrounding molecules by subtracting electrons to form a pair of electrons; in this way also the damaged molecule becomes a free radical and thus begins a chain reaction. Oxidizing species are often derived from oxygen, called reactive oxygen species (ROS), nitrogen, called reactive nitrogen species (RNS) and sulfur, called reactive sulfur species (RSS).

ROS include free radicals such as superoxide ($O_2^{\cdot-}$), hydroxyl ($\cdot OH$), peroxy ($ROO\cdot$), lipidperoxy ($LOO\cdot$), alkoxy ($RO\cdot$) and other non-radical reactive species such as hydrogen peroxide (H_2O_2), ozone (O_3), singlet oxygen (1O_2), hypochlorous acid ($HOCl$). While, RNS include nitrogen free radicals such as nitric oxide ($NO\cdot$) and nitrogen dioxide ($NO_2\cdot$) and non radical species such as peroxynitrite ($ONOO^-$), dinitrogen trioxide (N_2O_3). Lastly, RSS are often formed by the oxidation of thiols and disulfides into higher oxidation states, such agents include thiyl radicals, disulfides, sulfenic acids and disulfidesoxides [4]. In addition, RSS are also formed from thiols by reaction with ROS.

Moreover, the most common reactive species are ROS and RNS that can be produced from both endogenous and exogenous substances. Endogenous sources include mitochondria, cytochrome P450 metabolism, peroxisomes, neutrophils and macrophages during inflammation and excess of transition metals, as iron and copper. On the other hand, although oxygen is vital for aerobic bioprocesses, about 5% of inhaled oxygen is converted to reactive oxygen species.



($O_2^{\cdot-}$) is the primary oxygen free radical produced by mitochondria during electron transport chain (respiratory chain; oxidative phosphorylation). This oxygen reactive species is rapidly converted into hydrogen peroxide (H_2O_2) by the Superoxide Dismutase (SOD). Nonetheless, in the presence of the transition metals such as iron, H_2O_2 can produce $\cdot OH$ via the Fenton reaction, reactive hydroxyl radicals a far more damaging molecule to the cell.



Exogenous factors that can stimulate production reactive species are: pollution of the atmosphere, UV radiations, X-rays, gamma rays, intense physical exercise. The generation of reactive species is counterbalanced by the biological system through the action of enzymatic and non-enzymatic antioxidants, but the overproduction of these species induced oxidative stress which causes damage to essential bio-compounds such as proteins, lipids and DNA.

Reactive species have both harmful and beneficial effects. In fact, moderate levels of reactive species have important effects on cellular redox signaling [1] like activation of several cytokines and growth factor signaling, non-receptor tyrosine kinases activation, protein tyrosine phosphatases activation, release of calcium from intracellular stores, activation of nuclear transcription factors. Reactive species can also defense against infectious agents by phagocytosis, kill cancer cells by macrophages gene expression and help the synthesis of primordial life building blocks [5]. However, higher concentrations can have deleterious effects on many molecules including protein, lipid, RNA and DNA which leads to cell destruction causing several diseases such as Parkinson's diseases, inflammatory disease, cardiovascular, cancer, diabetes, Alzheimer's disease, cataracts, autism and aging [6, 7].

I.2. Oxidative damage to lipid, protein and DNA

The lipids cellular components involving polyunsaturated fatty acid residues of lipids are very sensitive to the damage caused by free radicals [8], especially glycolipids, cholesterol and phospholipids [9]. Reactive species such as $\cdot\text{OH}$, $\text{O}_2\cdot^-$ and H_2O_2 react with lipids resulting in the formation of various by-products including ketones, alkanes, carboxylic acids, aldehydes and polymerization products, which are highly reactive with other cellular components. Among the by-products formed we can mention: malondialdehyde (MDA), propanal, hexanal, and 4-hydroxynonenal (4-HNE). MDA and 4-HNE are known as bioactive marker of lipid peroxidation, due to its numerous biological activities resembling activities of reactive oxygen species [10]. In addition, lipid peroxidation in cell membranes can damage cell membranes by disrupting fluidity and permeability.

The overall process of lipid peroxidation develops of three steps (**Schema 1**): initiation, propagation, and termination.

➤ Initiation step.

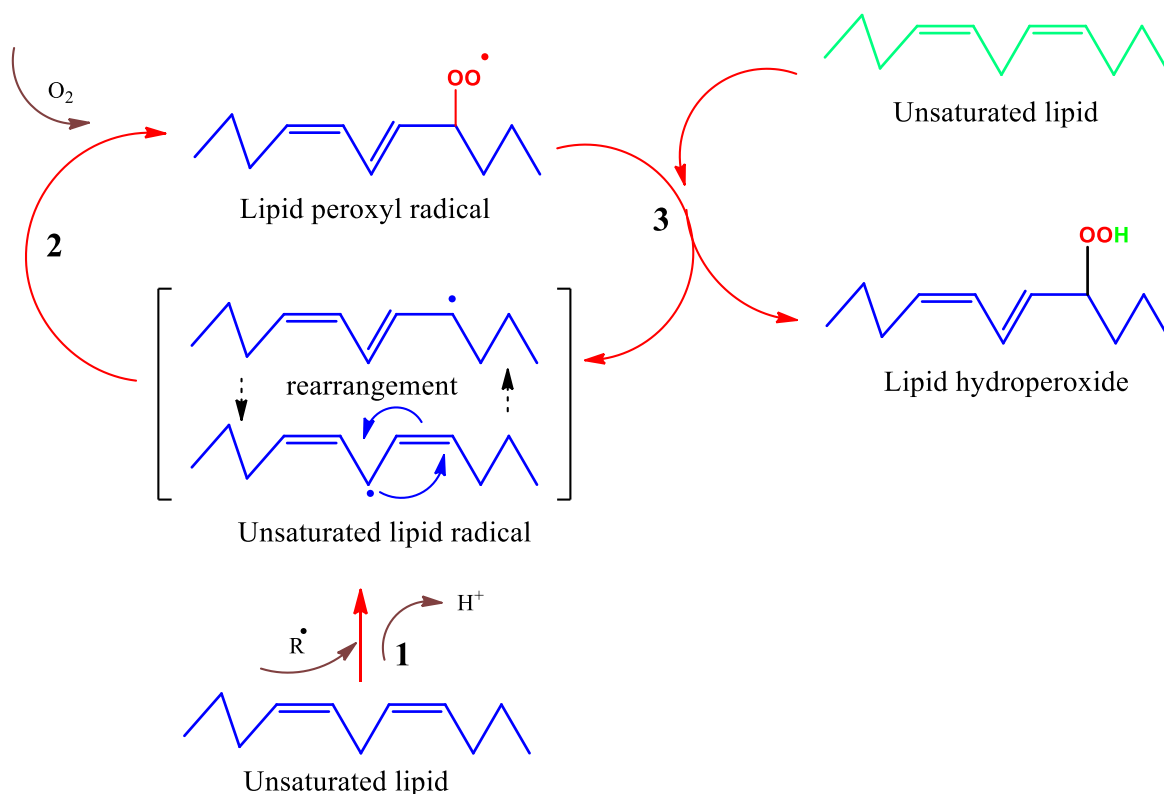
Prooxidant such as hydroxyl radical remove an allelic hydrogen, resulting to the formation of an unpaired electron on the carbon-centered lipid radical (L^\bullet). This radical is stabilized by rearrangement process to form a conjugated diene.

➤ Propagation step.

Conjugated diene can react with an oxygen molecule to form a lipid peroxy radical (LOO^\bullet). This radical can react with other lipid molecule abstracting a hydrogen to generating a new L^\bullet and lipid hydroperoxide ($LOOH$). Through this radical chain process, an oxidizing agent can oxidize many fatty acid molecules. LOO^\bullet can also be rearranged through a cyclization reaction to form endoperoxides which, by fragmentation, provides highly reactive compounds such as MDA [11].

➤ Termination step.

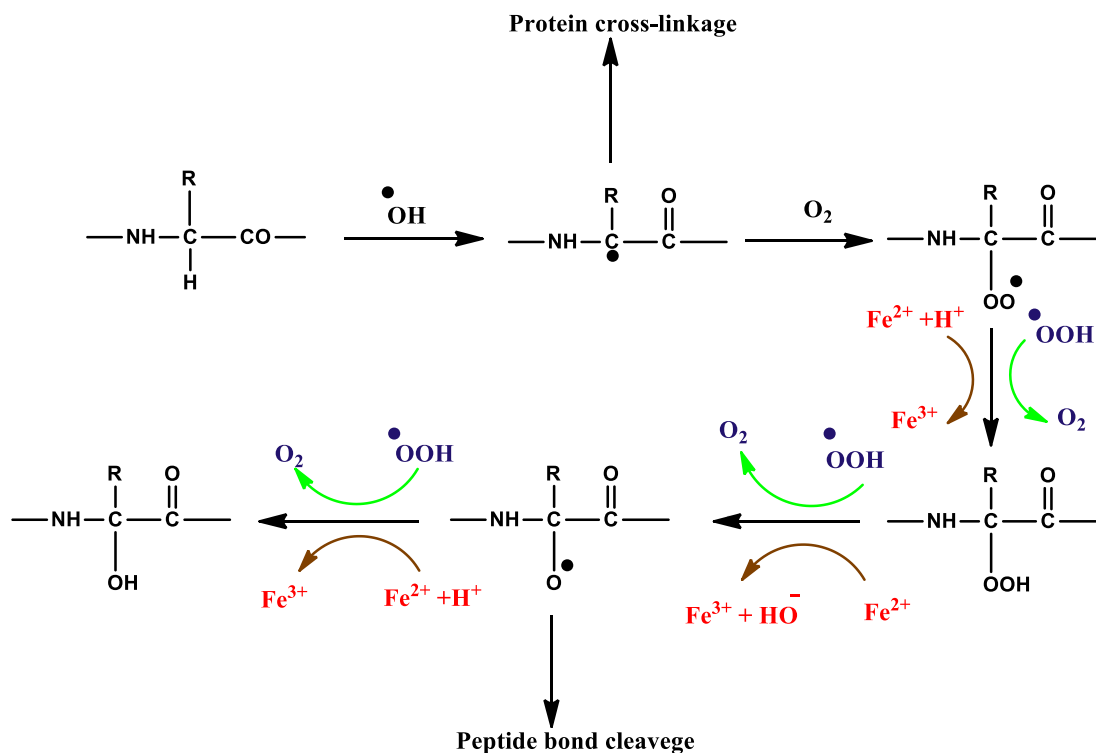
Radical chain reaction can be broke by antioxidants that donate a hydrogen atom to the LOO^\bullet and form non radical products ($LOOH$). An example of antioxidant is Vitamin E ($T-OH$) which reduce LOO^\bullet within the membrane, resulting in the formation of a lipid hydroperoxide and a radical of Vitamin E ($T-O^\bullet$). Vitamin E radical ($T-O^\bullet$) is reduced back to Vitamin E ($T-OH$) by ascorbic acid



Schema 1: Steps of lipid peroxidation

Proteins can be damaged directly via oxidation on their amino acid residues by ROS or by lipid peroxidation end-products. Amino acids subject to oxidation reaction are: tryptophan, cysteine, methionine, tyrosine, lysine, arginine, proline and histidine. However, histidine, cysteine, and methionine are highly susceptible to oxidation [12]. In some cases, specific oxidation of proteins may take place, for example the oxidation of cysteine residues can lead to the reversible formation of disulfide bonds and the methionine can be oxidized in methionine sulfoxide [13]. In addition, carbonyl groups may be introduced into the proteins by reactions with reactive aldehydes (MDA and 4-HNE) produced during lipid peroxidation.

In general, amino acid residues are attacked by $\cdot\text{OH}$ which tears away the α -hydrogen atom and form carbon-centered radical. The carbon-centered radical may undergo a crosslinking reaction to form a protein crosslink or may react rapidly with O_2 to form an alkylperoxyl radical intermediate which in turn undergoes a succession of reactions leading to fragmentation of the proteins (**Schema 2**).



Schema 2: Oxidation reaction of proteins

DNA is essential for life; however, it is subject to damage caused by interaction with various chemicals and environmental agents. Mitochondrial DNA is more exposed to ROS attack than nuclear DNA, because it is near to the ROS generated place. Like proteins, $\cdot\text{OH}$ is known as an important mediators of DNA damage. It reacts particularly with the purine

and pyrimidine bases as well as the deoxyribose skeleton. DNA modification can occur in several ways, including base degradation, single- or double-stranded DNA breaks, mutations, deletions or translocations, and cross linking with proteins. The transformation products of DNA bases in position C-8 of guanine by the $\cdot\text{OH}$ radical are 8-oxo-7,8-dihydro-2'-deoxyguanosine, hydroxymethylurea, urea, thymine glycol, thymine and open cycle adenine. Most of these DNA modifications are very relevant for carcinogenesis, and aging process [14], [15].

I.3. Oxidative stress and human diseases

Oxidative stress leads to the oxidation of lipids, DNA and proteins, which is associated with changes in their structure and functions. Indeed, the oxidative damage of these biomolecules can theoretically contribute to the increase of the activation of radical enzymes (cyclooxygenase, lipogenase), free iron, copper ions, or the disruption of the electron transport chains of the oxidative phosphorylation. These dysfunctions lead to primary or secondary physiopathological mechanisms of multiple acute and chronic human diseases such as neurodegenerative, cardiovascular, inflammatory and autoimmune diseases [14].

Carcinogenesis: in living cells, oxidizing specie such as superoxide anion, hydrogen peroxide, hydroxyl radical, nitric oxide and their biological metabolites also play an important role in carcinogenesis. In fact, ROS can cause tissue damage by reacting with lipids in cellular membranes, nucleotides in DNA, sulphhydryl groups in proteins and cross-linking/fragmentation of ribonucleoproteins. These effects cause cell mutagenesis and carcinogenesis. Lipid peroxides are also responsible for the activation of carcinogens [16].

Cardiovascular diseases: various pathophysiological conditions, including hypercholesterolemia, atherosclerosis, cigarette smoking, hypertension, diabetes and heart failure induce the activation of some enzymatic systems such as nicotinamide adenine dinucleotide phosphate (NADPH) oxidase, xanthine oxidase, lipoxygenase, nitric oxide synthase (NOS) and myeloperoxidase (MPO) contributing to increase the production of ROS. These stress conditions cause endothelial dysfunction by accelerated inactivation of $\text{NO}\cdot$. Furthermore, a loss of bioactivity of $\text{NO}\cdot$ in the vessel wall leads to loss of vasodilation, inflammation, platelet aggregation and growth of Smooth muscle cell that induce cardiovascular disease such as atherosclerosis and blood vessel stenosis [17,18].

Neurodegenerative: oxidative stress plays a potential role in the pathogenesis of neurodegenerative disorders. These diseases represent a primary health problem especially in the elderly population. The abnormal production of ROS and the excessive

accumulation of mitochondrial DNA mutations (mtDNA) cause a mitochondrial dysregulation leading to different pathologies such as Alzheimer's disease (AD), Parkinson's disease, Huntington's disease and amyotrophic lateral sclerosis and optic atrophy[19].

I.4. Antioxidants

To protect cells and body organ systems from oxidizing agents, human organism developed series of defense mechanisms. These defenses are provided by antioxidants that may be endogenous or exogenous and are classified according to their nature, origin or mechanism of action. In this work, is reported the classification based upon the nature of antioxidant.

I.4.1. Enzymatic antioxidants

Enzymatic antioxidants include superoxide dismutase (SOD), glutathione peroxidase (GPx), ascorbate peroxidase (APX), catalase (CAT) and Glutathione Reductase (GR).

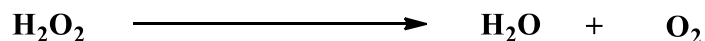
➤ SOD

Iron and manganese are the main SOD prosthetic groups in prokaryotes, whereas in eukaryotes the prosthetic groups of cytosolic SOD are copper and zinc. However, eukaryotic mitochondrial SOD also contains manganese as a prosthetic group. SOD enzymes catalyze the removal of superoxide radicals in a dismutation reaction where one superoxide radical is oxidized and another is reduced.



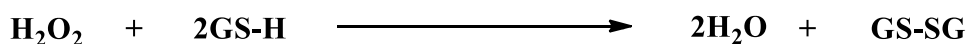
➤ CAT

The hydrogen peroxide produced can be degraded to water and oxygen by catalase.



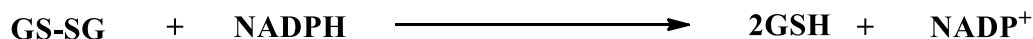
➤ GPx

H₂O₂ can be metabolized by peroxidase enzymes, such as the glutathione peroxidases (GPX prefers aromatic compounds like guaiacol and pyragallol), which use reduced glutathione as a co-factor that is oxidized by hydrogen peroxide. Therefore, glutathione peroxidase is mainly cytosolic selenoenzyme which attack hydroperoxides. The oxidized glutathione is recycled to its reduced form by glutathione reductase enzymes, thereby maintaining a high ratio of reduced/oxidized glutathione (GSH).



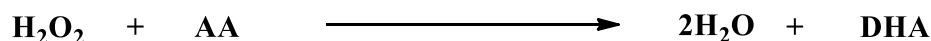
➤ GR

GR is a flavoprotein oxidoreductase which uses NADPH to reduce GSSG to GSH in order to maintain a high cellular GSH/GSSG ratio.



➤ APX

As GPx, APX reduces H₂O₂ to H₂O and DHA, using Ascorbic acid (AA) as reducing agent. The APX family comprises five isoforms based on different amino acids and location, i.e. cytosolic, mitochondrial, peroxisomal and chloroplastid [20].



I.4.2. Non-enzymatic antioxidants

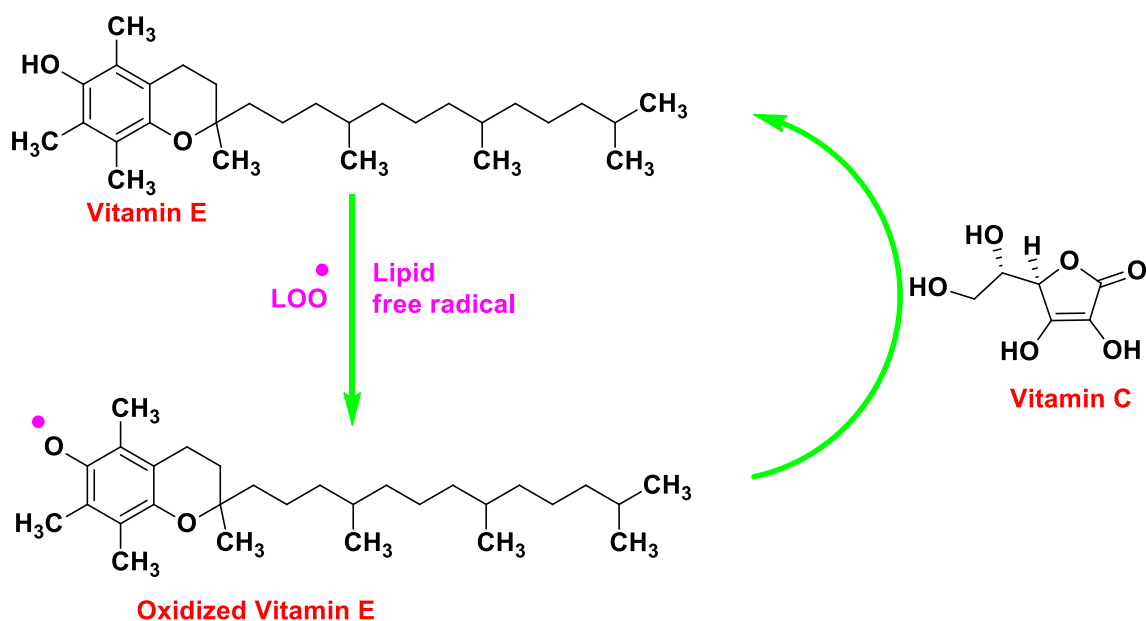
The non-enzymatic antioxidants form secondary defense against reactive species and damage induced by free radicals. In physiological condition, our organism is able to prevent oxidative stress by endogenous antioxidant systems or by taking antioxidant from food including vegetables, fruits, grain cereals, teas and other food products. GSH, Vitamin C, vitamin E, N-acetyl cysteine, carotenoids, coenzyme Q10, alpha-lipoic acid, lycopene, selenium, flavonoids and phenols are the main non-enzymatic antioxidants that are often brought from the diet.

➤ Glutathione

Glutathione (GSH) protects cells from the free radicals produced through oxidation/scavenges H₂O₂, ¹O₂, HO[•], and O₂^{•-} and protects the different biomolecules by forming adducts or by generating GSSG. It also plays a vital role in regenerating AA to yield GSSG. GSH is abundantly found in almost all cellular compartments like cytosol, mitochondria and chloroplasts. As GSH bonds it converts to its oxidized form, called glutathione disulfide. Then an enzyme glutathione reductase converts it back to its reduced state.

➤ Vitamin C (ascorbic acid) and vitamin E (α-tocopherol)

They are important small molecule antioxidants which react with free radicals to form stable radicals. Vitamin E [21] terminates the chain reaction of lipid peroxidation in biomembranes and lipoproteins, whereas Vitamins C scavenges aqueous-phase ROS by electron transfer and thus inhibit lipid peroxidation as well as reduces the oxidized vitamin E radicals leading to formation of ascorbate free radical. This radical can form dehydroascorbic acid by dehydroascorbate reductase. Therefore, vitamin E and Vitamins C function together to protect membrane lipids from damage [96] (**Schema 3**).

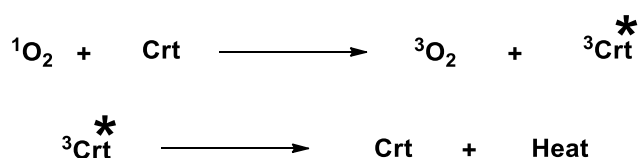


Schema 3: Vitamin C and E as antioxidant

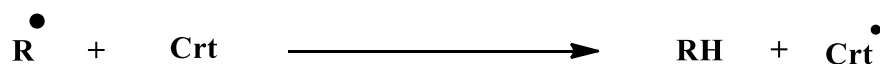
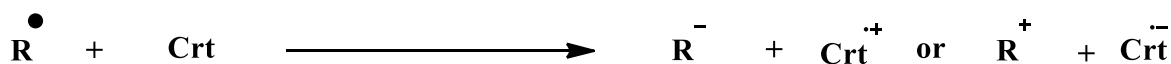
In addition, vitamin E protects body against colon, prostate and breast cancers, some cardiovascular diseases, ischemia, cataract, arthritis and certain neurological disorders. While Vitamin C is required for collagen synthesis by acting as a cofactor for non-heme iron/ α -ketoglutarate-dependent dioxygenases such as prolyl 4-hydroxylase and it is very important for neurotransmitters biosynthesis.

➤ Carotenoids

Carotenoids (Crt) are highly lipophilic molecules typically located inside cell membranes. The most important Crt present in human plasma include β -carotene, α -carotene, lycopene, lutein, zeaxanthin, β -cryptoxanthin, α -cryptoxanthin, γ -carotene, neurosporene, ζ -carotene, phytofluene and phytoene [22]. Crt are known to be important precursors of retinol (vitamin A) which is essential for vision and (photo) protection. They are very efficient physical quenchers of singlet oxygen and scavengers of other reactive oxygen species. In fact, Carotenoids exhibit their antioxidative activity by protecting the photosynthetic machinery in several ways: inhibition of lipid peroxidation to end the chain reactions; scavenging $^1\text{O}_2$ [23] and generating heat as a by-product; preventing the formation of $^1\text{O}_2$ by conversion of excess of energy to heat or dissipating the excess excitation energy, via the xanthophyll cycle.



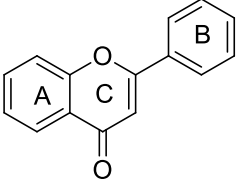
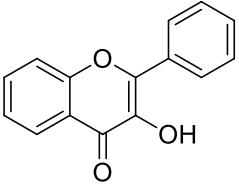
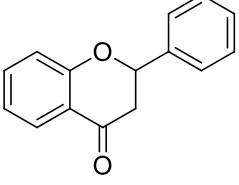
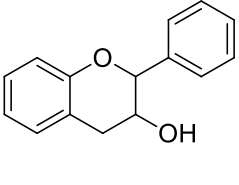
Carotenoids scavenge ROS and other free radicals following three main mechanisms: electron transfer between the free radical (R[•]) and Crt, resulting in the formation of a Crt radical cation (Crt^{•+}) or Crt radical anion (Crt^{•-}); radical adduct formation (RCrt[•]) and hydrogen atom transfer leading to a neutral Crt radical (Crt[•]) [24]



➤ Phenolic compounds

They have received considerable attention due to their antioxidant property. Their main source is dietary and they are widely present in the fruits such as apples, blackberries, blueberries, cantaloupe, pomegranate, cherries, cranberries, grapes, pears, plums, raspberries, aronia berries, and strawberries. They are also present in red wine, chocolate, black tea, white tea, green tea, olive oil and many cereal grains. Polyphenols are natural anti-oxidants and are classified in flavonoids and non-flavonoids.

Flavonoids are widely present in the plant kingdom, commonly found in fruits, vegetables, grains, bark, roots, stems, flowers, tea. Flavonoids are divided in subgroups, following the substitution of the C ring on which the B ring is attached and the degree of unsaturation and oxidation of C ring there are: flavones, flavonols, flavanones, flavanonols, flavanols or catechins, anthocyanins and chalcones, In addition, flavonoids are considered important components in several nutraceutical, pharmaceutical, medicinal and cosmetic applications. This can be attributed to their anti-oxidant, anti-inflammatory, anti-mutagenic and anti-carcinogenic properties coupled with their ability to modulate cellular enzymatic function (**Table 1**).

Name	Structure	Function
Flavone		<p>Baicalein protected H9c2 cardiomyocytes and also human embryonic stem cells-derived cardiomyocytes (hESC-CMs) against oxidative stress-induced cell injury. It exhibits anticancer activity against several cancers <i>in vitro</i>. Baicalein also decreased ROS generation and the number of death cells and activated Nrf2 pathway [25].</p>
Flavonol		<p>Flavonol decreased the DOX-induced apoptosis, ROS production, lipid peroxidation and NADPH oxidase activity. Isorhamnetin increased the production of anti-oxidant enzymes and modulated MAPK activity [26].</p>
Flavanone		<p>Hesperidin induced antiarrhythmic effects, reduction of inflammation, oxidative stress and cardiomyocytes apoptosis. Naringin restored ischemia/reperfusion injury inflicted by reactive oxygen species (ROS) by the increased activity of anti-oxidant enzymes [27].</p>
Flavan-3-ol		<p>Theaflavin-3,3'-digallate decreased ROS production, cellular damage and apoptosis [28].</p> <p>Catechin has antioxidant properties and reacts as a scavenger of free radicals. Catechins can also act as indirect antioxidant in conjunction with vitamins C and E and antioxidant enzymes, such as superoxide dismutase and catalase. [29]</p>

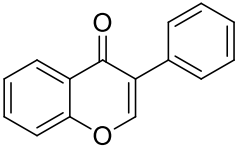
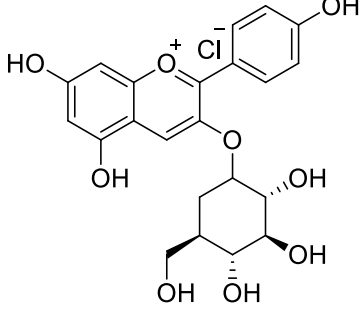
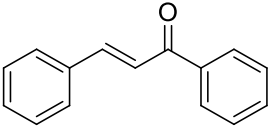
Isoflavone		Isoflavone has positive effects on oxidative stress-induced apoptosis in H9c2 cardiomyocytes. Calycosin enhanced the expression and activation of ER α / β and Akt phosphorylation and inhibited H ₂ O ₂ -induced cell injury and apoptosis[30].
Anthocynin		Malvidin increases left ventricular pressure, reduces cells apoptosis and necrosis. Anthocyanin reduces activation of Calpain and apoptosis and increases the activity of antioxidant enzymes [31]
Chalcone		Chalcone decreases the levels of pro-inflammatory cytokines and ROS in H9c2 cardiomyocytes. In addition, isoliquiritigenin improves the dysfunction of hypoxic cardiomyocytes [32].

Table 1: *Flavonoid compounds and their activities*

Non-flavonoid compounds include several subclasses and the most important classes are phenolic acids, stilbenes and lignans (**Table 2**).

Phenolic acids include benzoic acids such as protocatechuic acid and gallic acid, and cinnamic acids such as caffeic acid, ferulic acid, p-coumaric acid and sinapic acid. They are present in plants, fruits, coffee, and cereal grains [33]. These compounds may have beneficial effects on human health, and thus their study has become an increasingly important area of human nutrition research. Stilbene analogues are a heterogeneous group of natural phenols, abundant in grapes and berries and are widely known for their anti-inflammatory, cardiovascular protection, antiviral, antimicrobial and antioxidant properties [34].

The most common lignans are pinoresinol, lariciresinol, secoisolariciresinol, matairesinol, hydroxymatairesinol, syringaresinol and sesamin. Diets rich in foods containing plant lignans (grains, nuts and seeds, legumes, fruit, and vegetables) have been consistently associated with reductions in risk of cardiovascular disease [35] and cancer. Enterolignans,

which are the metabolites of the lignan plant derived from their conversion by intestinal bacteria, have several biological activities, including tissue-specific estrogen receptor activation, anti-inflammatory and apoptotic effects [36].

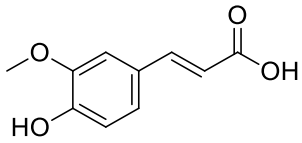
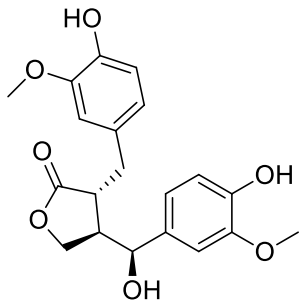
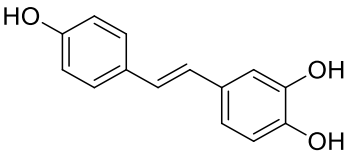
Compounds	Structure	Function
Phenolic acids (Ferulic acid)		Phenolic acids protect cardiomyocytes against H ₂ O ₂ -induced injury. Pyrrolidinyll caffeamide restores ischemia/reperfusion-induced oxidative stress in rats. It also reduces the levels of troponin and lipid peroxidation, improved cardiac functions [37]. Ferulic acid reduces oxidative stress.
Lignans (Hydroxymatairesinol)		Lignans(in particular sesamin) reduce the Ang II-induced apoptotic rate and ROS production in H9c2 cardiomyocytes. Sesamin also have anticarcinogenic and antioxidative properties. Lignans have anti-inflammatory potential via reduction of lipopolysaccharide-induced cellular oxidative stress. Schisandrin B significantly increases the levels of GSH redox cycling enzymes [38].
Stilbene (Resveratrol)		Resveratrol protects H9c2 cardiomyocytes from H ₂ O ₂ -induced cell injury, apoptosis necrosis and mitochondrial dysfunction. Resveratrol reduces ROS production and protects cell from fungal attack and sun damage. [39]

Table 2: Examples of non-flavonoid compounds

II. Sunlight, skin damages and and ossidative stress

II.1. Generality of sunlight

The sun is a solar-type star located at 1.496×10^{11} m from the Earth and its electromagnetic spectrum is very broad. It is from high frequencies such as X-rays and Gamma to low frequency waves such as radiofrequencies and microwaves. Ultraviolet rays, visible light, infrared are intermediate (**figure 1**). Energy and wavelength of these radiations can be related using a mathematical expression.

$$\text{Equation 1: } E = h \times \nu = h \times \frac{c}{\lambda}$$

Where **E** is the energy, **h** is the Planck's constant, **ν** is the frequency of electromagnetic radiation, **c** is the velocity and **λ** is the wavelength. Frequency is related to the wavelength by the relation $\nu = c/\lambda$ and **c** is about 300000 Km/s in the vacuum. Thus, the greater the wavelength of a radiation, the lower its frequency and consequently, lower is the energy transported by each photon.

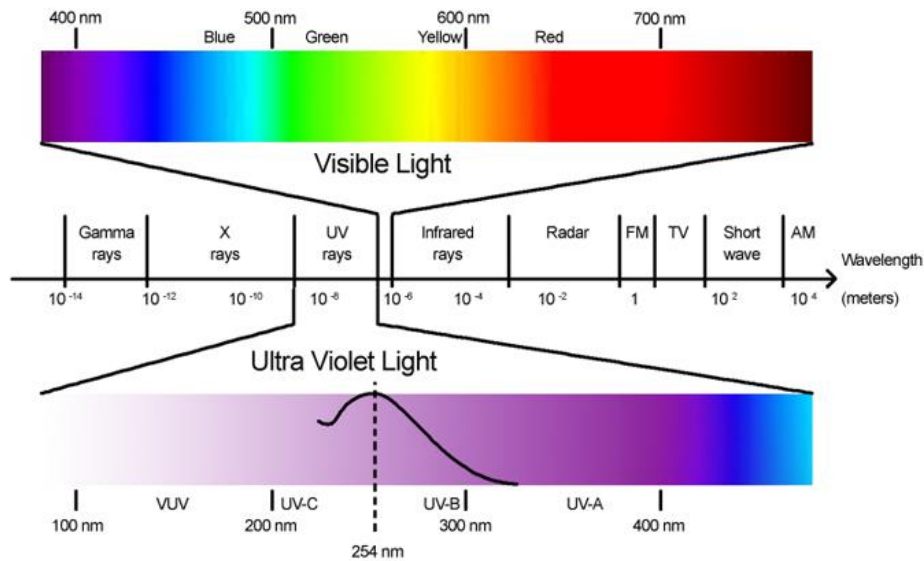


Figure 1: *Electromagnetic spectrum*

The Earth's atmosphere absorbs and disperses certain radiations, preventing all sunlight radiation from reaching the ground [40]. So sunlight that reach the Earth is constituted of 56% are infrared light photons (wavelength, 780-5000 nm), 39% visible light (400-780 nm), and 5% UV light (290-400 nm). These percentages may vary according to: altitude, latitude, atmospheric ozone content, cloud cover and season [41].

Latitude: The solar radiation varies according to our position on Earth. Closer to the equator, the sun's rays have a shorter distance to move into the atmosphere and therefore

less UV radiation can be absorbed. For each degree of latitude decrease, there is a 3% increase in UVB transmission [41]

Altitude: With increasing altitude, less ozone is available to absorb UV radiation. For each 300 m elevation, there is a 4% increase in UV radiation reaching the surface [43]. Any phenomenon leading to the alteration of the ozone layer causes a substantial increase in the transmission of UV to the Earth's surface.

Among electromagnetic radiations, the area that is of our interest is UV range. Ultraviolet radiation is the part of the electromagnetic spectrum located between the X-ray and the visible light. In fact, like all solar radiation, UV radiations move at the speed of light and it is undetectable by the human eye, but some animals, particularly some insects, can see them. UV rays range from 200 to 400 nm and classified in 3 bands according to their wavelength. Short wavelength UVC (200-290 nm) is the most harmful type of UV radiation. However, it does not reach the earth's surface because it is completely filtered out by the ozone. UVB (290-320 nm) constitute between 5 and 10% of the UV rays reaching the surface of the Earth. So, about 90% are absorbed by ozone. UVA (320-400 nm) is subdivided into two groups: UVA1 ($340 \text{ nm} < \lambda < 400 \text{ nm}$) and UVA2 ($320 \text{ nm} < \lambda < 340 \text{ nm}$). UVA represents 90 to 95% of terrestrial UV radiation. Therefore only 5-10% are blocked by the ozone layer [44].

II.2. Cutaneous physiology

The skin is one of the most important and largest organs of the body. In humans, it accounts for 16% of body weight and is composed on average of 70% water, 27.5% protein, 2% fat, 0.5% mineral salts and oligo-elements. It is the first barrier of protection of the body. In fact, the skin protects the body from harmful environmental factors [45] such as humidity, cold, sunlight, chemical and biological aggressions. In addition, the skin receives sensory stimuli from the external environment and regulates body temperature. It is the site of the synthesis of essential vitamin D thanks to the sunlight. The skin has a heterogeneous structure composed of three superimposed layers: epidermis, dermis and hypodermis.

II.2.1. Epidermis

The epidermis is the outermost layer of the skin; it is visible to the eye and constitutes a protective barrier of the surface of the body. It is responsible for the water-resistant barrier and preventing the entry of pathogens into the body. Its thickness depends on the region of the body; it is thinner on the eyelids and thicker on the palms of the feet and hands.

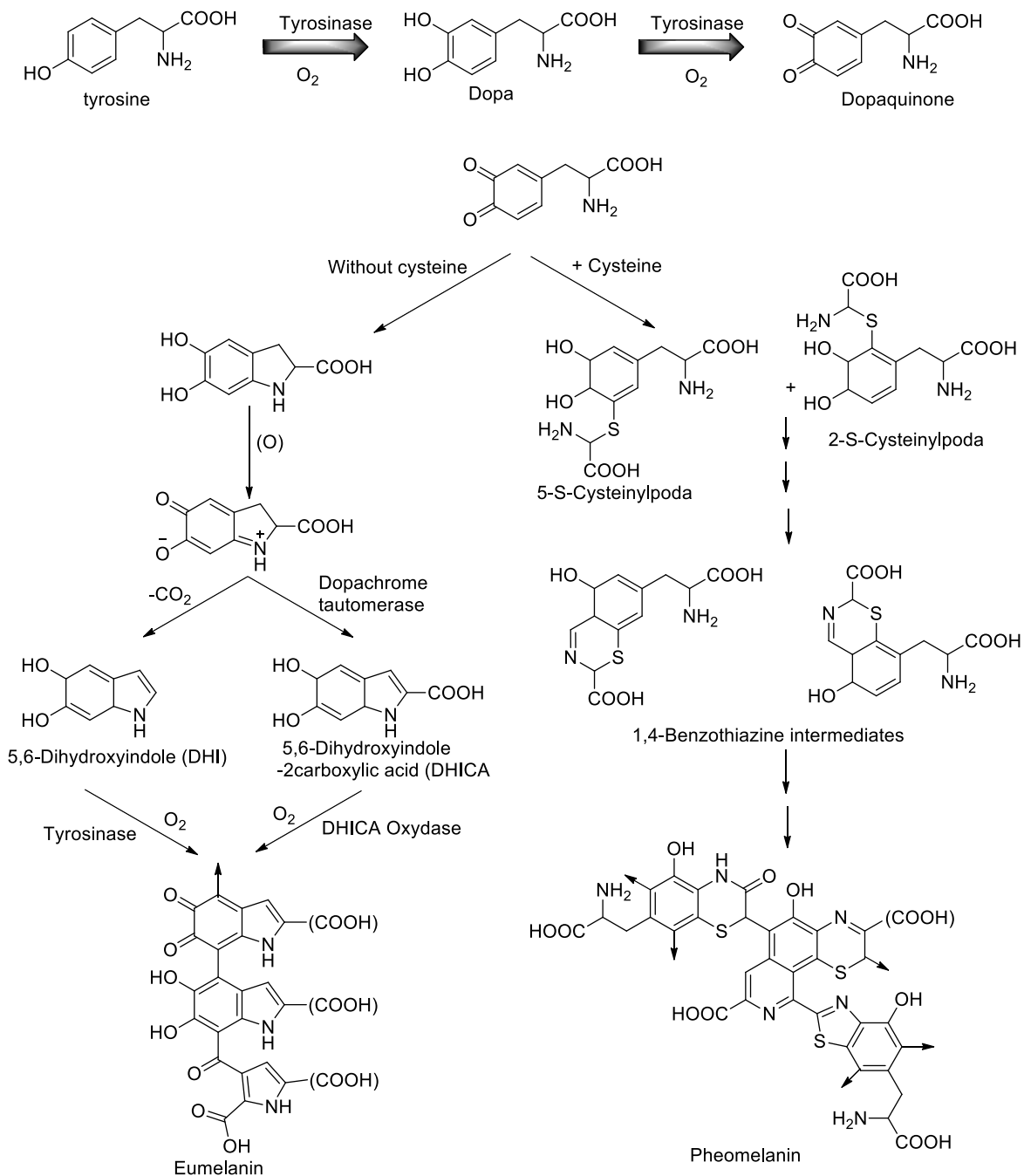
Moreover, the epidermis is mainly made up of epithelial cells called squamous cells. It is composed of four or five layers according to the area of the skin: cornified layer (stratum corneum, this is relatively waterproof and most of the barrier functions of the epidermis are localized there) [46], translucent layer (stratum lucidum, only in palms and soles), granular layer (stratum granulosum), spinous layer (stratum spinosum) and basal layer (stratum basale, they are closely associated with cutaneous nerves and seem to be involved in light touch sensation, it lies next to the dermis). The epidermis is constantly renewed to replace the damaged cells. The main function of the epidermal layer is the "barrier" means physical, chemical, micro-biological, and immunological protection. The epidermis consists of 4 types of cells: Keratinocytes, Melanocytes, Lymphocytes / Langerhans cells and Merkel cells.

Keratinocytes are the most numerous, representing about 90-95% of the cell population of the epidermis. It produces keratin, a resistant protective protein that constitutes the majority of the structure of the skin, hair and nails. Any defect in the expression of keratin leads to various diseases of the epidermis such as epidermolysis bullosa simplex, epidermolytic hyperkeratosis [47], hair such as monilethrix, pseudofolliculitis barbae [48]. The keratinocytes originate in the stratum basale, gradually they mature and move towards the stratum corneum. Once reached the most superficial layer, they undergo a process of keratinization (keratinocytes to corneocytes), creating the hard outer layer of the skin. This layer thus forms squamous cells that are flattened horizontally and replace dead cells, constituting an effective barrier preventing the entry of infectious agents into the body. One of the main roles of keratinocytes is the production of cytokines, involved in the initiation of the inflammatory response [49].

Melanocytes are cells located in the deepest layer of the epidermis. They are the second population (about 13%) of the epidermal cells. These cells are responsible for the synthesis of the melanin pigment which determines the color of the skin. Melanin is also found in hairs, eye, and some internal membranes. There are many different types of melanin with differing proportions. However, pheomelanin, eumelanin and neuromelanin are the most frequent. Both pheomelanin and eumelanin are found in skin and human hair, but eumelanin is the most abundant melanin in humans. Pheomelanin is found in red hair and red feathers while eumelanin is found in human black hair and in the retina of the eye [50], [51].

In the human skin, melanogenesis which is the production of color pigments eumelanin and pheomelanin occurs in the melanocytes, especially inside the organelles melanosomes by enzymatic or non-enzymatic reactions. In fact, upon exposure to UV radiation,

melanocytes increase the production of intracellular nitric oxide (NO); the latter triggers signal transduction cascades leading to a series of oxidative reactions involving the amino acid tyrosine [52]. Enzymatic pathway is regulated by at least three melanocyte-specific enzymes: Tyrosinase, TRP1 (Tyrosinase-Related Protein-1) which is 5,6-dihydroxyindole-carboxylic acid oxidase [53] and TRP2 (Tyrosinase-Related Protein-2) which is dopachrome tautomerase [54] but enzyme tyrosinase is known as the key enzyme in melanin synthesis. The oxidation of L-Tyrosine to L-DOPA is then catalysed by the action of tyrosinase enzymes. In the next step L-DOPA is oxidized to DOPA quinone, a key intermediate compound of two synthetic pathways. Depending on the conditions, DOPAquinone leads to the synthesis of eumelanin or pheomelanin (**Scheme 4**). The pathway of pheomelanin production involves cysteine or glutathione which, under the action of a glutamyl transpeptidase, can release a cysteine. The spontaneous reaction of cysteine with DOPAquinones results in the formation of 5-S-cysteinyl DOPA which polymerizes to form pheomelanins. The pathway of eumelanin production starts with the conversion DOPA quinone to leuco DOPAchrome and then DOPAchrome through auto-oxidation, and then in the presence of DOPAchrome tautomerase and dihydroxyindole-2-carboxylic acid oxidase, DOPAchrome is converted to 5,6-dihydroxyindole. Finally, the oxidation of 5,6-dihydroxyindole (DHI) to indole-5,6-quinone by tyrosinase leads the polymerization and the formation of eumelanin. The polymers of eumelanin would comprise many 5,6-dihydroxyindole (DHI) and 5,6-dihydroxyindole-2-carboxylic (DHICA) cross-linked polymers[55].



Scheme 4: Biosynthesis of eumelanin and pheomelanin

Synthesized melanin is then transferred from the cytoplasm of the melanocytes to the basal cytoplasm of the keratinocytes through melanocytic dendrites. Various hypothetical modes of melanin transfer have been demonstrated, such as cytophagocytosis, exocytosis, fusion of plasma membranes and transfer via membrane vesicles [56]. Most of these modes involving a phagocytosis step. In addition, melanogenesis and melanin transfer are induced by UVR which stimulate the production/secretion of autocrine or paracrine factors by keratinocyte [57, 58]. In fact, UV-induced pigmentation, leading to increase the dendricity

of melanocytes and the phagocytic activity of keratinocytes by upregulation of melanogenic enzymes. Therefore, keratinocytes and melanocytes are then known as the epidermal melanin unit.

Eumelanin and pheomelanin are chemically and physically different, eumelanin is a heterogeneous macromolecule form by units of 5,6-dihydroxyindole (DHI) and 5,6-dihydroxyindole-2-carboxylic acid (DHICA). The order of these units is aleatory and the ratio of DHI to DHICA depends on the origin of the pigment. Darker eumelanines are enriched in DHICA and Light-brown eumelanines contain more DHI units. Pheomelanin is derived from the sulphur containing cysteinyldopamelanin which lead to benzothiazine units. Eumelanin is a dark-brown to black pigment, insoluble in acid and alkali and contains nitrogen (6-9%) but no sulfur (0-1%), whereas pheomelanin is a yellow to reddish-brown pigment, soluble in alkali, and possesses both nitrogen (8-11 %) and sulfur (9-12%) [59]. On the other hand UV irradiation of pheomelanin produce free radical greater than those produced by eumelanin [60].

Melanin protects against sunlight induced burns, DNA damage, and skin cancer. These attributes of melanin are due to broad absorption spectrum. Eumelanin has been considered to perform a UV-protection function more than pheomelanin, because it has more chromophores, and it is more densely packed due to the branching of the polymer. Although melanin plays important protective roles, pigment can act as a potent photosensitizer leading to intense production of reactive oxygen species. Furthermore, during melanization, particularly in steps that can proceed without enzyme, toxic intermediates such as semiquinones, dopaquinone, indole-quinones are produced [61].

Lymphocytes or Langerhans cells constitute the third population of the epidermis layer and represent 1 to 3% of the total population. They are a subtype of white blood cells and are dendritic cells of medulla origin. There are three main types of lymphocytes: B (bone marrow) cells, T (thymus) cells, and natural killer cells. B cells produce antibody molecules, they are primarily responsible for humoral immunity, while natural killer cells are innate immune systems, they destroy cells infected by virus and tumor cells [62], and T cells ensure their own destruction as well as viruses and cancerous cells. In response to the pathogen, lymphocytes in particular Tcells can produce cytokines, which are small proteins that are important for immune system responses, inflammation and infections [63].

Merkel cells are found in the basal stratum of the epidermis separating the epidermis from the dermis layer and they have no dendrite [64]. These cells are very close to the nerve endings that receive the contact sensation and are more common in the skin exposed to the sun than in the covered skin. The richest regions of Merkel Cells such as the lips, palms,

fingers and soles of the feet are involved in tactile perception [65]. Merkel plays an important role in the secretion of neuropeptides and specific protein neurons, so they have a neuroendocrine function [66].

II.2.2. Dermis

Dermis is the second and thicker layer of the skin. It is located between the epidermis and the subcutaneous tissues. The dermis is composed mainly of connective tissues containing collagen and elastic fibers. Its structural tissue is divided into two sections: the thin upper layer called the papillary dermis and a thick lower layer called the reticular dermis. The papillary dermis, at the surface area of the skin, increases and seem as fingerprints called dermal papillae. Dermal papillae contain tactile receptors which are corpuscles of touch and nerves sensitive to heat, cold, pressure, pain and itching. The reticular dermis is the main site of dermal collagen and elastic fibers. The high concentration of these dermal proteins in the reticular region gives to the skin the properties of strength, extensibility and elasticity. Moreover, the spaces between the fibers are occupied by the roots of the hair, the sebaceous glands, the sweat glands, the skin receptors and the adipose cells [67], [68]. Properties of the dermis confer on it several functions, in particular sweat and oil production, blood bringing and hair growing [69].

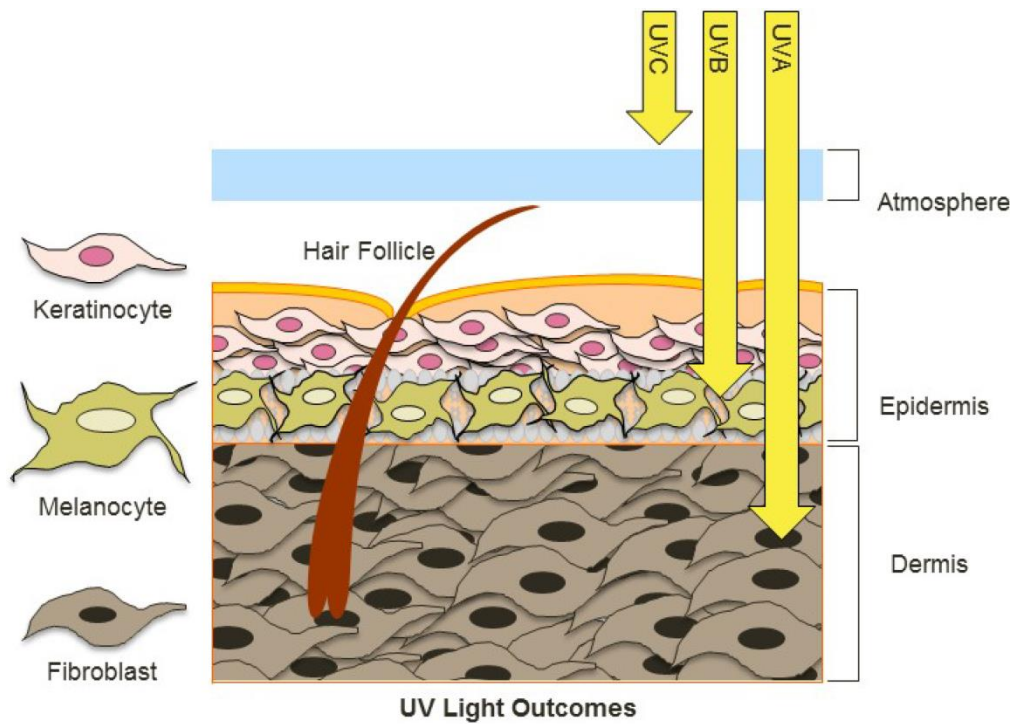
II.2.3. Hypodermis

The hypodermis or subcutaneous layer is the deepest layer of the skin. It is a fatty tissue composed of fibroblasts, adipose cells, connective tissue, larger nerves, blood vessels and macrophages. The distribution and thickness of the fat layer varies according to the personal diet, parts of the body and the sex of the individuals. In men, adipose tissue mainly develops in the abdomen and shoulders, whereas in women it is present mainly at the level of the belt, hips, thighs, buttocks and under the abdomen. Apart from the storage of the fat, hypodermis can also seal the skin to the underlying surface, provide thermal insulation, product the Leptin hormone and absorb shocks from impacts on the skin.

Of all the foregoing, the main functions of the skin are: protective barrier against external aggressions (physical, chemical and biological protection), regulate body temperature/ thermal insulator, infection protection site, immunological role (adaptation and activation of the immune system), sensory role (sensory nerves, thermoreceptors, etc ...) by means of the various receptors present on the surface of the skin and synthesis of vitamin D due to exposure to UV rays from the sun.

II.3. Skin damages by UV irradiation

As previously described, UV radiation range from 290 to 400 nm and it is the absorption range of many chromophores of the skin including DNA [70], RNA, proteins, lipids, trans-urocanic acid, and aromatic amino acids [71]. Skin, when excited by solar energy, emits a response, the extent of this response depends on the type and the quantity of UV absorbed, the color of skin. It follows that; effects from exposure to ultraviolet (UV) radiation can be harmful or beneficial. Indeed, moderate exposure to UV stimulates the secretion of tryptamines (melatonin) and the synthesis of melanin and vitamin D [72]. While overexposed to UV radiation causes harmful effects that can be acute or chronic. The major acute clinical effects of UV irradiation on human skin are sunburn in particular for the red skin (erythema), immunosuppression, mutation and tanning (darkening by improving melanogenesis) [70]. Chronic UV effects include premature aging of the skin, suppression of the immune system, damage to the eyes and skin cancer [73] which induced by mutation and immunosuppression. DNA photodamage is induced by both UVA and UVB radiations but with different mechanism. UVB radiations are absorbed directly by the DNA chromophores and induce base structural DNA damage, while UVA radiations cause the production of free radicals or ROS in the deep cells of the skin. These oxidizing species are toxic and, in turn, attack the DNA, and alter the functioning of the cell. Therefore, UVB radiation is more cytotoxic and mutagenic than UVA [72]. In addition, UVA causes premature cutaneous aging, by degrading collagen and inducing the production of free radicals in skin cells, causes premature cutaneous aging which results in the appearance of spots, thinning of the skin and the appearance of wrinkles 10 to 20 years after exposures. UVA and UVB lead to a weakening of the immune system and inflammation phenomena that could contribute to the promotion of cutaneous tumors [74]



UVC	UVB	UVA
-No effect	-Sunburn - Direct DNA Damage - Skin Cancer -Inflammation - Eye Cancer	- premature Aging - Indirect DNA Damage -Skin Cancer

Figure 2: *Effect of UV on the skin*

Sunburn or erythema is abnormal redness of the skin, caused by UV after overexposure to the sun. This phenomenon occurs a few hours after exposure. Biologically, it is a reaction of the body due to the direct DNA damage from mainly UVB [75], thus creating mutations in the cells and the superficial vessels of the skin. These mutations lead to the formation of cyclobutane pyrimidine dimers (CPDs) and pyrimidine (6-4) pyrimidone photoproducts (64 PPs) [76, 77]. The reaction is associated with certain infections, inflammation, and pain, hot or warm to the touch due to increased blood flow to the skin caused by dilation of the superficial blood vessels of the dermis. In some cases, body triggers several defense mechanisms, including DNA repair to reverse damages, apoptosis and peeling to remove irreparably damaged skin cells and increase melanin production to prevent future damage. UVA also contributes to the sunburn reaction in the summer months but its participation is low.

Tanning is the process whereby skin color is darkened. It can be the result of an increase in the number of melanocyte functions (pigment cells) which is the consequence of the increased activity of the enzyme tyrosinase. It is the auto-protection mechanism of the skin in response to UV radiation exposure that leads to the formation of a new melanin and an increase in the number of melanin granules in the epidermis. The process of tanning is caused by UVA and UVB. UVA radiation induces oxidative stress, which in turn oxidizes existing melanin and leads to rapid pigmentation or darkening of the melanin, but without any increase in melanin quantity [78]. UVB causes damage to DNA by absorbing cellular chromophore in direct action, increasing the production of melanin, tanning step is delayed and becomes visible two or three days after exposure [79].

Skin cancer is caused by abnormal growth of skin cells with the ability to invade neighboring tissue or metastasize. It occurs when unrepaired DNA lesions cause mutations (most often p53 tumor suppressor gene) [80] or genetic abnormalities promoting invasion, metastasis, proliferation and cell survival. Indeed, p53 is a nuclear transcription factor involved in many fundamental processes of the cell, such as genomic integrity maintenance, cell cycle arrest /apoptosis and DNA repair. Under normal conditions, p53 is expressed at an extremely low level whereas under stress conditions p53 is altered and induces DNA damage leading to generation of mutations. In human malignancies, p53 mutation is found in over 50% of cancer [81]. Skin is protected from sunlight damage by melanin that forms a plug on the DNA in the cells. The injuries of UV radiation exposure vary depending also on ability to block or repair sun induced damages. For this reason, darker skin has up to five fold the protection of lighter skin and a much lower risk of skin cancer. Certain types of skin cancer can spread to other organs and tissues, such as lymph nodes and bone. There are different types of skin cancer including basal cell carcinoma (BCC), squamous cell carcinoma (SCC) and melanoma which originates from the pigment-producing skin cells (melanocytes). Basal cell carcinoma (BCC) is the most common type of skin cancer. They are commonly found on the head, neck and areas subject to chronic sun exposure. Squamous Cell Carcinoma affects cells in the outer layer of the epidermis. It is the second most common form of skin cancer and it is typically more aggressive than basal cell carcinoma. It can spread to other body parts such as tissues, bones, and nearby lymph nodes. Squamous cells are found in many places of the body such as hands, head, neck, lips, and ears. **Melanoma** is the least common of skin cancer, but it is more likely to grow and spread. However it is the most dangerous, causing about 73 percent of all skin cancer-related mortality [82]. Melanoma originates in the pigment-producing melanocytes in the basal layer of the epidermis. The UV effects on human skin,

including DNA damage through the formation of dimeric photoproducts, gene mutations, oxidative stress, and immunosuppression, contributing to melanomagenesis [83].

Photoaging develops gradually with many years of regular exposure to intense solar radiation. It is manifested by abnormality damage such as loss of dilation of blood vessels and degradation of collagen and elastin fibers. This degradation is related to the formation of the enzyme metalloproteinase which lead to the decomposition of dermis constituents (Keratinocytes, melanocytes, fibroblasts and langerhan cells). The photo-aging phenomenon manifests itself both on the face and on the body, with fine wrinkles in the areas around the eyes, lips and nose, marked freckles, broken capillaries, spots and especially the solar elastosis, the cutaneous sagging that makes the skin soft and falling. Both UVB and UVA radiation contribute to photoaging, while, UVA has been shown to play a much larger role in photoaging than UVB [84].

Eyes damaged from UV absorption by the cornea can cause conjunctivitis or keratitis. These lesions are reversible and disappear in 1 or 2 days. However, repetition of eye disorders can lead to irreversible damage. Overexposure to UV can also increase the risks of eye diseases, including cataract, growths on the eye, retinal dystrophy and eye cancer [85].

II.4. UV-photoprotection

Protecting the skin against the harmful effects of ultraviolet radiation is important for maintaining the health of the skin. Despite natural photoprotection methods such as skin pigmentation, wearing clothes, hats and glasses, UV rays are able to penetrate and damage the skin. Therefore, the use of sunscreens becomes essential to protect the skin from several harmful effects.

In Europe, sunscreens are considered as cosmetic products. For this purpose, all UV filters before being placed on the EU market must be evaluated by the Scientific Committee for Consumer Safety and authorized by the Commission [86], [87], while in the United States suncreens are considered as over-the-counter (OTC) drugs and thus evaluated by the US Food and Drug Administration (FDA) [88].

The Cosmetics Directive 76/768/EEC, annex VII, the council of the European Communities has established 26 filters that can contain the sunscreen products and sets the maximum permitted concentrations and conditions of use for each one of them. In the United States, only 16 are authorized by the FDA. This could be explained by the fact that in the European Union the solar products are classified among the cosmetics product for which the acceptance process is faster. To provide suitable protection an UV filter should

be photostable, water resistant, nontoxic, photochemically inert, not penetrate through the stratum corneum and easy to formulate. Solar products may contain one or several UV filters active ingredients that can absorb, reflect or disperse photons from the sun. There are two types of filters: organic or chemical filters and inorganic or physical filters.

II.4.1. Organic or chemical filters

The organic filters are aromatic compounds sometimes associated with a carbonyl group designed to absorb UV radiation light and convert it into a small amount of heat. The absorption of UV radiation by the filter leads to transition of the molecule from a ground and stable state to an electronically excited and unstable state. If loss of energy is great, the excited electrons release the energy in the form of heat or fluorescence thus allowing the molecule to return to a stable state and the filter is defined “photostable” and assures its role of photoprotector. On the other hand, if excited electrons do not have sufficient energy to return to an initial state, the molecule remains in their unstable position and their structure can be modified or their chemical bonds can break, resulting in activity loss. In this case, the filter is “photounstable” (**Figure 3**). Photounstable filter induce phototoxic or photoallergic responses which, in the long term, may increase the risk of skin cancer or photo-aging. [89].

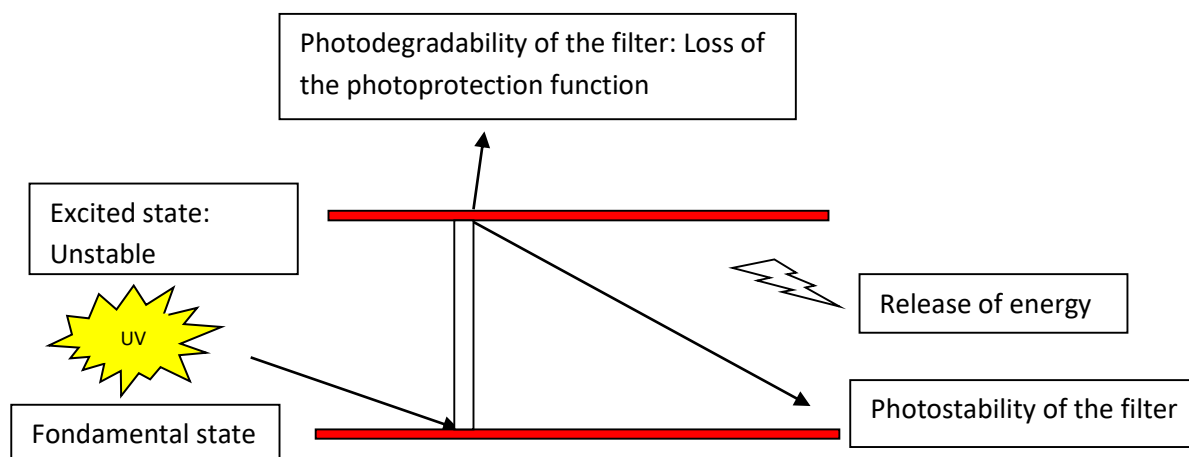


Figure 3: Operation of an organic UV filter

Chemical organic filters are classified into either UVA (benzophenones, anthranilates and dibenzoylmethanes) or UVB filters (PABA derivatives, salicylates, cinnamates and camphor derivatives) and broad spectrum UVB-UVA (Meroxyls, Tinosorb’s derivatives). These filters are almost always used in combination, especially with inorganic filters, since no single active agent, used at the levels currently permitted by the FDA [88] provides sufficiently high SPF (sun protection factor) protection or broad-spectrum absorption.

In addition, organic filters can be found not only in cosmetics but also in other personal care products, food packaging, pharmaceuticals, plastics, textiles, and vehicle maintenance products to prevent photodegradation of polymers and pigments.

I.4.2. Inorganic filter

Inorganic or physical UV filters work by reflection, absorption and scattering of both UV and visible light. The inorganic UV filters protect skin reflection or scattering [90]. However, some authors argue that even though inorganic UV filters diffuse, reflect, and / or absorb solar radiation, they protect the skin only by absorption [91]. Inorganic filters are zinc oxide, titanium dioxide, iron oxide, kaolin, ichthammol, talc [92]. By far, the most common are titanium dioxide (TiO₂) and zinc oxide (ZnO). Occasionally, iron oxide (Fe₂O₃) pigments are added to give the cosmetic a brown tinge to improve the appearance of the sunscreen product. In Europe only Titanium dioxide is permitted in sunscreen formulations. However, physical filters are not often cosmetically appreciated because they tend to be opaque and white on the skin due to high refractive index (ZnO refractive index = 1.9 and TiO₂ refractive index = 2.6) and the size of the molecules make their appearance unattractive. To overcome these disadvantages, some inorganic filters contained in sunscreen products are micronized and encapsulated in microspheres of dimethicone and silica. Micronization allows them to reach a nanometric size (20 to 30 nm for titanium dioxide and 60 to 120 nm for zinc dioxide), which leads to reduce the dispersion of light and to give transparency to creams. Considering that microparticles are in dispersion, they tend to agglomerate leading to the loss of the efficacy of the formulation [93]. In addition, The UV protection spectral range provided by TiO₂ is broad, extending from UVB to UVA region while the ZnO protection range peaks in the UVA spectrum.

However, TiO₂ and ZnO may undergo photochemical reactions generating highly oxidizing agents such as ·OH, O²⁻ H₂O₂ and ¹O₂, which are known to cause damage to DNA and RNA or alter the alteration of cellular homeostasis. To avoid this, the TiO₂ and ZnO particles are coated with dimethicone or silica, to stabilize them.

III. Infectious diseases induce oxidative stress

Infection is any damaging invasion of an organism's body tissues by harmful microorganism. These infectious organisms use host tissues to sustain itself, reproduce and colonize. They are known as pathogens and include bacteria, viruses, fungi and prions. The infection can be transmitted in various ways: contact with the skin, body fluids, contact with the feces, airborne particles and infected objects. The spread of the infection and its effect on the human body depend on the type of agent. However, mammalian hosts react to infections with an innate response, which often leads to inflammation, followed by an adaptive response (immune system), but sometimes colonies of pathogens pass through the body, at this stage infections become harmful causing an infectious disease. Infections by harmful microorganism can be either acute or chronic. Acute infections come and go rapidly; chronic infections develop more slowly and last longer.

III.1. Fungi

The organisms in kingdom fungi form several groups such as: mushrooms, yeasts, molds, rusts, smuts, puffballs, truffles and morels. They are eukaryotic organisms with sexual or asexual reproduction. These organisms are devoid of chlorophyll, they are therefore heterotrophic organisms and feed by absorbing nutrients from the organic material. But before absorbing, the hyphae of the fungus first release hydrolytic enzymes or acid to break down the organic material into smaller, easily ingested compounds. They can be saprophytes, commensal, parasites, symbionts and live in air, in water, on land, in soil, and on/or in plants and animals. Fungi are immovable like the vegetables, with the exception of some species of aquatic fungi that produce zoospores able to move through a scourge. They prefer to live in the presence of oxygen, but it is also possible to find optional anaerobes. The cell wall of fungi is constituted of chemical elements such as: polysaccharides, proteins, fats and waxes. Chitin is a very rigid polysaccharide consisting of N-acetylglucosamine residues. This polymer is the main cell wall constituent of all fungi [94].

For a long time, they have been placed with plants and included in the group of tallophytes despite being very different organisms. Then, they were placed by biologists in a kingdom in their own and their classification is constantly changing. But only five phyla are accepted today including the Chytridiomycota, the Zygomycota, the Ascomycota, the Basidiomycota and the Glomeromycota [95].

Chytridiomycota is a phylum of fungi with flagellated cells. It is the oldest evolutionary line of fungi, having aerobic zoospores [96]. This property gives them a saprotrophic or parasites character on a wide array of hosts such as algae, plants, mosses, insects, vertebrates and invertebrates [97]. The organisms of this phylum are presented in freshwater, brackish and marine habitats, and are also abundant in the soil. They are often microscopic but can also produce a mycelium.

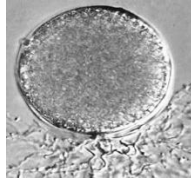


Figure 4: *Chytridiomycota structure*

Zygomycota is the most ecologically diverse group of fungi, it represent approximately 1% of the described species of true Fungi [98]. Contrary to Chytridiomycota, Zygomycota is the zygospor. This phyla is more evolved because it is completely disconnected from the aquatic environment and have no flagellate form. The organisms of this division act as saprophytes on substrates such as fruit, soil, and dung. While some are parasites of plants, insects, and small animals, while others form symbiotic relationships with plants [99]. In most zygomyceta, asexual reproduction through the formation of sporangiospores within sporangia cell is the most common form of reproduction. Sexual reproduction occurs when gametangials of different types of mating merge to form zygospores. Like all true fungi, zygomyceta produce cell walls containing chitin. It is grow primarily as mycelia, or filaments of long cells called hyphae.

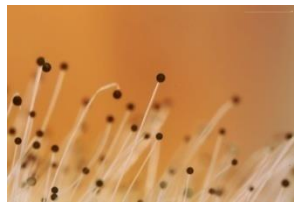


Figure 5: *Zygomycota structure*

Glomeromycota was formerly included within the Zygomycota, more recent genetic evidence shows that they are quite distinct from other fungi, which has made it possible to erect a new phylum [100]. It is a group of arbuscular mycorrhizal fungi, very important in the ecology and physiology of land plants. Glomeromycota is asexual organism and live in obligate symbiosis with plants [101]; More than 80% of extant land plants have a symbiotic with mycorrhizal fungi in their roots [102]. These microorganisms explore the host with mycelium.



Figure 6: *Glomeromycota structure*

Basidiomycota is a phylum of filamentous fungi composed of hyphae. Organisms of this phylum are unicellular or multicellular, sexual or asexual, and terrestrial or aquatic. Multicellular fungi are composed of networks of long hollow tubes called hyphae. They include mushrooms which are sexual reproductive structures. However, they also contain some microscopic fungi, such as rust and smut fungi that parasitise plants and some yeasts. In addition, they are found in terrestrial ecosystems, freshwater and marine housing [103]. Several Basidiomycota have a symbiotic lifestyle form. For humans, some Basidiomycota are a source of food nevertheless others cause human and animal diseases [104].



Figure 7: *Basidiomycota structure*

Ascomycota also known as Sac Fungi, include morels, truffles, brewer's yeast and baker's yeast, dead man's fingers, and cup fungi. Ascomycota and Basidiomycota form the subkingdom Dikarya. The mycelium of ascomycetes is usually made up of septate hyphae. Microscopic sexual reproduction by ascospores takes place in an ascus. However, some species of the Ascomycota are asexual by conidia. In symbiosis with algae most of Basidiomycota form lichens



Figure 8: *Ascomycota structure*

In short, the mycelium of Zygomycota and Chytridiomycota is not septated while that of Ascomycota and Basidiomycota is septated.

Fungi play a very important role in biotechnological applications such as the discovery in 1928 of penicillin produced by a fungal strain *Penicillium notatum* (Trichocomaceae,

division of Ascomycota), which is used for the biosynthesis of antibiotics used in pharmacopoeia [105]. In the same way, it has been shown that fungi have antibiotic and non-antibiotic bioactivity and the majority of organisms producing bioactive molecules are filamentous and a very small part of yeast organisms would be involved. Fermentation processes of certain yeasts such as brewer's yeast and baker's yeast (*Saccharomyces cerevisiae*) are used in many areas of the food industry and genetics / molecular biology [106].

However, fungi invade and grow in moist areas of the human body and plants causing fungal infection. Fungi utilize various mechanisms to deceive or destroy the immune cells and spread to various organs. Strangely, fungal infections on one part of the body can cause rashes on other parts of the body that are not infected. For example, a fungal infection on the foot may cause an itchy, bumpy rash on the fingers.

III.1.1. Fungal infection

Fungi infect billions of people every year, but still remain largely under-appreciated as pathogens of humans [107]. The types of infections caused by fungi can be classified in different ways: superficial infections, opportunistic infections and disseminated infections [108].

Superficial infections: the skin produces secretions, including sweat, sebum and antimicrobial peptides to defend against bacterial and fungal attacks. However some fungal species succeed in surpassing this defense and colonize the surface of the skin. At this time they become harmful and responsible for several skin infections such as pityriasis versicolor and tinea nigra. In addition, superficial fungal affect the outer layers of the body such as skin (epidermis), nails, hair and mucosa. The main groups of superficial fungal infections are: dermatophytosis (ringworm e tinea capitis, tinea pedis), superficial candidiasis (cutaneous, oropharyngeal, vaginal), diseases caused by *Malassezia* (pityriasis versicolor, seborrhoeic dermatitis) [109]

Dermatophytosis is fungal infection caused by dermatophytes that digest keratin of the epidermis and the integuments (nails and hair). Dermatophytes constitute a group of filamentous fungi adapted to keratin [110]. The dermatophytosis has proved to be among the most common and frequent fungal infections in the world, although other fungal infections such as Candidiasis, Cryptococcosis, Coccidiosis and Aspergillosis are becoming increasingly important. Depending on the stages of their life cycle, dermatophytes can be present in three anamorphic genera, identified as *Microsporium*, *Epidermophyton* and *Trichophyton* [111]. The predominant cause of dermatophytosis is

Trichophyton followed by *Epidermophyton* and *Microsporum* and within the genus *Trichophyton*, *Trichophyton rubrum* is the most predominant (69.5%)[112]. They are also grouped according to their sources of infection: geophilic (soil, generally saprophytic), zoophilic (animals) and anthropophilic (humans) [113]. Moreover, dermatophytosis is commonly known as tinea or ring-worm infections due to the characteristic ringed lesions [114]. Infection of humans is favoured by heat, humidity and poor hygiene. Clinical descriptions are based on the site of infection and we can distinguish: tinea pedis (foot), tinea capitis (scalp), tinea unguium (nail), tinea manuum (hands), tinea corporis or tinea circinata (non-hairy, glabrous region of the body), tinea barbae (bearded region of face and neck), tinea incognito (steroid modified), tinea imbricata (modified form of tinea corporis), tinea gladiatorum (common among wrestlers) and tinea cruris (“Jocks’ itch”; groin)[115]

Superficial candidiasis is usually caused by *Candida albicans* [116]. This organism is a common commensal in the mouth, vagina and gastrointestinal tract in healthy individuals. Superficial candidiasis can be classified as cutaneous, mucosal (vulvovaginal, balanopreputial, or oral), paronychia or onychia and chronic mucocutaneous candidiasis. Common sites of involvement include the skin folds (under the breasts, within the gluteal and inguinal folds, diaper area, under pannus, and the armpits). Most superficial infections result from some predisposing factors include heat, humidity, infancy, pregnancy, occlusion of epithelial surfaces, diabetes, obesity, and corticosteroid, Iron deficiency anemia and chemotherapy. In addition, vulvovaginal can occur at any age but is mainly seen in pregnant women and in women taking oral contraceptives.

Malassezia infection: *Malassezia* species are common lipid-dependent and lipophilic yeast that grow on normal human skin flora such as face, scalp, and chest. But abnormal overgrowth of some species can cause skin disorders, including pityriasis versicolor, seborrhoeic dermatitis, atopic eczema and folliculitis. Humidity and heat can promote yeast growth and some predisposing factors enclosed concomitant infections and food and flea allergies. *Malassezia* infection can complicate chronic central venous cannulation, mainly in neonates, manifesting as pulmonary infiltrates on upper trunk [117].

Opportunistic infections are infections that take advantage of weakness in the immune defenses. Opportunistic organisms are normal flora resident, they become pathogenic only when the immune defenses of the host is compromised. Immune-compromise can be induced by chronic diseases such as diabetes mellitus, lymphoma, leukemia, other hematologic cancers, burns, and therapy with corticosteroids, immunosuppressants, or antimetabolites, drug addiction, transplant and AIDS. The order of most common opportunistic fungal

infections are: Candidiasis (*Candida*), Aspergillosis (*Aspergillus*) and Cryptococcosis (*Cryptococcus*). Among *Candida* species, *Candida albicans* (75.8%) was the most prevalent species [118]. Furthermore, HIV-infected people are defenseless to opportunistic fungal infections that lead to morbidity and mortality. These weakened immune systems could be ascribed to the decreased of CD4+ cells level [119].

Disseminated fungal (also called systemic or deep-seated) infections are characterized by the presence of the fungal pathogen in the blood. The organisms responsible to the systemic fungal infection can be opportunistic fungal or true pathogenic fungi capable of invading and developing in the tissues of a normal host without recognizable predisposition [120]. These true (primary) fungi induce fungal infections such as Histoplasmosis, Blastomycosis, Coccidioidomycosis and Paracoccidioidomycosis. Systemic infection remains an important cause of mortality and morbidity in the immunocompromised patient.

III.1.2. Fungal infection and oxidative Stress

Phagocytic cells are the first line of defense against fungal infections which lead to the production of reactive species. Oxidative markers such as HNE, aconitase-2 and MDA [121] were observed in cells infected with fungal. Free radicals are produced via phagocytosis of fungi by human neutrophils and monocytes, and this situation is associated with dramatic changes of the oxidative metabolism. In fact, following stimulation by cytokines, phagocytic cells activate the assembly of the NADPH oxidase complex, which results in the generation of ROS. Increases in ROS cause oxidative stress in the cells resulting from imbalance of antioxidant and oxidant factors. These oxidants attack DNA and/or membrane lipids and cause chemical damage, including the healthy tissue. In addition, fungal infection also increased the mRNA expression and protein production of heme oxygenase-1 (HMOX1) and cyclooxygenase-2 (COX-2), with suppressed levels of antioxidant enzymes such as GPx1, peroxiredoxin-4 (PRDX4) and SOD1 [122].

III.1.3. Antimycotic drug

Antifungal agents can be grouped into three main classes based on their site of action: azoles, polyenes and 5-fluorocytosine. Beside these three classes we can cite others antifungals including allylamine and echinocandins. The antifungals are known to function by different mechanisms including inhibition of ergosterol biosynthesis by targeting the CYP450 14 α -demethylase (azoles); interaction with fungal membrane sterols (polyenes); inhibition of glucan synthase, which prevent the formation of β -glucan present in fungal

cell wall (echinocandins); inhibition of chitin synthase and squalene epoxidase (allylamine); interfering with pyrimidine metabolism, thus inhibiting nucleic acid synthesis (5-fluorocytosine) and inhibition macromolecular synthesis. In addition, the ergosterol which is one of the key components of the fungi cell membrane is the target of many of antifungal drugs.

Azole Antifungal Drugs: The azole antifungal agents have five-membered organic rings that contain either two or three nitrogen atoms (imidazole and triazole respectively). They can also contain sulfur atom (thiazoles). The clinically useful imidazoles are clotrimazole, miconazole, ketoconazole and econazole [123]. The most commonly used triazoles are itraconazole and fluconazole. The thiazole antifungal agent used for the topical treatment of fungal nail infections is abafungin. Azoles target the proteins responsible for ergosterol biosynthesis. In particular, Imidazole and triazole [124] classes inhibit the fungal cytochrome P450 enzyme 14 α -demethylase. While thiazole (abafungin) inhibits the enzyme sterol 24-C-methyltransferase, modifying the composition of the fungal membrane. In addition, abafungin has been shown [125], to have fungicidal and fungistatic effects on a wide variety of pathogens, including dermatophytes, yeasts (*Candida*) and moulds.

Imidazoles have a two-nitrogen azole ring in their structure and imidazole antifungals are predominantly used topically.

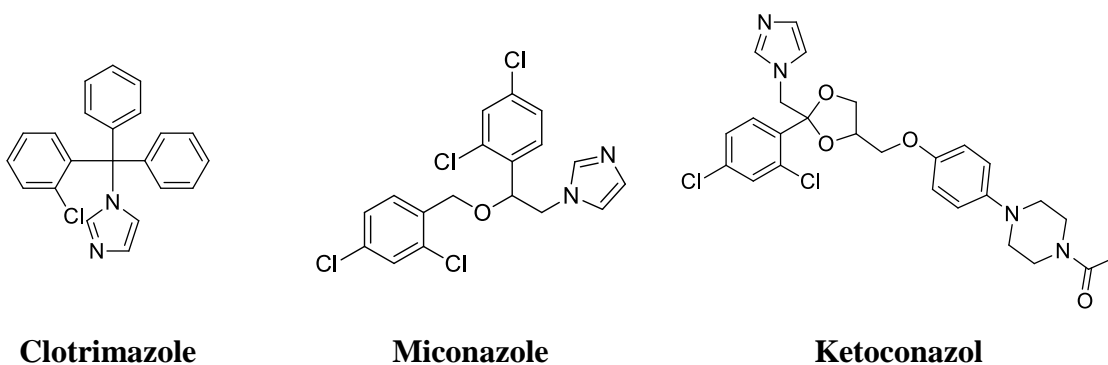


Figure 9: Imidazole antifungal drug

Triazoles have a two-nitrogen azole ring in their structure and triazoles antifungals are particularly 1,2,4-triazole rings, while thiazole contain both sulfur and nitrogen.

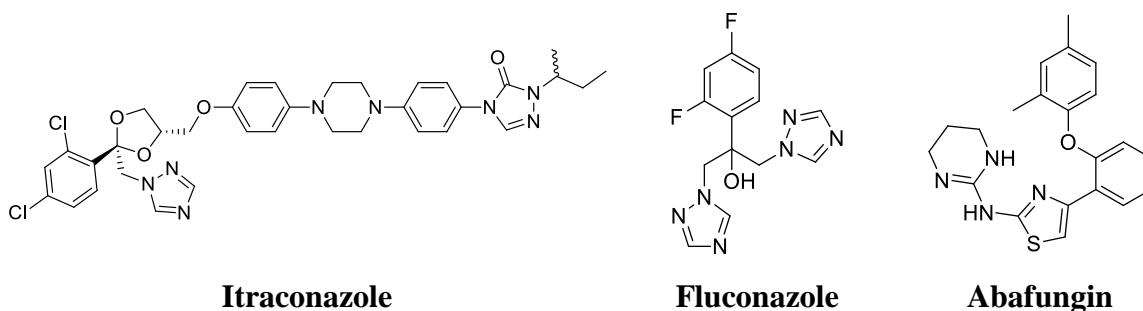


Figure 10: *Triazole and thiazole antifungal drugs*

Polyene Antifungal Drugs are macrocyclic compounds with a heavily hydroxylated region on the ring opposite the conjugated system. They have amphoteric character and their distinct characteristic is the presence of a chromophore formed by a system of three to seven conjugated double bonds in the macrolactone ring. Amphotericin, nystatin, and pimaricin interact with ergosterol in the cell membrane to form channels that open small pores into the membrane through which small molecules and ions leak from the inside of the fungal cell to the outside. This action therefore results in the loss of cytoplasmic components, the membrane-selective permeability, as well as the cell death. However, since the cholesterol present in human cell membranes is similar to the structure of ergosterol, the polyene also selects the human sterol, which leads to their toxicity. In addition, the polyene drugs are not soluble in water at physiological pH, are not absorbed orally, strongly absorb UV-visible light and are photolabile.

The common polyene antifungal drugs are Amphotericin B, nystatin, and natamycin. Amphotericin B is used primarily in the treatment of serious fungal diseases, such as cryptococcal meningitis, histoplasmosis, and blastomycosis.

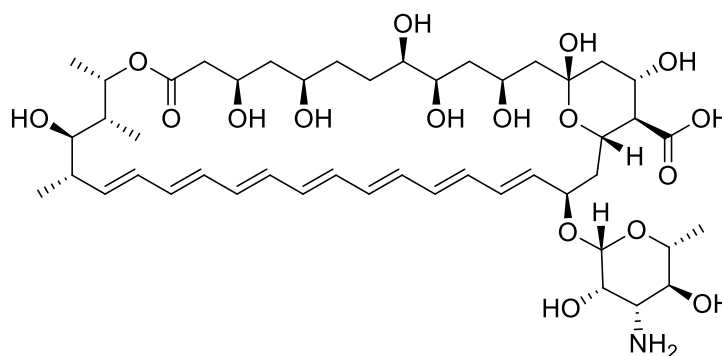


Figure 11: *Amphotericin B*

5-Fluorocytosine (5FC): is a fluorinated analog of cytosine. It inhibits both DNA and RNA synthesis via intra-cytoplasmic conversion to 5-fluorouracil. The latter is converted

to two active nucleotides: 5-fluorouridine triphosphate, which inhibits RNA processing thus disturbing the building of certain essential proteins, and 5-fluorodeoxyuridine monophosphate, which inhibits thymidylate synthetase and hence the formation of the deoxythymidine triphosphate important for DNA synthesis. Flucytosine is usually used for the treatment of serious infections caused by susceptible strains of *Candida* and *Cryptococcus*. 5FC is used in combination with other antifungals, such as amphotericin B and fluconazole, but only rarely as a single agent. In combination with amphotericin B it remains the treatment of choice for cryptococcal.

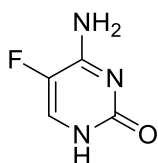


Figure 12: 5-Fluorocytosine

III.2. Virus

Viruses are very tiny germs (parasites) that cause infections. These infectious agent can replicates only inside the living cells of other organisms, they are incapable of reproducing on their own. Viruses depend on the organisms they infect (hosts) for their very survival. They are made of genetic material (DNA or RNA) inside of a protein coating, which the virus uses to replicate. Some viruses also have a fatty "envelope" covering.

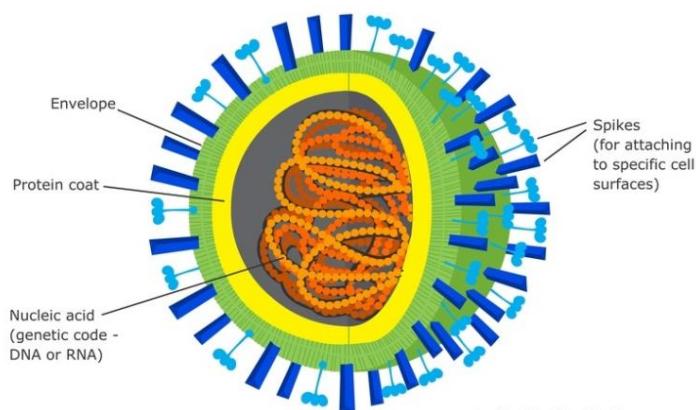


Figure 13: virus structure

The origins of viruses in the evolutionary history of life are not clear: some may have evolved from plasmids, pieces of DNA that can move between cells, while others may have evolved from bacteria.

In evolution, viruses are an important means of horizontal gene transfer, which increases genetic diversity. Some consider viruses to be a form of life, because they carry genetic

material, reproduce and evolve through natural selection. Viruses are grouped at different hierarchical levels of order, family, subfamily, genus and species on the basis of several properties including the morphology, the type of host, the chemical composition and the mode of replication. A virus family may consist of members that replicate only in vertebrates, only in invertebrates, only in plants, or only in bacteria however, certain families contain viruses that replicate in more than one of these hosts. Basic structural characteristics, such as genome type, virion shape and replication site, generally share the same features among virus species within the same family. Viruses that infect only bacteria are called a bacteriophage or simply a phage while viruses that infect animal or plant cells are referred to generally as animal viruses or plant viruses [126].

On the basis of structural characteristics, we might have:

- Five double-stranded DNA families: three are non-enveloped with icosahedral capsids (Adenoviridae, Papillomaviridae and Polyomaviridae) and two are enveloped (Herpesviridae and Poxviridae).

- One family of single-stranded DNA viruses that infect humans: Parvoviridae. These viruses are non-enveloped.

- One family of partly double-stranded DNA viruses: Hepadnaviridae (viruses are enveloped).

- Seven positive single-stranded RNA families: three non-enveloped (Astroviridae, Caliciviridae and Picornaviridae) and four enveloped (Coronaviridae, Flaviviridae, Retroviridae and Togaviridae). All the non-enveloped families have icosahedral nucleocapsids.

- Six negative single-stranded RNA families: Arenaviridae, Bunyaviridae, Filoviridae, Orthomyxoviridae, Paramyxoviridae and Rhabdoviridae. All are enveloped with helical nucleocapsids

- One family with a double-stranded RNA genome: Reoviridae.

- One family Anelloviridae and the genus Dependovirus.

- One additional virus (Hepatitis D virus) which has not yet been assigned to a family but is clearly distinct from the other families infecting humans.

Outside the host cell viruses are inert and are not able to generate energy. As obligated intracellular parasites, the replication phenomenon depends on the complicated biochemical machinery of the cell host. In the host cell, the virus releases its genome to allow its expression (transcription and translation) by the host cell [127]. In addition to being the causative agents of many diseases, viruses are important tools in cell biology research, particularly in macromolecular synthesis studies.

III.2.1. Viral infection

Viruses can infect all types of life forms, from animals to microorganisms and cause familiar infectious diseases such as cold, flu and warts. They also cause severe illnesses such as HIV/AIDS, smallpox, and Ebola. In human, viruses can affect many areas in the body, including the skin, brain, liver, reproductive, respiratory, and gastrointestinal systems.

Viruses can be transmitted in a variety of ways including sexual contact, contaminated objects, spread through touch, saliva, or even the air. In addition, some insects including ticks and mosquitoes viruses can act as "vectors," transmitting a virus from one host to another.

Skin conditions caused by viral infections include Herpes simplex (cold sores and genital herpes), Herpes zoster (shingles), Herpangina / vesicular stomatitis (oral ulcers), Molluscum contagiosum, viral warts (verrucae, genital warts or condylomas and squamous cell papillomas) and Milker's nodules. Viruses use three different routes to infect the skin: direct inoculation (papillomaviruses infect), regional spread from a specific internal focus (herpes infections), as well as systemic infection (varicella zoster infection).

Respiratory viral infections affect the lungs, nose, and throat and responsible virus include: Respiratory Syncytial Virus, influenza viruses, parainfluenza viruses, adenoviruses, and rhinoviruses. Rhinoviruses are the viruses that cause the common cold.

Sexually transmitted viral infections can be caused by some viruses such as:

- Herpes simplex virus-2 (HSV-2) causes genital herpes which is a common sexually transmitted infection. Herpes simplex virus-1 (HSV-1), the virus responsible for cold sores, can also causes genital herpes.

- The human immunodeficiency virus (HIV) is a virus that affects certain types of T cells in the immune system. The progression of the infection decreases the body's ability to fight disease and infection, leading to Acquired Immunodeficiency Syndrome (AIDS). HIV is transmitted by coming into contact with blood or bodily fluids of an infected person

- Human papillomavirus (HPV) causes genital warts or increases the risk of cervical cancer [128].

- Hepatitis B is a virus that causes inflammation in the liver. It is transmitted by contaminated blood and body fluids.

Food poisoning virus is a disease caused by eating or drinking food and/or water contaminated with viruses and includes:

- Norovirus is a gastrointestinal virus, also known as the "invernal vomiting virus" because the disease is more active in winter. However, norovirus can be contracted at any other time of the year.

- Hepatitis A virus usually transmitted person-to-person through the consumption of contaminated food or water or fecal-oral route,

- Rotavirus is the most common cause of diarrhoeal disease in infants and young children that can lead to dehydration [129].

Others types of viral infection are mononucleosis caused by epstein-Barr virus (EBV) which is herpes virus associated with fever, fatigue, swollen lymph nodes, and an enlarged spleen. The common transmission is widespread through saliva.

III.2.2. Viral infections and oxidative Stress

During infection by microorganisms such as viruses, microorganisms are detected, engulfed and then phagocytized by inflammatory cells including macrophages, neutrophils, and dendritic cells. Phagocytic cells produce reactive species by myeloperoxidase, NADPH oxidase, and nitric oxide synthase leading to an increased production of ROS and RNS. For this reason, expression of these enzymes serves as a suitable marker for inflammation which involves oxidative stress accompanied by alterations in antioxidants levels. These alterations, if unchecked, become deleterious to the cells and are responsible for acute or chronic oxidative stress that can lead to apoptotic cell-death and tissue damage. Some search shown that infections trigger the production of reactive oxygen (ROS) and nitrogen (RNS) species; in particular infections caused by the blood-borne hepatitis viruses (B, C, and D), human immunodeficiency virus (HIV), influenza A, Epstein-Barr virus and respiratory syncytial virus [130]. On the other hand, oxidative stress is a critical factor in the pathogenesis of a wide array of diseases, including neurodegenerative disorders such as Alzheimer's and Parkinson's diseases [6]. Infectious diseases too are likely associated with oxidative stress in a number of ways. Inflammation, organ damage combined with altered metabolism, and other factors such as iron overload in the case of hepatitis C are responsible for the development of oxidative stress in infected patients

However, the role of oxidative stress is not universally accepted by all researchers because it is plays a dual role in infections, thus ambiguities can be found in the literature [1].

IV. Focus on bioisosteric and isosteric concepts

The term isostere has a very broad meaning. It was introduced in 1919 by Langmuir, which states that isosteres are compounds (organic or inorganic) or groups of atoms having the same number of atoms and electrons. Examples: N_2 and CO, N_2O and CO_2 , N_3 - and NCO. He was then studied comparatively different molecules like N_3 - and NCO- or CO and N_2 and found that they have analogous physical properties. A further extension to the concept of isosteres came in 1925 by Grimm with “Hydride Displacement Law” and then in 1932 by Erlenmeyer which defines isosteres as atoms, ions or molecules in which the peripheral layers of electrons can be considered identical. Examples: atoms in the same column of the periodic table; Cl and CN and SCN and the -CH=CH- and -S- [131]. Pharmaceutical chemists exploited the extensive application of isosterism to modify of reference drug. These modifications gave rise to the bioisosterism term. Bioisostere was first defined in 1951 by Friedman as atoms or molecules that fit the broadest definition for isosteres and have the same type of biological activity. In drug design, this approach is now commonly used to optimize lead compound in order to:

- Improve selectivity.
- Reduce the side effects.
- Decrease toxicity.
- Improve pharmacokinetic i.e. absorption, distribution, metabolism and excretion (ADME) or pharmacodynamic i.e. receptor, enzyme or channel level behavior.
- Increase stability.
- Enhance the desired biological or physical properties of a compound without making significant changes in chemical structure [132].

IV.1. Bioisosteres in drug discovery

The development and application of bioisosteres in pharmaceutical industry have been adopted as a fundamental tactical approach useful to address a number of aspects associated with the design and development of drug candidates. Bioisosteres are mainly used to find hit and lead compounds by modifying known actives. Medicinal chemists have optimized the molecules by making relatively few changes to the structure taking into consideration their relevant properties such as size, shape, electronic properties, lipophilicity, pharmacophore characteristics, solubility and chemical reactivity. However, it is not always easy to perform bioisosteric modifications successfully because the chemical structure is an unreliable indicator of biological activity; small changes in a

molecule can have a profound impact on the activity, selectivity and pharmacokinetic parameters of the compound. Curiously, the chemically distinct entities can have almost identical biological activity profiles. Methods to identify bioisosteres are based on the fragment replacement, which consist to remove a portion of an active molecule, search a fragment database for a replacement moiety that will physically fit into the vacated space. Being an established and powerful concept in medicinal chemistry, the application of bioisosteres plays an important role in drug discovery and contributes to the productive application in the design and optimization of active compounds

IV.2. Classification of bioisosterism

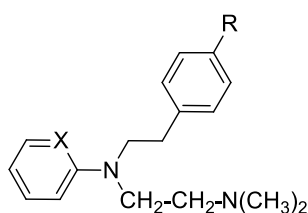
Bioisosteres have been classified into two broad categories: classical and non-classical. This classification depends on the degree of electronic and steric factors.

IV.2.1. Classical bioisosteres

Classical bioisosteres have been traditionally subdivided into five groups according to the degree of electronic and steric factors:

- (A) Monovalent atoms or groups example: Interchange of Hydroxyl and Amino Groups,
- (B) Divalent atoms or groups,
- (C) Trivalent atoms or groups,
- (D) Tetra-substituted atoms,
- (E) Ring equivalent.

Heterocyclic compounds are very important in medicinal chemistry; some of them are classified as ring equivalent bioisosteres. So, benzene and thiophene, thiophene and furan, and even benzene and pyridine exhibited similarities in many physical and chemical properties. In addition, the use of the classical bioisosteres benzene, thiophene, and pyridine resulted in analogues with retention of biological activity within different series of pharmacological agents. One of the successful uses of this modification resulted in the potent antihistamine Mepyramine which evolved by the replacement of the phenyl moiety in antegrin by a pyridyl group.



X = CH, R = H Antegrin X = N, R = OCH₃ Mepyramine

Figure 14: Bioisosteric ring equivalent

IV.2.2. Non-classical bioisosteres

Non-classical bioisosteres do not obey the steric and electronic rules and are divided into two groups: (A) rings vs noncyclic structures and (B) exchangeable functional groups [133].

Isosteres of carboxylic acid have been studied extensively since its replacement have typically focused on enhancing potency, reducing polarity, increasing lipophilicity (improve membrane permeability), enhancing pharmacokinetic properties and reducing the potential for toxicity.

Bioisosteric replacement of carbonyl or carboxylic group include: $-\text{COOH}$, $-\text{SO}_2\text{NH}_2$, $-\text{HCONH-}$, $-\text{COOR}$, $-\text{CONH}_2$, $-\text{CO}_2-$, $-\text{SO}_3\text{H}$, $\text{PO}(\text{OH})\text{NH}_2$, $-\text{F}$, NHCO- , $-\text{ROCO-}$ and Tetrazole.

Examples: replacement of $-\text{COOH}$ group in *para*- amino benzoic acid (PABA) by $-\text{SO}_2\text{NH}_2$ gives sulfanilamide (important class of antibacterial drugs) [133].



Figure 15: Bioisosteric relationship between $-\text{COOH}$ and sulfonamide group

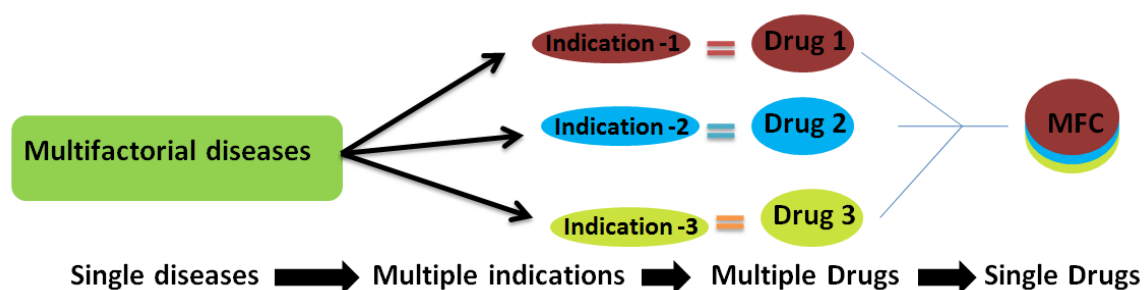
The replacement of $-\text{COOH}$ in γ -aminobutyric acid (GABA) by tetrazole group, resulting a tetrazole bioisostere of GABA, a potent antiepileptic agent.



Figure 16: Bioisosteric relationship between $-\text{COOH}$ and tetrazole group

V. Aim of work

Multifactorial diseases such as cancer, diabetes, Alzheimer's disease and Parkinson's disease are caused by a combination of genetic and / or environmental factors. These diseases have an extremely complex etiopathology and involve two or more physiopathological indications. However, it is not always easy to find drugs that can act on different sites. Over time, various strategies have evolved for effective treatment that includes cocktails and combined drugs. Although these approaches have improved patient compliance, side effects are considerable. As a result, the model is now moved to the design of a single chemical entity with multiple biological activities called multifunctional compounds (**Scheme 5**).



Scheme 5: *Multifunctional compounds*

In recent years, strategies based on the development of multifunctional compounds are attracting more and more attention from researchers as they are effective in the treatment of complex diseases that one of the main causes is oxidative stress. Oxidative stress is a deleterious process that can be a major mediator of damage to cellular structures, including lipids and membranes, proteins, and DNA leading to many chronic human diseases. For this reason it is important to protect or prevent body against free radical. In order to explore the possibility of a multi-target approach, we have taken into account that oxidative stress can be inducing by UV radiation and infection.

To this aim, our interest was in developing new compounds provided with UV-filter, antioxidant, antifungal and antiproliferative activities. To realize our project, we have chosen 2-Phenyl-1H-benzimidazole-5-sulphonic acid (a commercial UVB filter) as lead compound because it is easily modifiable and more, it has one of the investigated activities. Isosteric modification was the key tool for this study because it is a pharmaceutical chemistry strategy for the rational design of new drugs, applied with a lead compound. Its success in the development of new substances has observed significant growth in distinct therapeutic classes as widely used by the pharmaceutical industry to discover new

analogues of commercially interesting therapeutic innovations. In view of this, isosteric modifications have been carried out on PBSA, in particular position 1 and 4/6 to obtain respectively benzothiazole and imidazopyrimidine nucleus. PBSA was also modified on position 2 by introducing (poly)phenol ring or 5-membered ring on the phenyl ring and by substituting the functional group in position 5 of the benzimidazole ring with $-\text{COOH}$, $-\text{SO}_2\text{NH}_2$ and $-\text{H}$ (**Figure 17**).

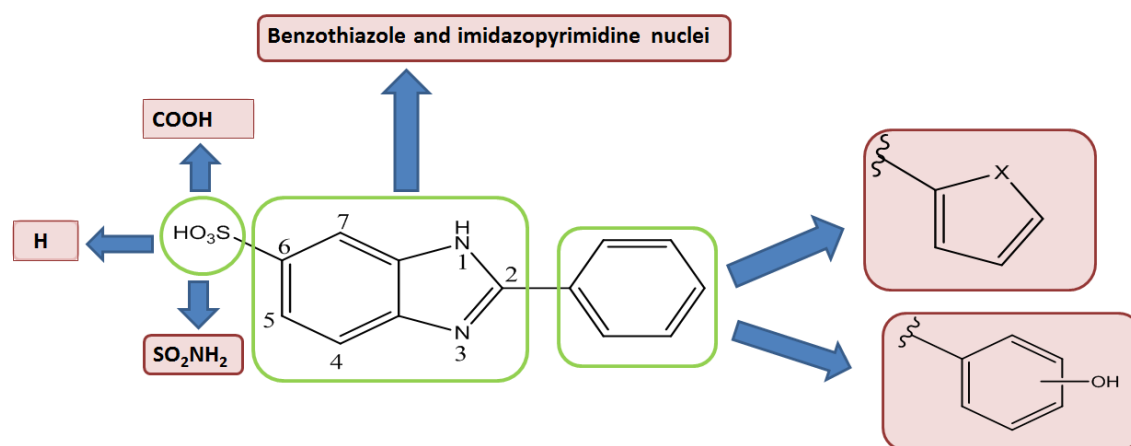


Figure 17: Modification of 2-Phenyl-1H-benzimidazole-5-sulphonic acid

VI. Results and discussion

Isosteric modification has been the key strategy for this study since that it is a commonly used approach in medicinal chemistry for the rational design of new drugs starting with a lead compound. To this purpose, PBSA was modified on benzimidazoles scaffold (in position 1, 2, 4 and 6) and phenyl ring as following:

- Modification in position 2 of benzimidazole, through isosteric substitution of phenyl ring by 5-membered ring; sulfonic acid moiety in position 5 was changed by -COOH or -H to obtain benzimidazole derivatives (**Figure 18**);

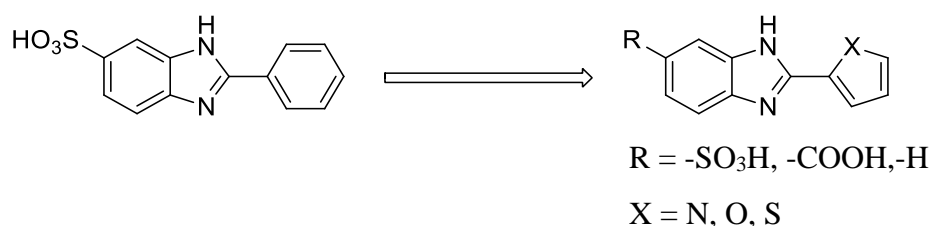


Figure 18: *Benzimidazole derivatives*

- Modification in position 1 of benzimidazole ring via isosteric substitution of nitrogen atom with sulfur atom to obtain benzothiazole nucleus, then in position 5, sulfonic acid moiety was replaced by -H, -COOH or -SO₂NH₂ and finally introduction of hydroxyl functional groups on phenyl ring to obtain benzothiazole derivatives (**Figure 19**);

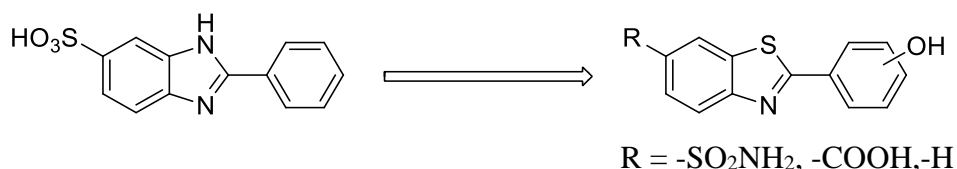


Figure 19: *Benzothiazole derivatives*

- Modification in position 4 and 5 by isosteric substitution of -CH- with -N- atom to obtain imidazolepyrimidine nucleus and introduction of hydroxyl functional groups on phenyl ring to obtain imidazopyrimidine (purine) derivatives (**Figure 20**).

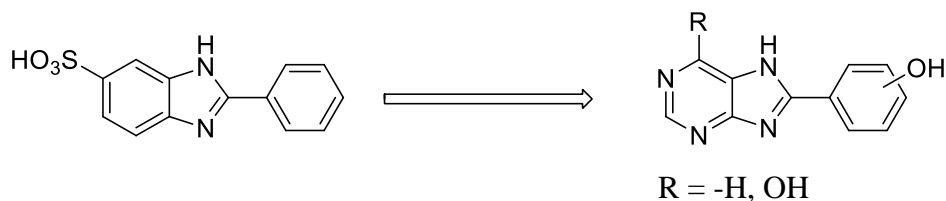
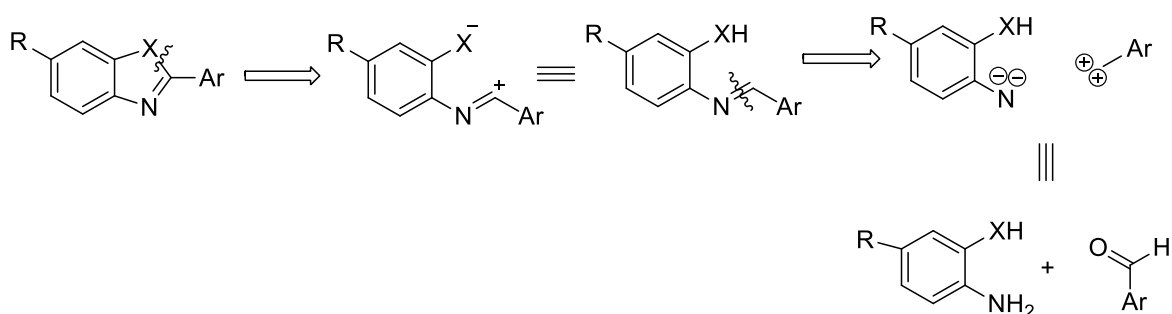


Figure 20: *Imidazopyrimidine derivatives*

All of these modifications led to the synthesis of a library of compounds which were then evaluated for their UV-filter, antioxidant, antifungal and antiproliferative activities.

First of all, the disconnection was made in order to get an idea about the starting reagents. Thus, an alternative retrosynthetic analysis for desired compounds is proposed (**Scheme 6**). Disconnection on 5- membered ring could lead to amino benzyl derivatives and aromatic aldehyde.



Scheme 6: Retrosynthetic pathway for desiderate compounds

VI.1. Benzimidazole derivatives

VI.1.1. Chemistry

Various modifications have been made to the PBSA in order to improve its UV filter potency and also confer on it other activities with the aim to obtain multifunctional compounds. For this purpose, the phenyl ring was replaced by 5-membered rings (pyrrole, thiophene and furan) which are isosteres of benzene. Sulfonic acid moiety in position 5 of the benzimidazole ring also was modified by carboxylic acid and hydrogen.

The synthesized compounds were classified into three groups, which have the same substituents in position 2 of the benzimidazole ring, but differ for the substituent in position 5.

- The first group maintains the sulfonic acid group in position 5 of the benzimidazole ring while the phenyl group is replaced by 5-membered rings.

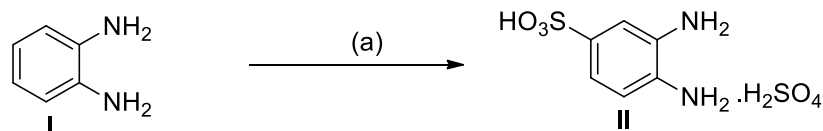
- The second group includes compounds substituted with carboxylic acid in position 5 of the benzimidazole ring and present 5-membered rings in position 2.

- The third group has no functional group on the benzimidazole ring and has 5-membered rings in position 2.

In the literature, several procedures are described for the synthesis of benzimidazole ring including condensation reaction of *o*-diaminobenzenes with carboxylic acids or its derivatives in the presence of oxidizing agent as catalyst [134]. After evaluation, we turned our attention to a method that allows to obtain desired compounds with good yield, at low

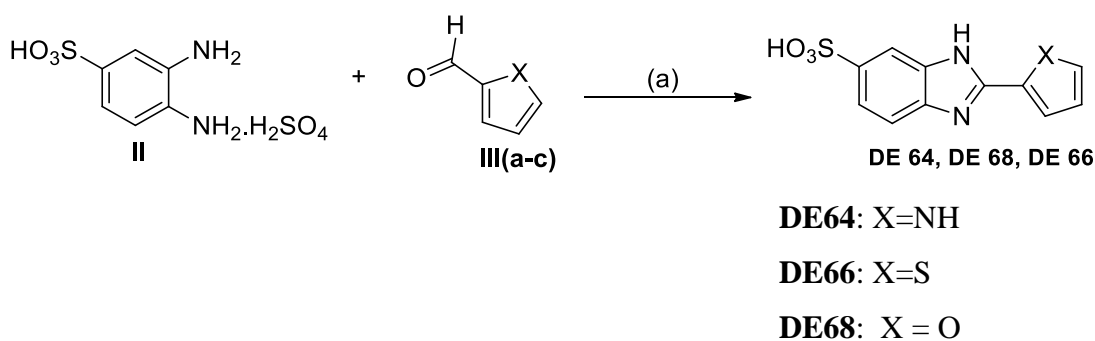
cost and in short times. This method consists in reacting the diamine and aldehyde in ethanol in the presence of Sodium bisulfite.

Compounds of group 1 were synthesized in two steps. The first step consisted to synthesize 3,4-diaminobenzenesulfonic acid (**II**) via sulfonation reaction from *o*-phenylenediamine (**I**) in the presence of concentrated sulfuric acid 95% (**Scheme 7**).



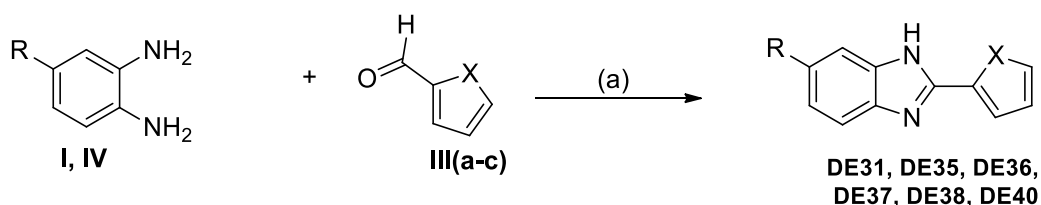
Scheme 7: Synthesis of compounds **II**. Reagents and conditions: (a) H_2SO_4 , reflux for 24h

Then, compound **II** was condensed with corresponding aldehydes following the modified procedure described in literature [134] (**Scheme 8**).



Scheme 8: Synthesis of 2-substitutedbenzimidazole-6-sulfonic acid. Reagents and conditions: (a) EtOH, NaHSO₃ in H₂O, Reflux

Compounds of groups 2 and 3 were synthesized in one step using respectively commercial 3,4-diaminobenzoic acid (**IV**) and *o*-phenylenediamine (**I**) with corresponding aldehydes following the same strategy reaction described below (**Scheme 9**).



Compound	R	X	Compound	R	X
DE 31:	H	S	DE 40:	COOH	S
DE 35:	H	NH	DE 36:	COOH	NH
DE 37:	H	O	DE 38:	COOH	O

Scheme 9: Synthesis of 2-substitutedbenzimidazole-6-carboxylic acid and 2 substituted benzimidazole. Reagents and conditions: (a) EtOH, NaHSO₃ in H₂O, Reflux

For a better discussion of the results, synthesized compounds are divided into three classes (Table 3). In each class the compounds are equally substituted in position 2 of the benzimidazole ring but with different substituents in position 6.

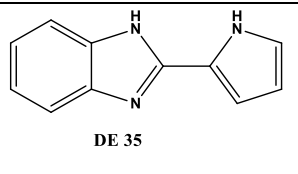
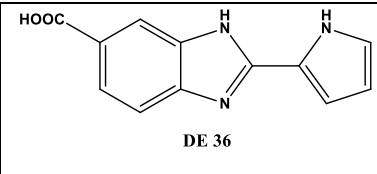
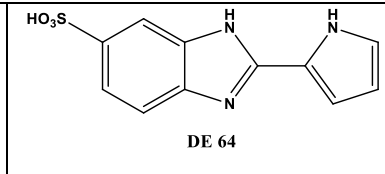
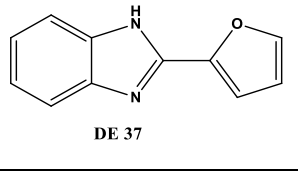
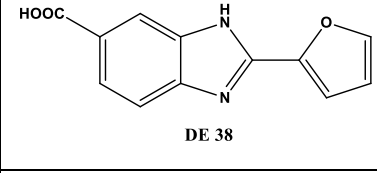
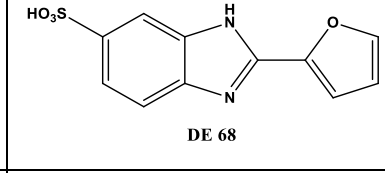
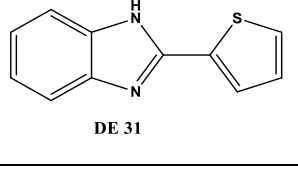
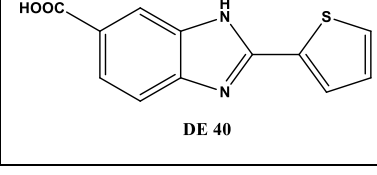
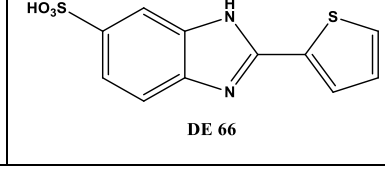
Class A	 DE 35	 DE 36	 DE 64
Class B	 DE 37	 DE 38	 DE 68
Class C	 DE 31	 DE 40	 DE 66

Table 3: Three classes of benzimidazole derivatives

VI.1.2. Biological evaluations

VI.1.2.1. Photoprotective activity

The spectral behavior of the test compounds dissolved in methanol was investigated firstly because the solar protection is related to the UV absorption. Absorption spectra were measured from 290 to 400 nm. Compounds **DE 35**, **DE 37** and **DE 31** have similar lamda max, however lamda max of **DE 31** is slightly higher than that of **DE 37**, which in turn is

slightly greater than that of **DE 35**. Substitution of -H by withdrawing group (-COOH and -SO₂NH₂) at the 6 position on the benzimidazole ring shown the bathochromic shift (**Figure 21**). This long wavelength absorption band is associated with the intramolecular charge transfer transition due to the transfer of the charge between the five-membered rings to the electron-withdrawing of benzimidazole and neighboring carboxylic or sulfonamidic chromophore.

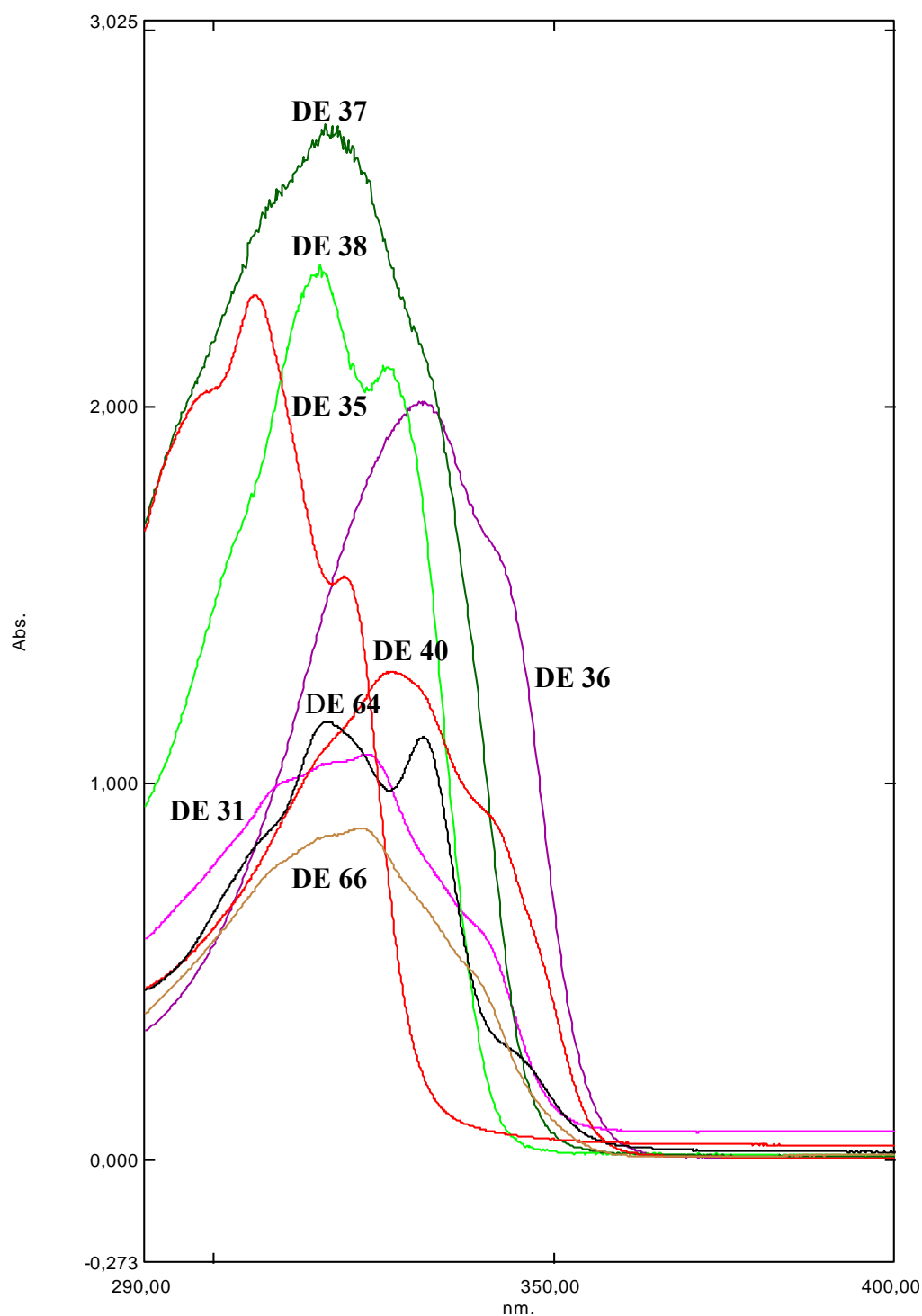


Figure 21: Spectral data of benzimidazole derivatives

Sun Protection Factor (SPF) is the UV energy required for producing a minimal erythema dose (MED) on protected skin, divided by the UV energy required producing a MED on unprotected skin. Therefore it is the theoretical amount of time we can stay in the sun without getting sunburned. This factor was first introduced in 1974 to evaluate the effectiveness of a sunscreen, only the *in vivo* method was officially accepted by the US Food and Drug Administration, and COLIPA. Due to the high cost, time consumption and some questions noble of the volunteers relating to *in vivo* SPF determination, *in vitro* photoprotection studies have been developed. The broadly applied *in vitro* method is the well-known Diffey-Robson approach [135] that is a spectrophotometrically-based measurement of transmission. The photoprotective activity of the synthesized compounds in methanol solution is shown in **Table 4**. Spectral data of samples were collected from 290 - 400 nm with the calculator software [136]. The software automatically determines theoretical COLIPA – SPF, COLIPA – UVAPF, critical wavelength value (λ_c) (see **Equation 2**, **Equation 3** and **Equation 4**) and UVA/UVB ratio as preliminary data.

Photoprotective activity of the sunscreen against UVB is reflected by SPF value. According to the results shown in **Table 4**, SPF values of all synthesized compounds was high compared to lead compound (PBSA) and the highest SPF value was **DE 37** characterized by the presence of furan in position 2 of the benzimidazole ring and without functional group in position 6. By maintaining -SO₃H group in position 6 and substituting the phenyl by the pyrrole, SPF value is increased. However, by maintaining the pyrrole and replacing -SO₃H with -COOH (**DE 64** vs **DE 36**), SPF is again increased. Then, substituting the functional group by an -H (**DE 36** vs **DE 35**), SPF is exponentially increased. The same results were obtained by replacing phenyl with thiophene (**PBSA** vs **DE 66**, **DE 40**, **DE 31**) and furan (**PBSA** vs **DE 68**, **DE 38**, **DE 37**). So, the photoprotective activity against the UVB radiations of the synthesized compounds does not depend only on the substitution in the 2-position of the benzimidazole ring, but also on the groups present in position 6. Therefore the structure activity relationship is: -H > -COOH > -SO₃H.

Moreover replacing the pyrrole with the furan (**DE 35** vs **DE 37**), the SPF value is increased. On the other hand, by substituting the pyrrole with thiophene, the SPF is decreased, for example **DE 35** vs **DE 31** SPF value of 13.13 to 7.03 respectively. Thus, by keeping the group present in the 6-position of benzimidazole and by varying the 5-membered ring at 2-position, the order of protection against UVB is as follows: furan > pyrrole > thiophene.

Protection against UVA rays was gave by UVA-PF which is considered efficient if it is greater than or equal to 1/3 of SPF. Given the obtained data, all the synthesized compounds

had UVA-PF values higher than that of the reference compound, but these values remained less than 1/3 of the SPF. Therefore, the synthesized compounds are not potential candidates for UVA protection.

Critical wavelength is the parameter that provides information on the broad-spectrum of UV-filter. It is classified in five numerical categories: 0 ($\lambda_c < 325$ nm), 1 ($325 \leq \lambda_c \leq 335$), 2 ($335 \leq \lambda_c \leq 350$), 3 ($350 \leq \lambda_c < 370$) and 4 ($\lambda_c \geq 370$). FDA considers the broad-spectrum sunscreen product should have a $\lambda_c \geq 370$ nm [137]. Based on this classification, none of the synthesized compounds showed a value of $\lambda_c \geq 370$ so they do not have a broad-spectrum profile.

In short, modifications on PBSA in position 2 by 5-membered rings and in position 6 by -COOH and -H led to enhanced UVB-filter activity.

Class	Compound	SPF	UVA-PF	UVA/UB	λ_c
	PBSA	3.40± 0.17	1.03± 0.08	0.29	322
A	DE 35	13.13± 0.70	1.16± 0.05	0.02	325
	DE 36	7.4± 0.23	1.10± 0.09	0.7	345
	DE 64	5.34± 0.39	1.22± 0.03	0.2	345
B	DE 37	20.06± 3.04	1.05± 0.06	0.3	333
	DE 38	16.66± 1.21	1.20± 0.10	0.5	332
	DE 68	10.96± 0.54	1.33± 0.05	0.29	342
C	DE 31	7.03± 0.42	1.49± 0.07	0.37	345
	DE 40	6.40± 0.12	1.42± 0.11	0.43	342
	DE 66	4.72± 0.17	1.43± 0.09	0.48	339

Table 4: Filtering activity of benzimidazole derivatives

VI.1.2.2. Antioxidant activity

The *in vitro* antioxidant potential of all the synthesized compounds was assessed by their ability to scavenge the stable radical 2,2-diphenyl-1-picrylhydrazyl (DPPH) through DPPH test and their ability to reduce ferric ions to ferrous ions via Ferric reducing antioxidant power (FRAP) test.

VI.1.2.2.1. DPPH test

The DPPH test allows to evaluate the antioxidant activity of the compounds against the DPPH radical which is a stable nitrogen-centered free radical.

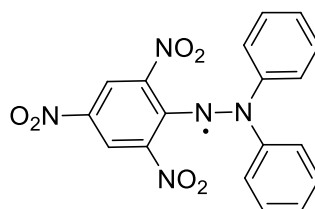
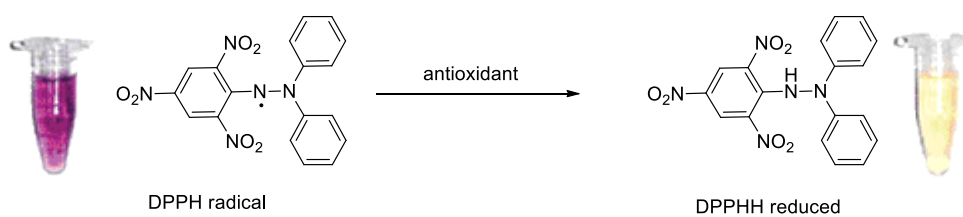


Figure 22: *1,1-diphenyl-2-picryl-hydrazyl radical*

The solution of DPPH radical is characterized by a deep purple color which changes to assume the pale yellow color in the presence of an antioxidant agent followed by the formation of DPPH.

This test is based on the determination of the reducing capacity of antioxidants against the radical DPPH at a wavelength of 517 nm, with a UV-visible spectrophotometer. In fact, DPPH radical is characterized by an absorption maximum at 517 nm that decreases in the presence of electron or hydrogen donor molecules.



Scheme 10: *Scavenger DPPH by an antioxidant compound*

The antioxidant power is then determined by measuring the decrease in absorbance of the DPPH radical at a wavelength of 517 nm after reaction with the test samples and the percentage of DPPH radical remaining is calculated using **Equation 5**.

Equation 5: DPPH radical-scavenging capacity (%) = $[1 - (A_1 - A_2) / A_0] \times 100\%$

Where A_0 was the absorbance of the control (without sample), A_1 was the absorbance in the presence of the sample, and A_2 was the absorbance without DPPH.

Then, the linear regression plots is carried out for calculating the effective concentration of the sample required to scavenge 50% of DPPH free radicals (IC_{50}).

From the results reported in **Table 5**, the reference compound is almost devoid of any antioxidant activity and the substitution of phenyl in the 2- position of benzimidazole by 5-membered rings gave the molecule an antioxidant activity more or less significant. To this effect, by substituting the phenyl with pyrrole (**DE 64**), a 53% inhibition of the DPPH radicals was observed. However, replacing the phenyl with furan (**DE 68**) or thiophene

(DE 66), inhibitions of 10.96 and 12.52% were respectively observed. Thus, the activity-structure relationship could be pyrrole >>thiophene \cong furan.

Replacing $-\text{SO}_3\text{H}$ with $-\text{COOH}$ and keeping pyrrole in position 2 (DE 64 vs DE 36), the scavenger activity is decreased. On the contrary, substituting with $-\text{H}$ (DE 64 vs DE 35), the activity is increased. However, keeping furan or thiophene and replacing $-\text{SO}_3\text{H}$ with $-\text{COOH}$ or $-\text{H}$ (compounds of class B and C) the activity is increased.

Compounds having a percent inhibition greater than or equal to 50% were screened to determine their IC_{50} and only DE 35 showed an acceptable value, $\text{IC}_{50} = 64.098 \mu\text{g/ml}$. This could be explained by the fact that DE 35 is the only compound in the series having the hydrogen-donating group.

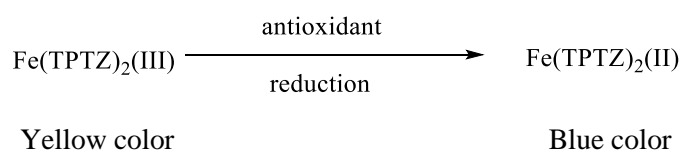
Class	Compound	DPPH (% inhibition)	DPPH IC_{50} ($\mu\text{g/ml}$)
	PBSA	< LOQ*	-
A	DE 35	70.00 \pm 3.25	64.098 \pm 3.21
	DE 36	33.00 \pm 1.28	2293.66 \pm 14.63
	DE 64	53.88 \pm 2.30	1093.09 \pm 8.65
B	DE 37	15.46 \pm 0.98	-
	DE 38	52.06 \pm 1.48	1416.38 \pm 21.40
	DE 68	10.96 \pm 0.56	-
C	DE 31	35.05 \pm 0.87	13163.00 \pm 55.84
	DE 40	30.23 \pm 1.45	1403.4 \pm 6.47
	DE 66	12.52 \pm 0.88	-

(- not tested)

Table 5: Antioxidant activity of the compounds through DPPH test. Each value was obtained from three different experiments (mean \pm SEM).

VI.1.2.2.2. FRAP Test

FRAP assay is the method developed to measure plasma antioxidant power. This method is also used to evaluate the antioxidant activity of pure or mixture compounds and it is based on the rapid reduction in ferric-tripyridyl-triazine (Fe^{III} -TPTZ) by antioxidants present in the samples forming ferrous-tripyridyl-triazine (Fe^{II} -TPTZ) (Scheme 11)



Scheme 11: Reduction of Fe^{3+} -TPTZ complex by antioxidant compound

In the presence of an antioxidant, the Fe^{3+} -TPTZ complex is reduced to the Fe^{2+} form and an intense blue color with an absorption maximum at 593 nm is observed. This antioxidant activity is determined by measuring the change in absorbance at 593 nm using Trolox as the standard for the calibration, then results are given as micromoles of Trolox per gram of sample.

Data obtained are shown in **Table 6**. Compounds **DE 35** and **DE 37** respectively characterized by the presence of pyrrole and furan in position 2 of the benzimidazole ring and both lacking a functional group in position 6 showed the good antioxidant profile. Whereas compound **DE 37** displayed the best activity (4462.64 $\mu\text{molT/g}$). By substituting furan with thiophene (**DE 37** vs **DE 31**), the activity is decreased exponentially. Therefore the activity-structure relationship could be furan > pyrrole >> thiophene.

Class	Compound	FRAP ($\mu\text{molT/g}$)
	PBSA	< LOQ*
A	DE 35	1085.57 \pm 0.88
	DE 36	108.89 \pm 2.98
	DE 64	239.912 \pm 1.79
B	DE 37	4462.64 \pm 18.29
	DE 38	26.67 \pm 2.89
	DE 68	< LOQ*
C	DE 31	75.89 \pm 5.43
	DE 40	181.84 \pm 2.66
	DE 66	82.16 \pm 0.22

LOQ* limit of quantification

Table 6: Antioxidant activity of the compounds through FRAP test. Each value was obtained from three different experiments (mean \pm SEM).

VI.1.2.3. Antifungal activity

VI.1.2.3.1. Anti-dermatophytes activity

Synthesized benzimidazole derivatives were investigated for their antifungal activity against five dermatophytes (*Microsporum gypseum*, *Microsporum canis*, *Trichophyton mentagrophytes*, *Trichophyton tonsurans* and *Epidermophyton floccosum*). Inhibition of the dermatophytes was evaluated by diffusion method in Sabouraud Dextrose Agar (SDA), using DMSO as a solvent. The rate of growth inhibition of dermatophytes was determined daily by measuring the diameter of the colony on each disk and the results determined as the average of three different experiments. All compounds were tested at the same concentration, namely 100 µg/mL and the results are shown in **Table 7**. For each class, compounds without functional group in position 6 of the benzimidazole ring (**DE 31**, **DE 35** and **DE 37**) showed good activity on all five dermatophytes with percent of inhibition more or less equal to 100%. Then, followed by compounds bearing -SO₃H with an inhibition range of 50-79%, except **DE 68** which did not have activity. Finally compounds with -COOH which did not have a significant activity on dermatophytes; on the contrary they rather favor the growth of certain fungi. Thus, the activity- structure relationship could be -H > -SO₃H >> -COOH. In addition, the presence of pyrrole, thiophene and furan in position 2 of the benzimidazole ring has no influence on the variability of the activity this is confirmed by Friedman which states that the bioisosteres have similar biological activity [131]. Interestingly, compounds **DE 31**, **DE 35** and **DE 37** displayed fungicide activity on all five dermatophytes at 100 µg/mL.

Class	Compound	<i>M. gypseum</i>	<i>M. canis</i>	<i>T. mentagrophytes</i>	<i>T. tonsurans</i>	<i>E. floccosum</i>
A	DE 35	99.07 ± 1.33	96.85 ± 3.56	96.26 ± 2.42	96.97 ± 0.62	101.75 ± 4.92
	DE 36	3.74 ± 1.49	8.66 ± 1.78	+	4.55 ± 1.34	21.05 ± 2.14
	DE 64	73.04 ± 3.67	72.11 ± 7.51	69.03 ± 1.84	56.58 ± 4.04	52.46 ± 6.58
B	DE 37	99.00 ± 0.28	98.32 ± 2.03	97.22 ± 4.53	94.74 ± 5.63	97.87 ± 4.23
	DE 38	+	18.72 ± 0.59	+	+	6.45 ± 1.47
	DE 68	8.00 ± 2.44	+	+	+	+
C	DE 31	100 ± 1.63	92.91 ± 1.33	98.13 ± 2.76	96.97 ± 1.34	94.74 ± 5.45
	DE 40	2.14 ± 0.59	20.30 ± 0.54	+	4.48 ± 0.90	6.45 ± 2.98
	DE 66	59.80 ± 6.12	65.91 ± 3.21	57.27 ± 1.09	50.75 ± 2.11	50.00 ± 3.26

+ the compound stimulates the growth of the fungus

Table 7: Percent growth inhibition of dermatophytes treated with the benzimidazole derivatives at 100 µg/mL. Each value was obtained from three different experiments (mean ± SEM).

From this first screening, compounds with percent inhibition close to 100% were further investigated by the determination of IC₅₀ which represents the concentration of the compound required to inhibit 50% of the growth of the fungus. The IC₅₀ results of **DE 31**, **DE 35** and **DE 37** against 5 dermatophytes are listed in **Table 8**, in comparison with the of the well-known antifungal agents Fluconazole and Econazole nitrate. The benzimidazole derivatives are very potent on *M. gypseum*, *M. canis*, *T. mentagrophytes*, *T. tonsurans* and *E. floccosum* with IC₅₀ values in the range of 0.97-3.80 µg/mL. All tested compounds are more active than Fluconazole, except on *E. floccosum*; however, they are less effective than Econazole nitrate. Compound **DE 35** showed the best activity, with IC₅₀ values on dermatophytes in the range 0.97-1.53 µg/mL.

Compound	IC ₅₀ (µg/mL)				
	<i>M. gypseum</i>	<i>M. canis</i>	<i>T. mentagrophytes</i>	<i>T. tonsurans</i>	<i>E. flocco sum</i>
DE 31	1.55 ± 0.03	2.14 ± 0.09	1.74 ± 0.11	2.42 ± 0.15	3.80 ± 0.07
DE35	1.53 ± 0.05	1.34 ± 0.02	1.38 ± 0.08	0.97 ± 0.06	1.07 ± 0.03
DE37	1.54 ± 0.02	1.58 ± 0.06	1.61 ± 0.10	1.89 ± 0.22	2.44 ± 0.05
Fluconazole	18.5 ± 1.23	29.6 ± 1.84	3.53 ± 0.26	19.41 ± 0.87	0.08 ± 0.005
Econazole nitrate	0.05 ± 0.0001	0.51 ± 0.02	0.006 ± 0.0001	0.13 ± 0.008	0.47 ± 0.015

Table 8: Concentration of the compound required to inhibit 50% of the growth of fungus.

Each value was obtained from three different experiments (mean ± SEM).

VI.1.2.3.2. Antifungal activity on *Candida albicans*

The antifungal activity of the synthesized compounds was also determined against *Candida albicans* (ATCC 10231). Minimal inhibitory concentration (MIC) of the synthesized agents was determined by broth microdilution method using RPMI 1640 + MOPS. The concentration of this strain ranged from 0.25 µg·mL⁻¹ to 12.48 µg·mL⁻¹. The growth in the tube was observed visually for turbidity and inhibition was determined by the absence of growth. MIC was determined by the lowest concentration of the sample that prevented the development of turbidity. The results shown in **Table 9** are representative of 24 hours of incubation arranged in triplicate. Compounds **DE 38**, **DE 40**, **DE 64** and **DE 66** showed activity against *Candida albicans*. Only **DE 38** and **DE 40** exhibited good activity (MIC = 16 µg/mL). It is important to note that, contrary to the results observed on dermatophytes, the non-substituted compounds in position 6 of benzimidazole have no activity on the yeasts. This can be explained by the fact that each fungus has its own morphology and defense systems.

Class	Compound	<i>Candida albicans</i> (MIC $\mu\text{g/mL}$)
A	DE 35	-
	DE 36	-
	DE 64	64
B	DE 37	-
	DE 38	16
	DE 68	-
C	DE 31	-
	DE 40	16
	DE 66	64

Table 9: *Anti-Candida albicans* activity of synthesized compounds. The antibacterial tests were carried out three times, and the average values were taken as the MICs.

VI.1.2.4. Antiviral activity

Antiviral activity was tested against herpes simplex virus-1 (KOS), herpes simplex virus-2 (G), herpes simplex virus-1 TK-KOS ACVr, vaccinia virus, Adeno virus-2 and Human Coronavirus (229E) in HEL cell cultures; vesicular stomatitis virus, Coxsackie virus B4, Respiratory syncytial virus in HeLa cell cultures. Cytotoxicity of compounds was evaluated in parallel with the antiviral activity namely, microscopic evaluation of the cell morphology of the confluent cell monolayer which either had or had not been inoculated with virus. Cytotoxic concentration and concentration producing 50% inhibition of virus-induced cytopathic effect were determined by measuring the cell viability with the colorimetric formazan-based MTS. Reference compounds used were: Brivudin, Cidofovir, Ganciclovir, Acyclovir for virus in HEL cell cultures and ribavirin and DS-10.000 for virus in HeLa cell cultures. The antiviral activity of the compounds is expressed as the concentration required to inhibit viral cytopathogenicity by 50% (EC_{50}) and results are shown in **Tables 10-11**. None of the synthesized compounds showed specific antiviral activity.

Class	Compound	Cytotoxic concentration ^a (μM)	Antiviral EC ₅₀ ^b (μM)					
			Herpes simplex virus-1 (KOS)	Herpes simplex virus-2	Herpes simplex virus-1 TK-KOS ACVr	Vaccinia virus	Adeno virus-2	Human Coronavirus (229E)
A	DE 35	>100	>100	>100	>100	>100	>100	>100
	DE 36	>100	>100	>100	>100	>100	>100	>100
	DE 64	>100	>100	>100	>100	>100	>100	>100
B	DE 37	>100	>100	>100	>100	>100	>100	>100
	DE 38	>100	>100	>100	>100	>100	>100	>100
	DE 68	>100	>100	>100	>100	>100	>100	>100
C	DE 31	>100	>100	>100	>100	>100	>100	>100
	DE 40	>100	>100	>100	>100	>100	>100	>100
	DE 66	>100	>100	>100	>100	>100	>100	>100
Brivudin		>250	0,01	250	0,1	5,8	-	-
Cidofovir		>250	4,5	3,4	2,8	50	10	-
Acyclovir		>250	0,6	0,6	2	>250	-	-
Ganciclovir		>250	0,01	0,01	0,2	>100	-	-

^a50% Cytotoxic concentration, as determined by measuring the cell viability with the colorimetric formazan-based MTS assay. ^bconcentration producing 50% inhibition of virus-induced cytopathic effect, as determined by as determined by the MTS method.-not detected

Table 10: Cytotoxicity and antiviral activity of compounds in human embryonic lung (HEL) cell cultures

Class	Compound	Cytotoxic concentration ^a (μM)	Antiviral EC ₅₀ ^b (μM)		
			Vesicular stomatitis virus	Coxsackie virus B4	Respiratory syncytial virus
A	DE 35	>100	>100	>100	>100
	DE 36	>100	>100	>100	>100
	DE 64	>100	>100	>100	>100
B	DE 37	>100	>100	>100	>100
	DE 38	>100	>100	>100	>100
	DE 68	>100	>100	>100	>100
C	DE 31	>100	>100	>100	>100
	DE 40	>100	>100	>100	>100
	DE 66	>100	>100	>100	>100
DS-10.000		>100	>100	>100	0,8
Ribavirin		>250	112	250	10

^a50% Cytotoxic concentration, as determined by measuring the cell viability with the colorimetric formazan-based MTS assay.

^bconcentration producing 50% inhibition of virus-induced cytopathic effect, as determined by measuring the cell viability with the colorimetric formazan-based MTS assay.

Table 11: Cytotoxicity and antiviral activity of compounds in HeLa cell cultures

VI.1.2.5. Antiproliferative activity

Antiproliferative activity of benzimidazole derivatives against human T-lymphocyte cells (CEM), human cervical carcinoma cells (HeLa), human pancreatic carcinoma cells (Mia Paca-2) and human melanoma cells (SK-Mel 5) was evaluated. According to the obtained results (Table 12), none of the tested compounds showed a specific antiproliferative activity except the **DE35** compound, which displayed good activity against SK-Mel 5 with $IC_{50} = 9.7 \mu\text{M}$ but having discrete selectivity index (SI= 3.20).

Class	compound	IC_{50} (μM)					SI			
		CEM	HeLa	Mia-Paca2	SK-Mel5	Hek293	CEM	HeLa	Mia-Paca2	Sk-Mel5
A	DE 35	14 \pm 1	37 \pm 0	15 \pm 9	9.7 \pm 1.7	31 \pm 3	2.21	-	2.07	3.20
	DE 36	> 100	> 100	> 100	> 100	> 100	-	-	-	-
	DE 64	31 \pm 21	\geq 100	28 \pm 10	> 100	67 \pm 47	2.16	-	2.39	-
B	DE 37	ND ^[a]	ND ^[a]	ND ^[a]	ND ^[a]	ND ^[a]				
	DE 38	75 \pm 35	> 100	> 100	> 100	> 100	1.33	-	-	-
	DE 68	> 100	\geq 100	\geq 100	\geq 100	> 100	-	-	-	-
C	DE 31	> 100	> 100	\geq 100	86 \pm 17	> 100	-		-	1.16
	DE 40	50 \pm 10	> 100	80 \pm 12	> 100	> 100	2	-	1.25	-
	DE 66	34 \pm 2	> 100	43 \pm 34	> 100	\geq 100	2.94	-	2.33	-

^[a]not detected

Table 12: Inhibitory effects of benzothiazole derivatives on the proliferation of CEM, HeLa, Mia Paca-2 and SK-Mel 5

VI.2. Benzothiazole derivatives

Benzothiazole and its derivatives are known to be very important intermediates for their biological activities such as anti-diabetic, Alzheimer's disease, antimicrobial, anthelmintic, anticancer, analgesic, anticonvulsant, trypanocidal, antifungal, neuroprotective and anti-inflammatory [139]. For these reasons, benzothiazole scaffold is attractive for development of multifunctional compounds

VI.2.1. Chemistry

In this part, modifications of the lead compound PBSA were applied to obtain benzothiazole derivatives. To this purpose, benzimidazole ring was modified by replacing

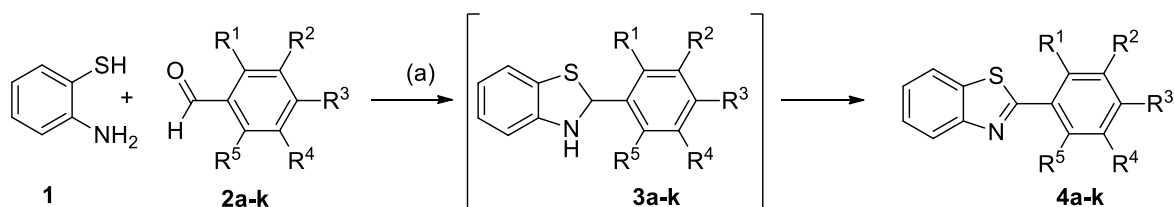
nitrogen in position 1 by sulfur and in position 5, sulfonic acid moiety was changed by -COOH or -H. The phenyl ring was modified by introducing hydroxyl groups, in different position of the ring.

To achieve this goal we turned our attention on the synthesis procedures reported in literature. Several methods of the synthesis of benzothiazole derivatives have been described including the condensation reaction of 2-aminothiophenol with substituted nitriles, carboxylic acids, aldehydes, acyl chlorides or esters [138]. The 2-aminothiophenol reacts first with reagents noted above to give a thiol substituted Schiff's base which then cyclizes in presence of various oxidants to give the desired benzothiazole derivative. Some oxidizing agents, such as polyethylene glycol-400, sodium hydrosulfite ($\text{Na}_2\text{S}_2\text{O}_4$), TMSCl , $\text{H}_2\text{O}_2 / \text{Fe}(\text{NO}_3)_3$, Dowex 50W [139], FeCl_3 , scandium triflate, ionic liquid [pmIm] Br [140], ceric ammonium nitrate $(\text{NH}_4)_2\text{Ce}(\text{NO}_3)_6$, $\text{PhI}(\text{OAc})_2$, $\text{Mn}(\text{OAc})_3$, $\text{Th}^+\text{ClO}_4^-$, $\text{Pb}(\text{OAc})_4$ and I_2 [141], have been used to effect the cyclocondensation of aminothiophenols and aromatic aldehydes to give benzothiazoles in good yield.

After evaluating these methods, we have chosen the simple and effective procedure which involve condensation of 2-aminothiophenol with aldehydes using sodium hydrosulfite as efficient catalyst. The progress of the reaction was monitored by thin layer chromatography. The corresponding 2-substituted-benzothiazoles were obtained in excellent yields and pure products were got by recrystallization or column chromatography.

➤ **2-arylbenzothiazoles unsubstituted on the benzothiazole ring**

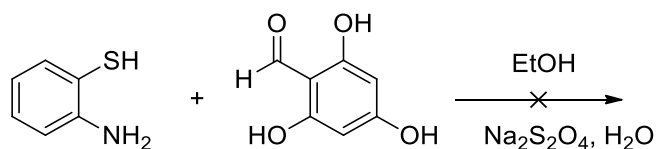
2-substituted benzothiazoles were synthesized via condensation of commercially available 2-aminothiophenol (**1**) and corresponding benzaldehyde (**2a-k**) in refluxing ethanol in one step in the presence of $\text{Na}_2\text{S}_2\text{O}_4$ (**Scheme 12**). The same reaction under free catalyst gave a mixture of benzothiazoline and benzothiazole. Therefore, oxidation of the intermediate benzothiazoline (**3a-k**) was accelerated by $\text{Na}_2\text{S}_2\text{O}_4$.



	R ¹	R ²	R ³	R ⁴	R ⁵
A	H	H	H	H	H
B	OH	H	H	H	H
C	H	OH	H	H	H
D	H	H	OH	H	H
E	H	H	OCH ₃	H	H
F	OH	H	OH	H	H
G	OH	H	H	OH	H
H	H	OH	OH	H	H
I	H	OH	OCH ₃	H	H
J	H	OH	H	OH	H
K	OH	H	OH	OH	H

Scheme 12: Synthetic route of compounds **4a-k**. Reagents and conditions: (a) EtOH, Na₂S₂O₄ in H₂O, Reflux

Electron-donating substituents on the aromatic ring of aldehyde decrease the yield and increase the time of the reaction. This effect is cumulative, so the higher the -OH number, the lower the yield; whereas the present of -OCH₃ substituents in the position *para* increase the yield and decrease the time of the reaction. However synthesis of 2,4,6-trihydroxyphenyl benzothiazole was unsuccessful; this could be due to the steric hindrance.



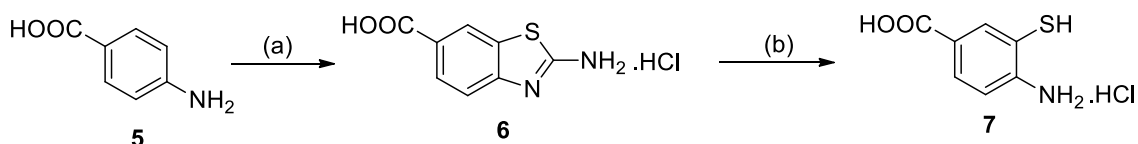
Scheme 13: Attempts of the synthesis of **2,4,6-trihydroxyphenylbenzothiazole**

➤ **2-arylbenzothiazoles substituted on the benzothiazole ring**

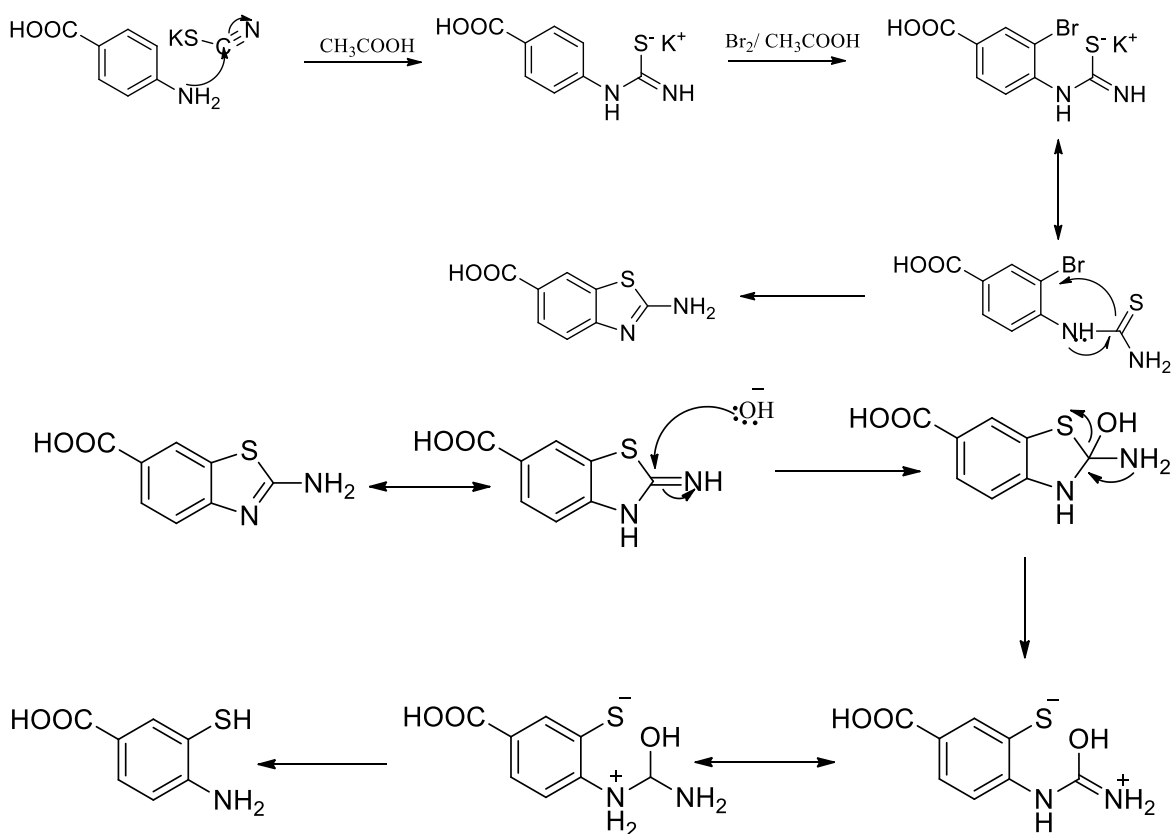
The synthesis of 2,6-disubstituted benzothiazole involve several steps. The initial step is the preparation of intermediates 2-aminobenzothiazole-5-carboxylic acid hydrochloride **7** and

4-amino-3-mercaptobenzenesulfonamide **10** according to a modified literature method [142].

Treatment of 4-aminobenzoic acid with potassium thiocyanate in the presence of bromine in acidic condition at low temperature (0-5°C) gave **6** which was converted into 4-amino-3-mercaptobenzoic acid **7** (Scheme 14) by alkaline hydrolysis in a low yield due to the fact that -NH₂ group of **6** has the possibility to tautomerize into the imino form and consequently strongly limits the reaction Scheme 15. Firstly, attack of nitrogen lone pair of aniline on electrophilic carbon of potassium thiocyanate took place. The second step was the bromination reaction in ortho of the amine, followed by the cyclization in situ to give 2-aminobenzothiazole.



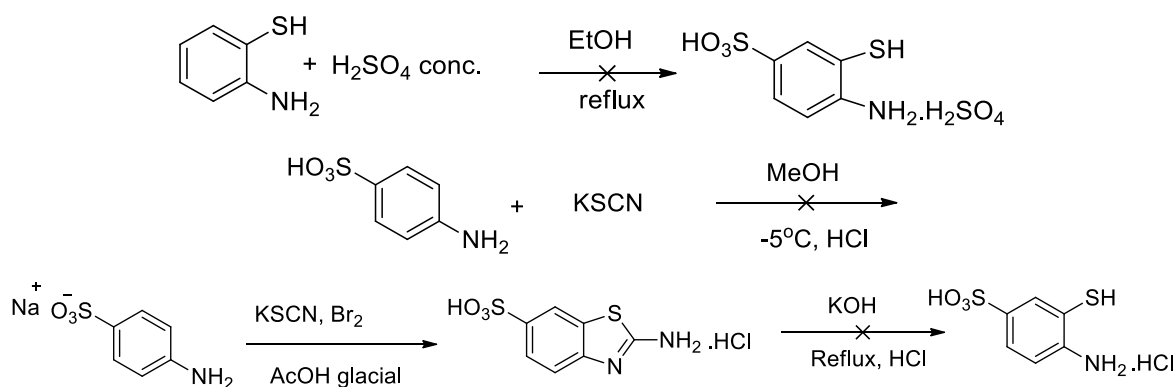
Scheme 14: Synthetic route of 4-amino-3-mercaptobenzoic acid. Reagents and conditions: (a) MeOH, KSCN, Br₂, -5°C, HCl; (b) KOH, Reflux, HCl



Scheme 15: Proposed mechanism for the formation of 4-amino-3-mercaptobenzoic acid

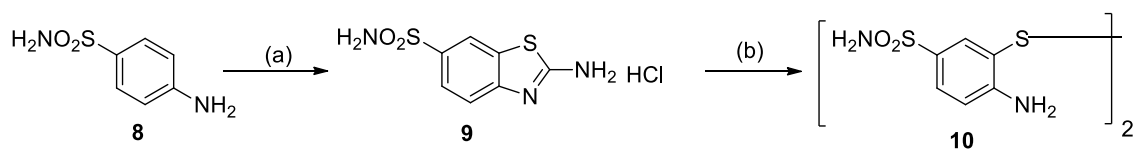
Preparation of 4-amino-3-mercapto benzenesulfonic acid

Like all aromatic compounds, the first attempt at the synthesis of 4-amino-3-mercapto-benzenesulfonic acid was the sulfonation reaction of 2-aminothiophenol, but the reaction was unsuccessful. The second attempt was the exploitation of the method described above by taking 4-aminobenzenesulfonic acid as starting material but the results were still unsatisfactory **Scheme 16**.



Scheme 16: Attempts of the synthesis of 4-amino-3-mercapto benzenesulfonic acid

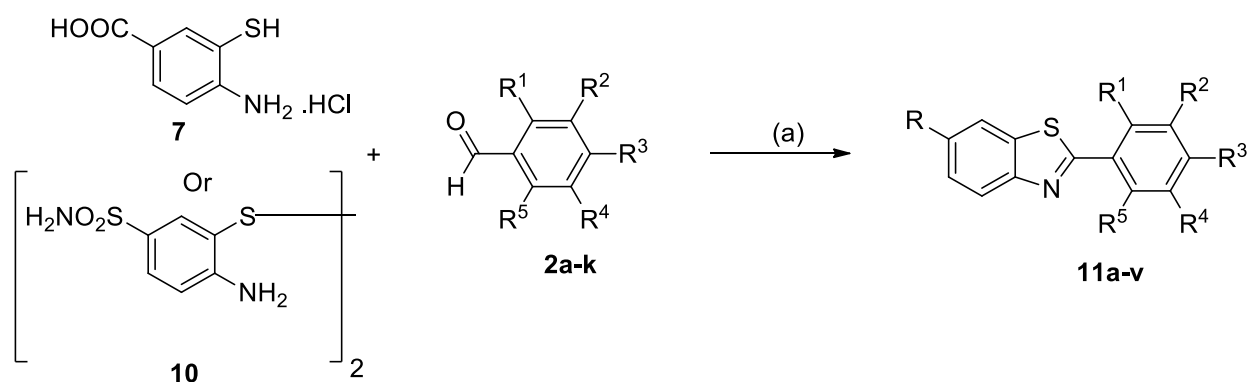
After these series of unsatisfying results, attention was then turned toward formation of 4-amino-3-mercapto-benzenesulfonic using 4-aminobenzenesulfanamide as starting material. To this end, we exploited the method previously described (the synthesis of compound **7**). To optimize the reaction condition of 2-aminobenzothiazole-6-sulfanamide, two solvents were tried: acetic acid and methanol. Acetic acid was found to be the most suitable reaction media giving a high reaction rate and good yield of the product. Treatment of 2-aminobenzothiazole-6-sulfanamide with aqueous potassium hydroxide followed by acidification gave bis(2-amino-4-benzenesulfonamide)disulfide (**Scheme 17**) instead of 4-amino-3-mercapto benzenesulfonic acid. Therefore, the thiazole ring was opened but the sulfonamide group didn't hydrolyze to a sulfonate. Since that $-\text{SO}_2\text{NH}_2$ and $-\text{SO}_3\text{H}$ are isosteres, we proceeded with $-\text{SO}_2\text{NH}_2$ group.



Scheme 17: Synthetic route of bis(2-amino-4-benzenesulfonamide) disulfide (**10**).

Reagents and conditions: (a) AcOH, KSCN, Br₂ in AcOH, -5°C, NH₃; (b) KOH, Reflux, HCl.

Subsequently, condensation of **7** or **10** with benzaldehyde (**2 a-k**) yielded corresponding benzothiazole compounds (**11a-v**), summarized in **Scheme 18**. To evaluate the catalytic efficiency of sodium hydrosulfite, all reactions were then run in ethanol under free catalyst; reaction with bis(2-amino-4-benzenesulfonamide) disulfide gave corresponding 2-Arylbenzothiazoles with good yield while reaction with 4-amino-3-mercaptobenzoic acid gave less than 50% of desired compounds.



	R	R ¹	R ²	R ³	R ⁴	R ⁵		R	R ¹	R ²	R ³	R ⁴	R ⁵
a:	COOH	H	H	H	H	H	l:	SO ₂ NH ₂	H	H	H	H	H
b:	COOH	OH	H	H	H	H	m:	SO ₂ NH ₂	OH	H	H	H	H
c:	COOH	H	OH	H	H	H	n:	SO ₂ NH ₂	H	OH	H	H	H
d:	COOH	H	H	OH	H	H	o:	SO ₂ NH ₂	H	H	OH	H	H
e:	COOH	H	H	OCH ₃	H	H	p:	SO ₂ NH ₂	H	H	OCH ₃	H	H
f:	COOH	OH	H	OH	H	H	q:	SO ₂ NH ₂	OH	H	OH	H	H
g:	COOH	OH	H	H	OH	H	r:	SO ₂ NH ₂	OH	H	H	OH	H
h:	COOH	H	OH	OH	H	H	s:	SO ₂ NH ₂	H	OH	OH	H	H
i:	COOH	H	OH	OCH ₃	H	H	t:	SO ₂ NH ₂	H	OH	OCH ₃	H	H
j:	COOH	H	OH	H	OH	H	u:	SO ₂ NH ₂	H	OH	H	OH	H
k:	COOH	OH	H	OH	OH	H	v:	SO ₂ NH ₂	OH	H	OH	OH	H

Scheme 18: Synthesis of compounds **11a-v**. Reagents and conditions: (a) EtOH, Na₂S₂O₄ in H₂O, Reflux

To better interpret the experimental results, the compounds are divided into classes. In each class the compounds are equally substituted on the phenyl ring but with different substituents in position 6 on the benzothiazole ring (**Table 13**).

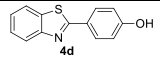
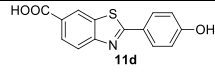
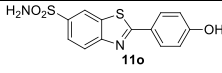
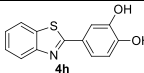
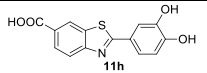
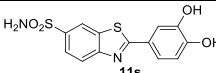
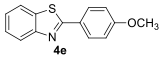
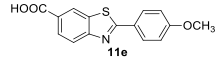
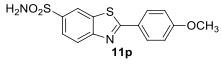
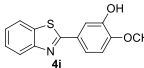
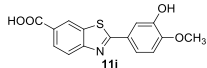
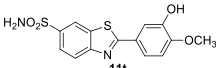
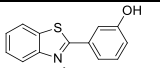
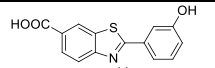
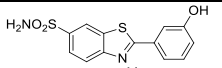
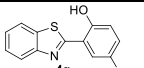
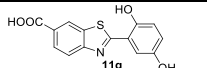
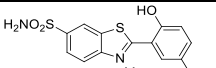
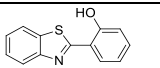
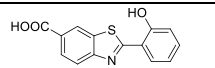
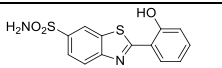
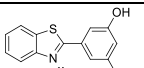
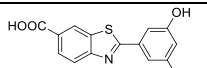
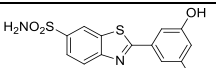
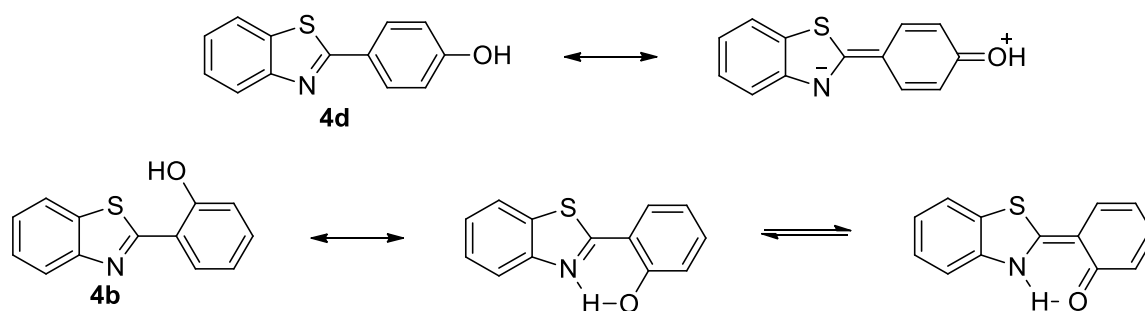
A				F			
B				G			
C				H			
D				I			

Table 13: Subdivision of compounds into classes

VI.2.2. Biological evaluations

VI.2.2.1. Photoprotective activity

In the first part of this study, we examined the spectral behavior of synthesized compounds dissolved in dimethyl sulfoxide, since solar protection is related to the UV absorption of the substances. Absorption spectra were measured from 290 to 400 nm. The wavelength of maximum absorption (λ_{\max}) is closely related to stereoelectronic effects, which can be affected by substituents on the aryl or benzothiazole group that alter the electron density of compounds. The spectral absorption data of the molecules dissolved in DMSO are shown in **Figure 24**. The long wavelength absorption band of **4d** is red-shifted relative to **4c** and can be attributed to the presence of -OH group in *para* position which lead the resonance interaction of lone pair of oxygen and π cloud of phenyl and benzothiazole group. That wavelength is increased if -OH is at *ortho* position, due to the presence of the formation of an intramolecular hydrogen bond between nitrogen of benzothiazole group and hydrogen of hydroxyl group, which increase the resonance character of phenolic group with benzothiazole moiety (see **Scheme 19**). Substitution of *para*-OH by *para*-methoxy has no remarkable change on the absorption spectra.



Scheme 19: Delocalization of electrons over the π -conjugated molecule

The absorption spectrum of **4c** is similar to 2-phenylbenzothiazole (**4a**) one. This could be explained by the fact that, lone pair of -OH group at *meta* position will be localized on the phenyl ring rather than delocalized over the whole molecule and therefore, it has very little effect on the absorption spectrum. But λ_{\max} of **4j** is slightly higher than that of **4c** because both *meta* positions are occupied that is confirmed by Joykrishna Dey and al. [143] which stipulated that, red- shift is observed when the number of auxochrome groups increase. The same result is obtained with **4h**, analogue of **4d** with the second -OH in *meta* position; **4i** analogue of **4e** with the second -OH in *meta* position; **4g** analogue of **4b** with the second -OH in *meta* position 5'-OH and **4f** which have the combined effect described in the **Scheme 19**. The presence of three -OH on the phenyl moiety (**4k**, **11k** and **11v**) makes the molecule more rigid and promotes the shift at the longest wavelength absorption band compared to the other compounds. But although **4g** has only two hydroxyl groups, its spectrum is similar to the spectrum of **4k**.

Substitution of H by withdrawing group (-COOH and -SO₂NH₂) at the 6 position on the benzothiazole moiety shown the bathochromic shift. This long wavelength absorption band is associated with the intramolecular charge transfer transition due to the transfer of the charge between the electron donor group (phenolic group) to the electron-withdrawing of benzothiazole and neighboring carboxylic or sulfonamidic chromophore. The order of λ_{\max} along the series is - H <<-SO₂NH₂<-COOH see **Figure 23**. Therefore absorption range increase with the trend of the increasing electron-withdrawing ability. This could be mainly due to the significant stabilization of the LUMO leading to a smaller HOMO-LUMO energy space.

In short, beyond the position and the number of -OH on the phenyl ring, the presence of an electron-acceptor group at the 6 position of benzothiazole ring, as well as the extent of conjugation favors the bathochromic shift of the molecule.

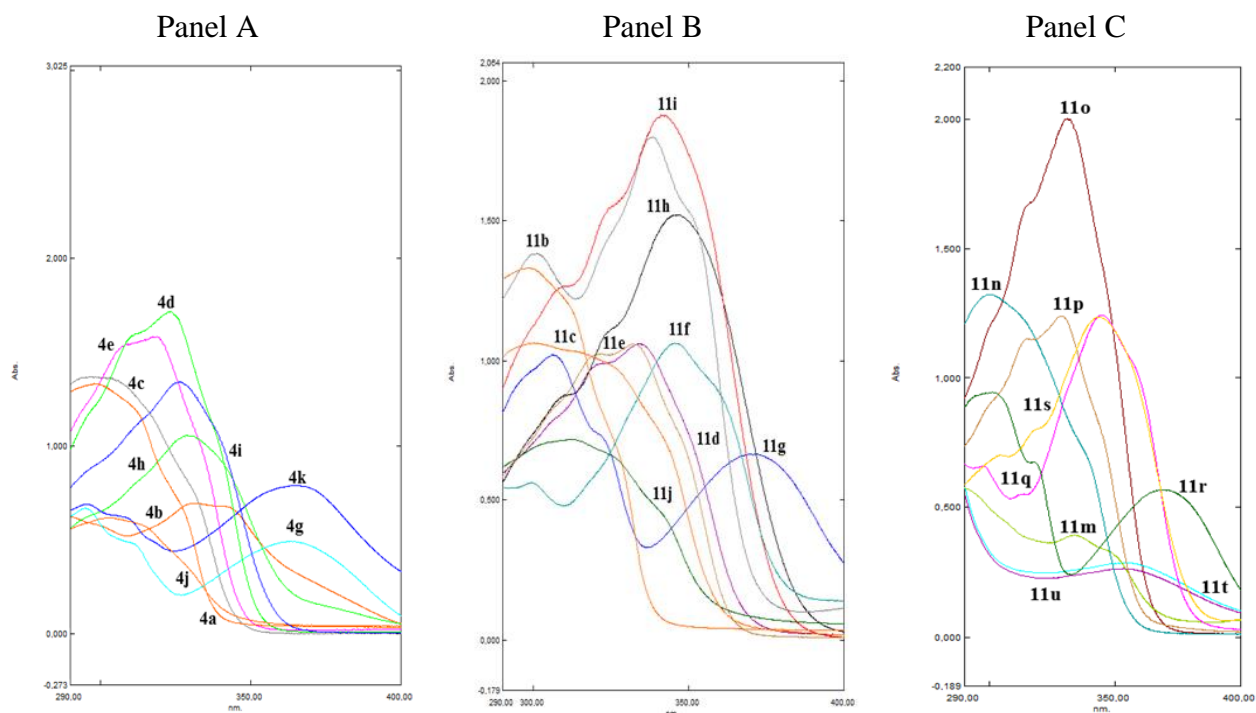


Figure 23: Spectral data of benzothiazole derivatives; compounds **4a-k**(panel A), **11a-j**(panel B) and **11l-u**(panel C).

Indeed there are two mainly types *in vitro* method: measurement of absorption or the transmission of UV radiation by a thin film of sunscreen agent on the quartz plate or biomembranes and spectrophotometric assay of dilute solutions of sunscreen agent. In order to study the synthesized compounds more deeply, both method were employed. Firstly, a pre-screening test was carried out by determination of absorption characteristics of all candidates dissolved in solution (DMSO). Then, some compounds were introduced in formulation (O/W emulsion) and their transmission spectrum was determined using PMMA plate.

VI.2.2.1.1. *In vitro* studies of dilute solutions of target compounds by spectrophotometry

Spectral data of samples were collected from 290 - 400 nm with the calculator software [136]. The software automatically determines theoretical COLIPA – SPF, COLIPA – UVAPF, critical wavelength value (λ_c) and UVA/UVB (paragraph V.1.2.1). To better interpret the obtained results, the compounds were disposed by classes. The photoprotective activity is shown in **Table 14**.

All the synthesized compounds, in general, showed a significant photoprotection activity respect to the lead compound **4a** and the reference PBSA. Photoprotective activity of the sunscreen against UVB is reflected by SPF value. Thereby, among all classes of compounds having a single substituent on the phenyl ring, those without substituent at the 6-position of the benzothiazole moiety have good photoprotective profile, followed by compounds having -SO₂NH₂, and finally compounds having -COOH. Except class **D**, whose compound bearing -COOH showed the best SPF value. From these results it is evident to note that isosteric substituent at the sixth position of benzothiazole ring does not have significant effects for the sun protection. Of everything indicated, we could say that, the presence of hydrogen atom at the 6 position of benzothiazole ring increases SPF value, therefore reactivity order is -H > -SO₂NH₂ > -COOH. On the contrary, among the compounds having more than one substituent on the phenyl ring, those bearing -COOH group showed the best UVB profile. However, the order of SPF values according to the substitution on the phenyl ring is the following: *para* > *ortho* > *meta* for compounds having H or -SO₂NH₂ at 6 position of benzothiazole moiety, while compounds with COOH at position 6 on the ring benzothiazole have the following order: *meta* > *ortho* > *para*. Compounds of class **B** (*para*-methoxy substituent on the phenyl ring) showed lower value than compounds of class **A**, indicating that *para*-hydroxy group is better than *para*-methoxy.

By maintaining fixed compounds of class **A** and introducing an -OH in position *ortho* or *meta* to obtain compounds of classes **E** and **F** respectively, SPF values decrease. In the same way, introduction of -OH in *meta* position of compounds of class **D** (*ortho*-OH) and class **C** (*meta*-OH) gave respectively compounds of classes **H** (two -OH in position 2 and 5) and **I** (two -OH in position 3 and 5) with lower SPF. Curiously compounds of class **J** with three -OH on the phenyl ring showed SPF values similar to those with two -OH. This means that, the SPF factor does not depend only on the number of -OH on the phenyl ring but also on their position. Interestingly, replacing *para*-hydroxy with *para*-methoxy (class **F** to **G**) the SPF values increase. Nevertheless, this result is contrary to that previously described (class **A** to **B**). In summary, compounds endowed with the best SPF are those unsubstituted at the benzothiazole ring especially compound **4d** with -OH in *para* position on the phenyl ring. Protection against UVA rays was given by UVAPF which is considered efficient if it is greater than or equal to 1/3 of SPF. Compounds of the same class presented similar UVAPF values despite they are different at the 6 position, but compounds with -SO₂NH₂ are slightly less effective than others. Compounds **11h** of class **F** and **11k** of class **J** are the best candidate against UVA (with UVAPF \cong 7) characterized both by the presence of -OH in *meta* and *para*-position of the phenyl ring then followed by compounds

of class **G** (3-OH, 4-OMe). Thus, the effect of the electron donor group (hydroxyl or methoxy) in the *meta* and *para*-position of the phenyl ring appears to be important for protection against UVA.

Critical wavelength is the parameter that provides information on the broad spectrum of UV-filter. It is classified in five numerical categories: 0 ($\lambda_c < 325$ nm), 1 ($325 \leq \lambda_c \leq 335$), 2 ($335 \leq \lambda_c \leq 350$), 3 ($350 \leq \lambda_c < 370$) and 4 ($\lambda_c \geq 370$). FDA considers the broad-spectrum sunscreen product should have a $\lambda_c \geq 370$ nm[137]. Under that classification, compounds of classes **H** and **J** have fallen into category “4”, as well as compounds **11f** (class **E**), **11t** (class **G**) and **11u** (class **I**). Whereas compounds of classes **A**, **D**, **E** (except **11f**), **F** and **11i** (class **G**) have fallen into category “3” and compound of classes **B**, **C** and **4i** fell into “2”. Lastly, compounds **4a** and **PBSA** are rated “1”. Therefore all synthesized compounds showed $\lambda_c > \text{PBSA}$ except compound **4a**. Interestingly, compounds of classes **H**, **J** and compounds **11f**, **11t** and **11u** can be considered potential broad-spectrum filters.

Finally, we also determined the UVA/UVB absorbance ratio, which is an important parameter to provide good idea of the absorbance through the entire UV spectrum. According to the latest EU recommendation and **PBSA** data, all synthesized compounds have good UVA/UVB values, apart from **4a**, **4d**, **4e**, **4c** and **11n**.

Classes	Compound	SPF	UVAPF	UVA/UVB	λ_c (nm)
	PBSA	3.40 ± 0.17	1.03 ± 0.08	0.29	322
	4a	8.38 ± 0.29	0.13 ± 0.01	1.8	331
A	4d	25.86 ± 2.06	1.57 ± 0.02	0.81	353
	11d	6.19 ± 0.98	2.23 ± 0.08	0.81	353
	11o	19.41 ± 1.75	2.35 ± 0.10	0.32	350
B	4e	14.23 ± 1.43	1.30 ± 0.04	0.1	335
	11e	6.54 ± 0.87	1.88 ± 0.12	0.65	349
	11p	8.91 ± 0.45	1.80 ± 0.09	0.45	347
C	4c	10.05 ± 0.11	1.18 ± 0.07	0.13	335
	11c	8.84 ± 0.64	1.71 ± 0.02	0.36	346
	11n	9.42 ± 0.06	1.46 ± 0.05	0.18	340
D	4b	7.56 ± 0.59	2.57 ± 0.06	0.86	355
	11b	18.03 ± 1.15	4.09 ± 0.14	0.62	358
	11m	6.59 ± 0.83	3.45 ± 0.22	0.77	360
E	4f	6.62±0.07	3.34±0.13	1.62	356
	11f	3.43±0.49	4.62±0.05	1.61	370
	11q	3.85 ± 0.31	4.41 ± 0.11	1.63	364
F	4h	5.51 ± 0.96	2.33 ± 0.16	0.9	358
	11h	7.42 ± 0.13	7.35 ± 0.41	1.74	367
	11s	5.39 ± 0.09	4.71 ± 0.08	1.40	365
G	4i	9,13 ± 0.34	5.94 ± 0.15	0.42	350
	11i	17.33 ± 1.45	5.95 ± 0.26	1.02	361
	11t	11.87 ± 0.07	5.80 ± 0.33	0.96	380
H	4g	2.82 ± 0.49	2.50 ± 0.17	0.66	381
	11g	7.34 ± 0.49	3.32 ± 0.24	0.40	384
	11r	5.47 ± 0.07	2.76 ± 0.01	0.40	382
I	4j	3.38 ± 0.16	1.52 ± 0.09	0.45	345
	11j	4.45 ± 0.23	1.57 ± 0.07	0.45	353
	11u	3.06 ± 0.06	1.72 ± 0.02	0.95	380
J	4k	3.87 ± 0.012	4.71 ± 0.08	0.86	385
	11k	5.16 ± 0.33	7.50 ± 0.42	1.25	389
	11v	3.65 ± 0.15	4.20 ± 0.19	1.34	384

Table 14: Filtering activity of benzothiazole derivatives in DMSO

VI.2.2.1.2. In vitro sun protection factor of the Cosmetic formulation

The synthesized molecules were introduced at the concentration of 1% in a cosmetic formulation in order to evaluate their UV -filter activity. For this, Diffey and Robson [135] *in vitro* method based on the measurement of transmission of ultraviolet radiation on Polymethylmethacrylate (PMMA) plate was used. Values of the SPF, UVAPF, UVA/UVB and λ_c are shown in **Table 15**.

Compound **4j** characterized by the presence of -OH in position 3 and 5 on the phenyl ring showed the best SPF value (SPF = 4.15). This value is very significant since the formulation contains only 1% of active ingredient. Compounds **4d**, **4k** and **11g** with at least one hydroxyl group in *ortho* or *para* position of the phenyl ring have SPF value greater than the compound lead. However, substitution of -OH by -OCH₃ (**4e**) reduces the activity of the compound (3.2 to 2.7 respectively). The same result is observed by modifying **4h** to obtain **4i** (2.10 to 1.59 respectively). Consequently, -OCH₃ group favors less the UV filtering activity than the -OH group. Among the 6-substituted benzothiazoles, only **11g** and **11r** (-OH groups in 2,5-position) have SPF values greater than 2. Data of compounds **4b**, **4c** and **4h** are similar although they have neither the same -OH number nor the same substitution position. Regarding λ_c , compounds **4g**, **4h**, **4k**, **11d**, **11g**, **11o** and **11r** exhibited $\lambda_c > 370$ nm. All synthesized compounds have UVA-PF value greater than or equal to 1/3 of SPF. The UVA/UVB ratio of all synthesized compounds is greater than the lead compound (PBSA).

In short, taking into consideration the spectral data of dilute solutions and cosmetic formulations, compounds **4g**, **4h**, **4k**, **11d**, **11g**, **11o** and **11r** were potential candidates for broad-spectrum UV filters while compounds **4d** and **4j** only for UVB protection. The particularity of these potential candidates is marked by the presence of -OH in position *para* or *orto* of the phenyl ring. It is also important to emphasize that the number and the position of auxochrome (-OH and -OCH₃) influence on the photoprotective activity.

compound	SPF	UVA-PF	UVA/UVB	λ_c (nm)
PBSA	3.02 ± 0.89	1.04 ± 0.06	0.26	333
4b	2.17 ± 0.26	1.43 ± 0.12	1.01	356
4c	2.18 ± 0.08	1.08 ± 0.05	0.66	332
4d	3.2 ± 0.21	1.20 ± 0.11	0.63	338
4e	2.7 ± 0.17	1.12 ± 0.08	0.63	335
4g	2.66 ± 0.21	1.84 ± 0.16	0.71	385
4h	2.10 ± 0.13	1.80 ± 0.10	1.22	389
4i	1.59 ± 0.10	1.14 ± 0.07	1.89	342
4j	4.15 ± 0.34	1.20 ± 0.19	0.42	336
4k	3.66 ± 0.29	3.24 ± 0.26	0.81	385
11e	1.77 ± 0.14	1.22 ± 0.13	0.89	348
11p	1.46 ± 0.11	1.09 ± 0.09	0.82	345
11d	1.57 ± 0.09	1.79 ± 0.10	1.12	389
11o	1.99 ± 0.18	3.59 ± 0.24	1.35	391
11g	3.71 ± 0.27	3.15 ± 0.21	0.86	384
11r	2.12 ± 0.19	2.56 ± 0.25	1.18	386
11j	1.74 ± 0.16	1.28 ± 0.11	0.88	366

Table 15: Photoprotection results of benzothiazole derivatives in formulation (O/W)

VI.2.2.1.3. Photostability study by spectral analysis

Photostability of compounds is evaluated using one of the criteria developed by Garoli and al. [144], which is based on the measurement of SPF before and after UV exposition. The loss of sunscreen protection after exposure to sunlight is expressed as the residual effectiveness after exposure (%). The *in vitro* % SPF_{eff.} and % UVA-PF_{eff.} of compounds are calculated according to the **Equation 6** and **Equation 7** respectively and are reported in **Table 16**. A sunscreen is considered photostable if its residual percentage is greater than or equal to 80.

From the results obtained, % SPF_{eff.} and % UVA-PF_{eff.} values of compounds ranged from 80.18 to 100. Therefore, these compounds are considered photostable especially **11e** with a degradation rate less than 2%. However, the compounds **4b** and **4g** exhibited a degradation rate more or less 20%. Both compounds have an hydroxyl in *orto* position of the phenyl ring. Interestingly, the substitution of the benzothiazole ring in position 6 with -COOH or -SO₂NH₂ increases the photostability of the compounds. Moreover, compounds with -SO₂NH₂ are more photostable.

Entry	% SPF _{eff.}	% UVA-PF _{eff.}
4b	83.42	98.00
4c	99.07	99.07
4d	94.06	98.07
4e	93.33	99.07
4g	80.18	98.36
4i	92.45	98.26
4j	93.25	98.07
11e	99.99	100
11p	95.78	100
11d	97.45	99.85
11o	95.21	100
11g	88.72	99.00
11i	93.45	99.12
11j	95.67	99.09
11r	98.11	99.54
11u	96.13	100

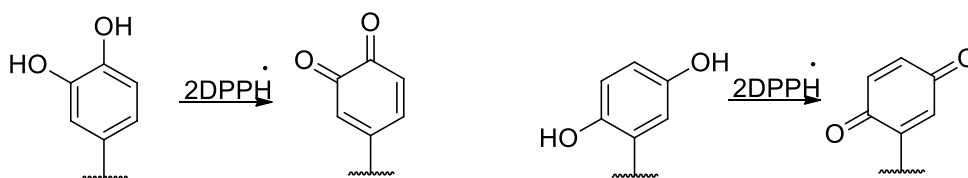
Table 16: Evaluation of photostability of benzothiazole compounds

VI.2.2.2. Antioxidant activity

Synthesized compounds were evaluated for their *in vitro* antioxidant activity by DPPH and FRAP assays (paragraph V.1.2.2).

To better interpret the results of the DPPH test, we first evaluated the percentage inhibition of the DPPH radical by synthesized compounds at the same concentration, namely 1 mg/mL (**Table 17**). Compounds of classes **F** (3,4-dihydroxy) and **H** (2,5-dihydroxy) have a percentage of inhibition close to 100%. But, substituting -OH with -OCH₃ to obtain class **G** (3-hydroxy, 4-methoxy) the percentage of inhibition decreases. Compounds of class **A**, with *para* hydroxyl on the phenyl ring, did not exhibit any particular activity with respect to the radical under consideration. However, contrary to what is stated above, replacing -OH with -OCH₃ (class **B** compounds) the percentage of inhibition considerably increases (**4e** and **11e**). Therefore, only methoxy group has good activity but associated with a hydroxyl, its activity decreases. In addition, among compounds of class **D**, only **11m** with -OH in *ortho* position of phenyl ring and -SO₂NH₂ in 6 position of the benzothiazole ring displayed a good inhibition. Alike, for compounds of class **C** (*meta*-hydroxyl), only compound **11c** with -COOH in 6-position on benzothiazole ring has good inhibition. However, all compounds of class **I** with two *meta* substituted (3,5-dihydroxy) have good inhibition.

From this first screening, only compounds with good inhibition ($\% \geq 50$) were further investigated for the determination IC_{50} which represents the concentration of a compound required to inhibit 50% of DPPH radical. The results are expressed in $\mu\text{g/mL}$ (**Table 17**). Structure-activity relationship analysis indicated that various factors such as the nature of substituents in position 6 of benzothiazole ring, as well as the number and position of the electron donor group (-OH and -OCH₃) on the phenyl ring are very important for the radical scavenging activity. All compounds of class **F** and **H** especially those without electron attractor group on the benzothiazole ring (**4h** and **4g**) showed good inhibition, with IC_{50} values between 6.42 and 11.29 $\mu\text{g/mL}$. This could be due to the fact that, polyphenols having two -OH groups in the 2,5- and 3,4-positions react twice with DPPH radical to form a very stable conjugated diketone structure (see **Scheme 20**). Apart from the stability due to the conjugation of diketone, we also have the hydrogen bonds between two hydroxyl for the 3,4-dihydroxy compounds and between one hydroxyl and nitrogen of the benzothiazole ring for the 2,5-dihydroxy compounds. But introduction of methoxy group at position 4 on the phenyl ring (compounds of class **G**) drastically reduced the activity in comparison to compounds of class **F**, due to the lack of stabilities mentioned above. Surprisingly, the compounds **11c** with *meta*-hydroxyl have a good activity, but those having two meta substituted (3,5-dihydroxy) have no activity. Curiously, compounds of class **J**, although having three -OH group, are less active than their parent compounds (compounds of class **H**). This could be explained by the fact that the presence of the third -OH prevents the resonance described in **Scheme 20**.



Scheme 20: Stabilization of phenol by resonance

Results of FRAP test are similar to those of DPPH test; molecules with a better antioxidant profile are those of classes **F** and **H** which bear two hydroxyl groups respectively in positions 3, 4 and 2, 5- of the phenyl ring. The compounds of classes **A** and **D** having *para* and *ortho*-hydroxyl on the phenyl ring respectively have moderate values, however, the class **A** compounds are slightly more active than those of class **D**, which is explained by the fact that the proton *ortho*-phenol could form a hydrogen bond with the nitrogen atom of the benzothiazole ring, which disadvantages the transfer of the proton. Among compounds of class **C**, compound **11c** bearing -COOH on the benzothiazole ring have a good activity

(2045.37 $\mu\text{molT/g}$). Instead, both **4c** and **11n** have very low values (respectively 48.605 and 17.357 $\mu\text{molT/g}$). The introduction of the *para*-methoxy group (classes **B** and **D**) has reduced activity with respect to classes **A** and **F**. So *para*-methoxy is not conducive to this activity.

Summary, considering the above mentioned results, in DPPH and FRAP assays, molecules with better antioxidant profile are compounds of classes **F** and **H**, which bear two hydroxy groups at positions 3, 4 and 2, 5- of the phenyl ring. The best is compound **4g** according to DPPH, whereas according to FRAP, the best is **11h**.

Classes	Compound	DPPH %Inhibition	DPPH IC ₅₀ (μ g/ml)	FRAP μ molT/g
	4a	43.6 \pm 0.11	974.49 \pm 4.78	167.01 \pm 3.34
A	4d	11.60 \pm 0.32	-	123.00 \pm 5.92
	11d	30.75 \pm 0.89	-	402.17 \pm 1.95
	11o	31.22 \pm 0.45	-	65.60 \pm 1.18
B	4e	45.27 \pm 0.61	-	206.88 \pm 6.64
	11e	71.70 \pm 0.58	322.70 \pm 6.29	173.83 \pm 5.05
	11p	15.48 \pm 0.33	-	90.95 \pm 3.64
C	4c	16.27 \pm 0.06	-	48.61 \pm 0.40
	11c	94.64 \pm 1.22	28.97 \pm 0.56	2045.37 \pm 18.68
	11n	22.73 \pm 0.69	-	17.36 \pm 0.81
D	4b	30.72 \pm 0.47	-	264.75 \pm 5.84
	11b	18.00 \pm 0.36	-	20.60 \pm 0.85
	11m	58.22 \pm 0.87	-	197.80 \pm 5.07
E	4f	72.83 \pm 0.58	822.63 \pm 8.16	187.64 \pm 5.15
	11f	22.37 \pm 0.52	-	50.32 \pm 1.54
	11q	23.89 \pm 0.48	-	91.31 \pm 3.25
F	4h	84.65 \pm 0.93	7.2 \pm 0.11	6021.15 \pm 25.84
	11h	94.74 \pm 0.66	11.29 \pm 0.07	7402.73 \pm 22.78
	11s	94.36 \pm 0.82	7.96 \pm 0.55	5273.01 \pm 15.01
G	4i	65.00 \pm 0.31	561.62 \pm 18.13	3247.656 \pm 56.72
	11i	28.02 \pm 0.87	-	712.515 \pm 10.75
	11t	10.98 \pm 0.11	-	65.39 \pm 0.35
H	4g	94.32 \pm 1.15	6.42 \pm 0.28	6268.43 \pm 25.16
	11g	96.41 \pm 0.89	7.61 \pm 0.28	7321.64 \pm 34.73
	11r	96.23 \pm 0.77	9.09 \pm 0.24	7115.91 \pm 14.46
I	4j	77.5 \pm 4.76	159.55 \pm 6.20	273.486 \pm 15.38
	11j	57.9 \pm 0.82	-	175.98 \pm 1.78
	11u	19.93 \pm 1.54	-	73.33 \pm 1.42
J	4k	23.78 \pm 0.82	-	4876.44 \pm 34.54
	11k	72.73 \pm 3.67	43.01 \pm 2.93	1960.24 \pm 18.43
	11v	53.20 \pm 95	186.89 \pm 5.46	513.04 \pm 2.66

- not detected

Table 17: Antioxidant activity of benzothiazole derivatives

VI.2.2.3. Antifungal activity

VI.2.2.3.1. Antidermatophyte activity

Each tested substance was dissolved in dimethylsulfoxide (DMSO) and investigated for its antifungal activities against five dermatophytes responsible for the most common dermatomycoses: *Microsporum gypseum*, *Microsporum canis*, *Trichophyton mentagrophytes*, *Trichophyton tonsurans* and *Epidermophyton floccosum*. Inhibition of the dermatophytes was evaluated by measuring the colony diameter at each disk. The biological results are presented in **Table 18**. Compound **4h** showed the highest antifungal activity. It is active against all five dermatophytes, in particular against *Microsporum gypseum*, *Trichophyton tonsurans* and *Epidermophyton floccosum* with a percentage of inhibition close to 100%. Significant activity was observed for compounds **4f** and **4g** against *Microsporum gypseum* and *Epidermophyton floccosum*. Compounds **4c** and **4j** showed good activity against *Microsporum gypseum* and *Epidermophyton floccosum* respectively. However, no activity was observed for compounds substituted at position 6 of benzothiazle ring. This suggests that, electron withdrawing substituent decrease the antifungal activity.

Classes	Compound	<i>M. gypseum</i>	<i>M. canis</i>	<i>T. mentagrophytes</i>	<i>T. tonsurans</i>	<i>E. floccosum</i>
	4a	21.57 ± 0.45	18.94 ± 2.31	++	10.45 ± 1.09	+
A	4d	24.24 ± 2.39	12.75 ± 1.02	6.12 ± 2.86	7.02 ± 0.76	7.50 ± 0.23
	11d	15.84 ± 1.53	10.81 ± 0.32	+	11.86 ± 3.11	18.18 ± 2.05
	11o	17.35 ± 2.45	8.27 ± 1.22	5.13 ± 0.56	+	+
B	4e	7.53 ± 1.10	19.01 ± 1.34	1.00 ± 0.04	15.25 ± 3.29	10.87 ± 2.34
	11e	19.80 ± 2.93	16.22 ± 1.23	9.71 ± 2.01	20.34 ± 3.90	9.09 ± 1.02
	11p	+	0.00 ± 1.45	4.72 ± 1.29	0.00 ± 1.02	+
C	4c	62.31 ± 8.39	34.43 ± 0.10	28.85 ± 3.22	18.18 ± 1.73	40.48 ± 3.02
	11c	+	11.11 ± 2.09	0.00 ± 0.90	22.22 ± 4.56	+
	11n	31.63 ± 4.17	18.05 ± 3.10	29.06 ± 1.02	1.64 ± 0.54	+
D	4b	13.98 ± 2.14	14.88 ± 3.29	+	18.64 ± 0.85	6.52 ± 0.38
	11b	27.72 ± 1.02	18.02 ± 2.38	4.85 ± 0.84	27.12 ± 4.01	6.82 ± 1.74
	11m	18.37 ± 0.20	12.03 ± 1.32	11.11 ± 0.63	+	++
E	4f	62.12 ± 0.56	36.41 ± 2.92	19.98 ± 3.11	31.95 ± 1.02	50.31 ± 2.01
	11f	9.18 ± 0.99	6.84 ± 1.00	+	36.51 ± 1.65	++
	11q	4.55 ± 0.04	6.36 ± 0.92	5.98 ± 1.03	4.76 ± 0.54	2.13 ± 0.77
F	4h	94.62 ± 5.09	68.60 ± 2.21	56.0 ± 1.36	96.61 ± 4.02	93.48 ± 0.32
	11h	10.20 ± 0.54	4.27 ± 1.29	+	11.11 ± 0.33	++
	11s	9.09 ± 0.20	+	+	7.94 ± 0.94	0.00 ± 1.28
G	4i	32.31 ± 3.73	9.02 ± 0.02	3.85 ± 1.33	++	0.00 ± 1.78
	11i	+	12.31 ± 1.99	1.80 ± 0.21	1.69 ± 0.39	0.00 ± 0.93
	11t	+	1.50 ± 0.45	10.92 ± 2.67	7.94 ± 1.83	17.86 ± 2.55
H	4g	50.46 ± 2.01	28.69 ± 2.67	17.31 ± 0.98	18.18 ± 1.03	71.43 ± 8.40
	11g	4.49 ± 0.55	6.15 ± 0.42	+	3.39 ± 0.17	4.17 ± 0.34
	11r	+	0.00 ± 0.34	6.84 ± 1.03	7.94 ± 0.98	+
I	4j	46.46 ± 0.44	35.29 ± 0.23	36.73 ± 1.06	36.84 ± 2.30	62.50 ± 3.01
	11j	+	8.46 ± 1.39	2.70 ± 0.09	0.00 ± 0.01	18.75 ± 2.63
	11u	11.24 ± 2.34	6.02 ± 0.82	5.88 ± 0.84	7.94 ± 0.42	12.50 ± 1.05
J	4k	12.40 ± 3.51	5.69 ± 1.33	+	1.30 ± 0.60	8.62 ± 1.52
	11k	7.44 ± 0.89	+	+	10.39 ± 1.89	+
	11v	7.44 ± 0.55	0.81 ± 0.23	0	6.49 ± 0.43	+

+, ++ the compound stimulates the growth of the fungus

Table 18: Percent growth inhibition of dermatophytes treated with the benzothiazole derivatives at 100 µg/mL. Each value is the mean of three measurements

Since compound **4h** showed good activity against *Microsporium gypseum*, *Trichophyton tonsurans* and *Epidermophyton floccosum* with a percentage of inhibition close to 100%, IC₅₀ was determined for these three dermatophytes in comparison with reference compounds Fluconazole and Econazole Nitrate. According to the results presented in **Table 19** compound **4h** is more active against *E. floccosum* with an IC₅₀ value of 11.63 µg/mL, followed by *M. gypseum* and finally *T. tonsurans*. Both fluconazole and econazole nitrate are more active than **4h**.

Compound	IC ₅₀ (µg/mL)		
	<i>M. gypseum</i>	<i>T. tonsurans</i>	<i>E. floccosum</i>
4h	26.95 ± 1.04	43.31 ± 1.85	11.63 ± 0.24
Fluconazole	18.5 ± 1.23	19.41 ± 0.87	0.08 ± 0.005
Econazole Nitrate	0.05 ± 0.0001	0.13 ± 0.008	0.47 ± 0.015

Table 19: Concentration of the compound required to inhibit 50% of growth of fungus

VI.2.2.3.2. Anti-candida Activity

The *in vitro* antifungal activity of benzothiazole derivatives against *Candida albicans* (paragraph V.1.2.3.2), is reported in **Table 20** (only active compounds against *Candida albicans* were shown). Minimal inhibitory concentration (MIC) of the synthesized agents was determined by broth microdilution method. The results shown are representative of 24 hours of incubation arranged in triplicate. Compounds **4h**, **4f**, **4k**, **11k** and **11v** compounds showed good activity. However, compounds **4f** and **4k** characterized respectively by the presence of -OH groups in positions 2, 4 and 2, 4, 5 of the phenyl ring and no functional group on the benzothiazole ring are more effective with a range of MIC of 4-8µg/mL.

Compound	<i>C. albicans</i> (MIC µg/mL)
4f	4
4h	32
4k	8
11k	64
11v	128

Table 20: Anti-*Candida albicans* activities of benzothiazole derivatives. The average values were taken as the MICs

VI.2.2.4. Antiviral activity

Antiviral activity was tested against herpes simplex virus-1 (KOS), herpes simplex virus-2 (G), herpes simplex virus-1 TK-KOS ACVr, vaccinia virus, Adeno virus-2 and Human Coronavirus (229E) in HEL cell cultures; vesicular stomatitis virus, Coxsackie virus B4, Respiratory syncytial virus in HeLa cell cultures (paragraph V.1.2.4). The antiviral activity of the compounds is expressed as the concentration required to inhibit viral cytopathogenicity by 50% (EC₅₀) and results are shown in **Tables 21-22**. Compounds **11g** and **11r** exhibited antiviral activity against Adeno virus-2 and Human Coronavirus in HEL cells. None of the synthesized compounds showed specific antiviral activity in HeLa cells. However some compounds showed cytotoxic activity; the most cytotoxic of the series are **4f**, and **4g** with cytotoxic concentration of 37.1 and 38.1 μM respectively in HeLa cells.

Class	compound	Cytotoxic concentration ^a (μM)	EC ₅₀ ^b (μM)					
			Herpes simplex virus-1 (KOS)	Herpes simplex virus-2	Herpes simplex virus-1 TK-KOS ACVr	Vaccinia virus	Adeno virus-2	Human Coronavirus (229E)
	4a	> 100	> 100	> 100	> 100	> 100	> 100	> 100
A	4d	> 100	> 100	> 100	> 100	> 100	> 100	> 100
	11d	> 100	> 100	> 100	> 100	> 100	> 100	> 100
	11o	> 100	> 100	> 100	> 100	> 100	> 100	> 100
B	4e	> 100	> 100	> 100	> 100	> 100	> 100	> 100
	11e	> 100	> 100	> 100	> 100	> 100	> 100	> 100
	11p	> 100	> 100	> 100	> 100	> 100	> 100	> 100
C	4c	> 100	> 100	> 100	> 100	> 100	> 100	> 100
	11c	> 100	> 100	> 100	> 100	> 100	> 100	> 100
	11n	> 100	> 100	> 100	> 100	> 100	> 100	> 100
D	4b	> 100	> 100	> 100	> 100	> 100	> 100	> 100
	11b	> 100	> 100	> 100	> 100	> 100	> 100	> 100
	11m	> 100	> 100	> 100	> 100	> 100	> 100	> 100
E	4f	> 100	> 100	> 100	> 100	> 100	> 100	> 100

	11f	> 100	> 100	> 100	> 100	> 100	> 100	> 100
	11q	> 100	> 100	> 100	> 100	> 100	> 100	> 100
F	4h	> 100	> 100	> 100	> 100	> 100	> 100	> 100
	11h	> 100	> 100	> 100	> 100	> 100	> 100	> 100
	11s	> 100	> 100	> 100	> 100	> 100	> 100	> 100
G	4i	> 100	> 100	> 100	> 100	> 100	> 100	> 100
	11i	> 100	> 100	> 100	> 100	> 100	> 100	> 100
	11t	> 100	> 100	> 100	> 100	> 100	> 100	> 100
H	4g	91.8 ± 1.2	> 100	> 100	> 100	> 100	> 100	> 100
	11g	> 100	> 100	> 100	> 100	> 100	36.6 ± 3.2	50±2
	11r	> 100	> 100	> 100	> 100	> 100	39.1 ± 2.5	50±1
I	4j	> 100	> 100	> 100	> 100	> 100	> 100	> 100
	11j	> 100	> 100	> 100	> 100	> 100	> 100	> 100
	11u	> 100	> 100	> 100	> 100	> 100	> 100	> 100
J	4k	> 100	> 100	> 100	> 100	> 100	> 100	> 100
	11k	> 100	> 100	> 100	> 100	> 100	> 100	> 100
	11v	> 100	> 100	> 100	> 100	> 100	> 100	> 100
Brivudin		>250	0,01	250	0,1	5,8	-	-
Cidofovir		>250	4,5	3,4	2,8	50	10	-
Acyclovir		>250	0,6	0,6	2	>250	-	-
Ganciclovir		>250	0,01	0,01	0,2	>100	-	-

^a50% Cytotoxic concentration, as determined by measuring the cell viability with the colorimetric formazan-based MTS assay.

^bconcentration producing 50% inhibition of virus-induced cytopathic effect, as determined by as determined by the MTS method.

- not detected.

Table 21: *Cytotoxicity and antiviral activity of compounds in human embryonic lung (HEL) cell cultures*

Class	compound	Cytotoxic concentration ^a (μ M)	EC ₅₀ ^b (μ M)		
			Vesicular stomatitis virus	Coxsackie virus B4	Respiratory syncytial virus
	4a	> 100	> 100	> 100	> 100
A	4d	> 100	> 100	> 100	> 100
	11d	> 100	> 100	> 100	> 100
	11o	> 100	> 100	> 100	> 100
B	4e	> 100	> 100	> 100	> 100
	11e	> 100	> 100	> 100	> 100
	11p	> 100	> 100	> 100	> 100
C	4c	> 100	> 100	> 100	> 100
	11c	> 100	> 100	> 100	> 100
	11n	> 100	> 100	> 100	> 100
D	4b	> 100	> 100	> 100	> 100
	11b	> 100	> 100	> 100	> 100
	11m	> 100	> 100	> 100	> 100
E	4f	37.1 \pm 2.8	> 100	> 100	> 100
	11f	> 100	> 100	> 100	> 100
	11q	> 100	> 100	> 100	> 100
F	4h	77.1 \pm 3.2	> 100	> 100	> 100
	11h	> 100	> 100	> 100	> 100
	11s	> 100	> 100	> 100	> 100
G	4i	> 100	> 100	> 100	> 100
	11i	> 100	> 100	> 100	> 100
	11t	> 100	> 100	> 100	> 100
H	4g	38.1 \pm 1.9	> 100	> 100	> 100
	11g	> 100	> 100	> 100	> 100
	11r	> 100	> 100	> 100	> 100

I	4j	> 100	> 100	> 100	> 100
	11j	> 100	> 100	> 100	> 100
	11u	> 100	> 100	> 100	> 100
J	4k	> 100	> 100	> 100	> 100
	11k	> 100	> 100	> 100	> 100
	11v	> 100	> 100	> 100	> 100
DS-10.000		>100	>100	>100	0,8
Ribavirin		>250	112	250	10

^a50% Cytotoxic concentration, as determined by measuring the cell viability with the colorimetric formazan-based MTS assay.

^bConcentration producing 50% inhibition of virus-induced cytopathic effect, as determined by as determined by the MTS method.

Table 22: Cytotoxicity and antiviral activity of compounds in HeLa cell cultures

VI.2.2.5. Antiproliferative activity

Antiproliferative activity of target compounds against human T-lymphocyte cells (CEM), human cervix carcinoma cells (HeLa), human pancreas carcinoma cells (Mia Paca-2) and human melanoma cells (SK-Mel 5) was evaluated *in vitro* and summarized in **Table 23**. The results were expressed as IC₅₀ values (as μM concentration) and normal kidney epithelial cells (HEK293) were chosen as control of cytotoxicity and/or selectivity.

Among synthesized compounds **4e**, **11n** and **11o** were the most potent candidates against Mia Paca-2 cells with IC₅₀ values of 6.6, 5.5 and 6.5 μM respectively, but inactive against HeLa and CEM cells (IC₅₀>50 μM). However, **4e** also displayed good activity against SK-Mel 5 cells while **11n** were moderately active. Compounds **4g** and **4h** exhibited an excellent antiproliferative activity against CEM and SK-Mel 5 cells with IC₅₀ < 10 μM and a moderate activity against HeLa and Mia Paca-2 (IC₅₀> 20 μM) cells. **4k** showed the best activity against SK-Mel 5 cells and it also displayed good inhibitory activity against CEM. Interestingly, substitution of the *para* hydroxyl group of compound **4d** with methoxy leads to compound **4e** endowed with increased antiproliferative activity against Mia Paca-2 cells (52 to 6.6 μM respectively). Similarly, the introduction of -SO₂NH₂ at the 6-position on the benzothiazole ring, **11o**, increased potency. Curiously, in this case, substitution by *para*-methoxy has the same effect on Mia Paca-2 cells as substitution by -SO₂NH₂ in position 6 on benzothiazole, therefore activity of **4e** \cong **11o**. The shift of the hydroxyl along phenyl

group didn't have significant effect on the activity, whereas the introduction of a second or third hydroxyl group (compound **4g**, **4h** and **4k**) led to an increase in the antiproliferative activity on the CEM and SK-Mel 5 cells.

After introduction of the -SO₂NH₂ group into the benzothiazole skeleton of **4c** to obtain **11n**, an increase in activity against Mia Paca-2 cells was observed but activity against CEM, HeLa and SK-Mel 5 cells decreased. Apart from **4c** and **4d**, the introduction of -SO₂NH₂ into the backbone reduced the activity against Mia Paca-2 cells. All tested compounds showed low antiproliferative activity towards HeLa cell line, except compound **4h** with an inhibition activity less than 30 μM. To our surprise, replacement of the -SO₂NH₂ with -COOH led to almost total loss of activity.

On the basis of cytotoxicity screening, all unsubstituted compounds on the benzothiazole ring were cytotoxic to normal HEK293 except compound **4e** and **4i** with *para* methoxy on phenyl ring, suggesting the importance of *para*-methoxy for antiproliferative activity. However electron-withdrawing group -SO₂NH₂ on the benzothiazole ring decreased the cytotoxicity of the target compound, except compound **11o** and **11s** characterized by the presence of *para* hydroxyl on phenyl group. Compounds bearing -COOH on the benzothiazole ring (**11a-11k**) were inactive against both normal and cancer cells.

The Selectivity Index (SI) was determined by comparing the IC₅₀ (μM) obtained on the healthy cells (HEK) with that obtained on cancer cells (CEM, HeLa, Mia-Paca-2 and SK-Mel 5). From the results presented in **Table 23**, we observed that compounds **4e**, **11n** and **11o** were respectively 15, 18 and 5 fold more selective toward Mia-Paca-2 cells, while compounds **4g** and **4k** were approximately 6 fold more selective for CEM cells. **4e**, **4i** and **4k** showed selectivity for SK-Mel 5 cells. Compounds **4k** were 25 fold more selective for SK-Mel 5 cells that could be due to the presence of three hydroxyls on the phenyl ring. These observations revealed that, compounds **4g** and **4k** are the best candidates since they exhibited the most selective cytotoxicity for both CEM and SK-Mel 5 tumor cells line. The particularity of these compounds is the presence of -OH in position 2 and 5 on the phenyl ring. Therefore, these two positions are very important for the sought activity.

Class	compound	IC50 μ M					SI			
		CEM	HeLa	Mia-Paca-2	SK-Mel5	HEK293	CEM	HeLa	Mia-Paca-2	SK-Mel5
	4a	> 100	> 100	≥ 100	82 ± 23	> 100	-	-	-	1,22
A	4d	52 ± 0	46 ± 10	52 ± 10	51 ± 3	50 ± 2	0.96	1.09	0.96	0.98
	11d	77 ± 32	> 100	> 100	> 100	> 100	1.30	-	-	-
	11o	64 ± 24	67 ± 25	6.5 ± 0.5	33 ± 6	32 ± 4	0.50	0.48	4.92	0.97
B	4e	> 100	> 100	6.6 ± 3.3	14 ± 2	≥ 100	-	-	15.15	7.14
	11e	> 100	> 100	> 100	> 100	> 100	-	-	-	-
	11p	> 100	> 100	47 ± 16	> 100	≥ 100	-	-	2.13	-
C	4c	38 ± 2	44 ± 8	62 ± 14	17 ± 10	46 ± 2	1.21	1.05	0.74	2.71
	11c	> 100	> 100	72 ± 39	> 100	> 100	-	-	1.39	-
	11n	58 ± 19	77 ± 12	5.5 ± 3.1	43 ± 1	≥ 100	1.72	1.30	18.18	2.33
D	4b	63 ± 16	93 ± 10	> 100	34 ± 10	> 100	1.59	1.08	-	2.94
	11b	> 100	> 100	> 100	≥ 100	> 100	-	-	-	-
	11m	> 100	≥ 100	> 100	≥ 100	> 100	-	-	-	-
E	4f	52 ± 0	46 ± 10	52 ± 10	51 ± 3	50 ± 2	0.96	1.09	0.96	0.98
	11f	> 100	> 100	≥ 100	> 100	> 100	-	-	-	-
	11q	> 100	> 100	≥ 100	> 100	73 ± 38	-	-	-	-
F	4h	8.2 ± 5.7	29 ± 16	40 ± 21	5.4 ± 0.3	15 ± 4	1.83	0.52	0.38	2.78
	11h	> 100	> 100	> 100	> 100	> 100	-	-	-	-
	11s	19 ± 5	45 ± 9	41 ± 22	25 ± 2	14 ± 5	0.74	0.31	0.34	0.56
G	4i	51 ± 15	≥ 100	> 100	25 ± 3	≥ 100	1,96	-	-	4,00
	11i	> 100	> 100	80 ± 25	95 ± 7	> 100	-	-	1.25	1.05
	11t	59 ± 13	80 ± 29	≥ 100	> 100	≥ 100	1.69	1.25	-	-
H	4g	2.0 ± 1.6	74 ± 29	38 ± 3	5.3 ± 0.5	13 ± 5	6.50	0.18	0.34	2.45
	11g	> 100	> 100	66 ± 35	> 100	> 100	-	-	1.52	-
	11r	22 ± 6	90 ± 14	72 ± 21	> 100	62 ± 17	2.82	0.69	0.86	-
I	4j	32 ± 5	38 ± 6	52 ± 4	28 ± 2	33 ± 9	1.03	0.87	0.63	1.18
	11j	> 100	> 100	≥ 100	> 100	> 100	-	-	-	-
	11u	89 ± 15	> 100	≥ 100	74 ± 6	≥ 100	1.12	-	-	1.35
J	4k	18 ± 2	> 100	> 100	4.0 ± 0.2	> 100	5.56	-	-	25.00
	11k	91 ± 13	> 100	> 100	64 ± 26	> 100	1.10	-	-	1.56
	11v	> 100	> 100	> 100	> 100	> 100	-	-	-	-

Table 23: Inhibitory effects of benzothiazole derivatives on the proliferation of CEM, HeLa, Mia Paca-2 and SK-Mel 5

VI.2.2.6. Benzothiazole derivatives block hERG potassium channels expressed in HEK293 cells

In order to have an idea of the mechanism of compounds presenting a good antiproliferative profile, we studied the effect of these derivatives on the modulation of human ether-a-go-go related gene (hERG) current. hERG is a gene that codes for a protein highly selective for potassium channel. These protein channels are widely expressed, mainly in the cardiac tissues, neuronal tissues, brain, adrenal gland, thymus, retina and and some cancer cells [145]. Indeed, the ion channels are transmembrane proteins that regulate the flow of ions through biological membranes. In particular, potassium channels represent the most diverse group of ion channels and play an important role in several functions such as muscle excitation, regulation of blood pressure, proliferation of several types of cancer, such as prostate, colon, and glioma [146]. It has been shown that, hERG potassium channels are overexpressed in many types of human cancers as well as in primary human cancers [147]. In addition, it was shown that over-expression of hERG channels in HEK-293 cells greatly increased the proliferation, tumor cell invasion and metastasis. The blockade or inhibition of hERG in these cells induced both antiproliferative and antimigratory effects [148]. Therefore hERG channels reduce proliferation and impair invasiveness in a variety of cancer cell types. Seen those mentioned above, the interest in the study of hERG channels has increased exponentially, mainly because of its involvement in many cellular events such as repolarization and proliferation of cells. Therefore, given their multifunction, these channels are potential therapeutic targets for cancer treatment by application of hERG channel blocking.

One of precise method for determination of the compounds' potencies in K⁺ channel inhibition is patch-clamp electrophysiology. QPatch automated patch clamp system was used to evaluate the blockade of hERG potassium channels expressed in HEK293 cells. Three different concentrations (0.1, 1 and 10 μ M) of benzothiazole derivatives were tested and recapitulated in **Table 24**. E-4031 (methanesulfonanilide class III antiarrhythmic agent) is the reference compound for this assay. The percent inhibition of the peak tail current was measured, the concentration of drugs needed to yield a 50% blockade of the hERG current (IC₅₀) was obtained by fitting the data to a Hill equation (**Equation 8**).

4g reduced hERG to 60.32 \pm 2.43 % with pIC₅₀ equal to 5.32 (IC₅₀= 4.79 μ M) while **4e**, **11c**, **4k** and **11d** had an inhibition less than 50%. In comparison with the reference compound, **4g** is a potential candidate for blocking hERG potassium channels.

Compound	pIC ₅₀	% inhibition
4e	< 5	12.09 ± 5.05
4g	5.32 ± 0.04	60.32 ± 2.43
4k	< 5	41.17 ± 2.94
11c	< 5	20.73 ± 1.79
11d	< 5	8.07 ± 4.08
E-4031	7.55 ± 0.08	96.32 ± 0.9

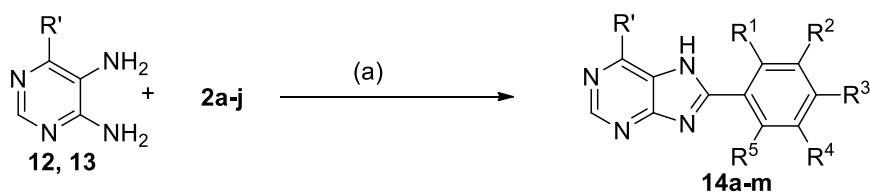
Table 24: *Inhibition of hERG channels by benzothiazole derivatives*

VI.3. Imidazopyrimidinederivatives

Imidazopyrimidine (Purine) derivatives and analogues possess a wide variety of biological properties such as antitumor, antitubercular, antifungal and antiviral activities [149]. For this reason, (di)substituted purine derivatives were synthesized in order to explore the possibility of their multi-target approach

VI.3.1. Chemistry

Like several heterocyclic compounds, the new class of purine compounds was synthesized through free solvent reaction and the principle is based on the melting point's difference. In one step we directly obtained the expected compounds. Condensation reaction of 6-hydroxy-4,5-diaminopyrimidine hemisulfate (**12**) or 4,5-diaminopyrimidine (**13**) with the corresponding mono and poly-benzaldehyde by heating under free solvent condition gave products **14a-m** (Schema 21). These products were purified by crystallization using appropriate solvents.



	R'	R ¹	R ²	R ³	R ⁴	R ⁵
a:	OH	H	H	H	H	H
b:	OH	OH	H	H	H	H
c:	OH	H	OH	H	H	H
d:	OH	H	H	OH	H	H
e:	OH	H	H	OCH ₃	H	H
f:	OH	OH	H	OH	H	H
g:	OH	OH	H	H	OH	H
h:	OH	H	OH	OH	H	H
i:	OH	H	OH	OCH ₃	H	H
j:	OH	H	OH	H	OH	H
k:	H	H	H	OH	H	H
l:	H	H	H	OCH ₃	H	H
m:	H	OH	H	H	OH	H

Scheme 21: Synthesis of compounds **14a-m**. Reagents and conditions: (a) Heat, free solvent, free catalyst.

VI.3.2. Biological Evaluation

VI.3.2.1. Photoprotection activity of purine derivatives

Purines derivatives were evaluated for their photoprotective activity using *in vitro* method described in paragraph V.1.2.1. SPF, UVA-PF, λ_c and the UVA/UVB ratio are shown in **Table 25**. The electronic transition responsible for the absorption spectra of substituted purines, depends on the HOMO-LUMO energy gap since substituted imidazopyrimidines are characterized by π - π^* and n- π^* ; these transitions are centred generally in the UV region between 220 and 300 nm. The presence of different substituents may cause a red shift or a blue shift in the transition and may generate novel bands. The appearance of novel fine structures reflects both the possibility that the system will assume new conformations, whether electronic transitions take place between the different vibrational energy levels possible for each electronic state.

The presence of aromatic group gives a bathochromic effect for all the components proposed and novel transitions appear as consequence of a highly conjugated system.

The -H group in position 6 of imidazopyrimidine ring has a major influence in the band-shift: comparing **14e** and **14l**, the spectrum presents a red-shift of the transition and higher energy transition disappears; while **14g** and **14m**, the two higher energy transitions of **14g** disappear, but on the contrary the transition band at lower energy has a blue-shift in **14m**.

Also the position of the functional group in the phenyl ring influences the number and the wavelength of the bands. Comparing **14b**, **14c** and **14d**, the *ortho* and *para* substitutions have a higher resonance effect respect to the *meta* position. The same behavior is registered for **14g** and **14h**. The mesomeric effect reflects on a red-shift of the transition and a finest structure of bands. The combination of the inductive effect of several -OH groups on the molecule gives a red-shift that indicates a lower energy level of the ground state and novel conformation seem to be possible as reason of the appearance of novel bands on the spectrum.

Comparing **14d** and **14k**, the major influence on the wavelength and the structure of the band depends on the substituent in position 6 of imidazopyrimidine ring (**Figure 24**). The contribution given in the inductive and mesomeric effect makes this position crucial in the definition of the energy asset of the entire molecules.

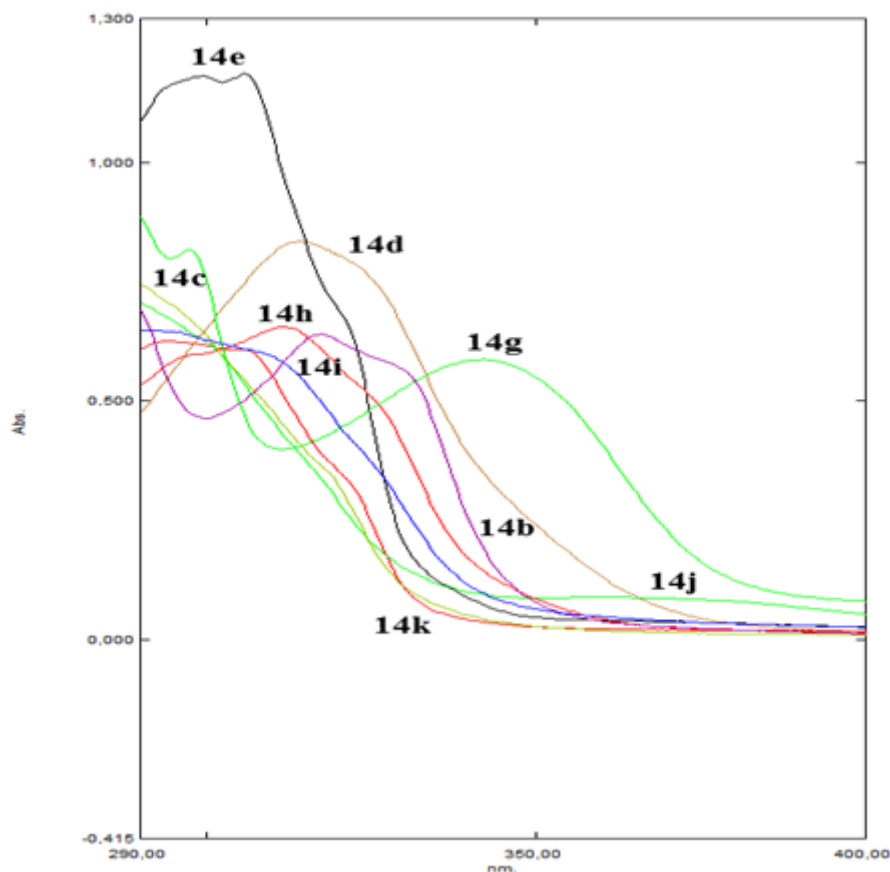


Figure 24: Spectral data of imidazopyrimidine derivatives

SPF value of **14b**, **14i** and **14k** characterized by the presence of *ortho* or *para*-OH of the phenyl ring are higher than lead compound (**PBSA**). Any other changes are inadequate for filtering activity. The UV-filtering activities for compounds **14k** and **14i** are remarkable as

compared to the others. This demonstrates that substitution of a phenyl sulfonic acid by a pyrimidine is compatible and even improves UV filtering capabilities as compared to the model **PBSA**. Interestingly, compound **14d** had a lower value in comparison with **14e** (methoxy-substitution at the 8-phenyl ring), indicating that the *para*-methoxy is better as compared with hydroxyl. Compounds **14j** and **14m** having two -OH in position 3,5 and 2,5, respectively of phenyl ring, had a lower value of SPF. However, compounds **14b** and **14i** had the same value of protection in spite of the presence of respectively *para*-OH and *meta*-OCH₃/*para*-OH on their aromatic group. But compound **14h** was less active than **14i**. Compounds **14h**, **14g** and **14j** featured two -OH on the aromatic moiety, on different position, and also a 6-OH on the purine ring and their activity order was **14g**, **14j** and **14h**. In this case we may advance the hypothesis that, having an OH group at position 6 increases the compound's activity.

In conclusion, compounds endowed with the best SPF (**14k** and **14l**) were those unsubstituted at the pyrimidine ring and featured by a methoxy or hydroxyl moiety in *para*-position. Any other modification decreased activity.

Another parameter important for determining the broad spectrum of the UV-filter is the critical wavelength λ_c . According to the classification shown in paragraph **V.1.2.1**, compounds **14d**, **14g**, **14m** and **14j** were rated as '4' while compounds **14e**, **14b**, **14k**, **14h**, **14i** and **14l** were rated as '2' and compound **14c** was rated as '1'. Therefore, the sole interesting compounds were **14d**, **14g**, **14j** and **14m**.

Finally, The UVA-PF values of all synthesized compounds were greater than the UVA-PF value of PBSA.

Taken together, these compounds were designed using **PBSA** as model compound. Compounds **14d**, **14g**, **14j** and **14m** could be defined as the best candidates for the development of broad-spectrum sunscreens although less efficient for UVA protection. However, considering only UVB absorbance **14k** and **14l** were really good candidates for further studies. Thus, the possible use strongly depends on the final application, only UVB or a wider range. An interesting final consideration is that the lack of the -OH group at the purine ring strongly increases UVB protection but reduces UVA filtering capabilities.

Compound	SPF	UVAPF	UVA/UVB	λ_c (nm)
PBSA	3.10± 0.09	1.03± 0.08	0.29	322
14b	3.17± 0.02	1.24± 0.02	0.62	340
14c	1.69± 0.08	1.04± 0.05	0.65	332
14d	1.45± 0.01	1.33± 0.05	0.95	381
14e	2.73± 0.12	1.09± 0.09	0.42	337
14g	2.19± 0.03	1.93± 0.12	1.01	371
14h	1.77± 0.15	1.10± 0.17	0.72	340
14i	2.55± 0.17	1.16± 0.01	0.54	349
14j	1.81± 0.13	1.67± 0.03	1.02	371
14k	8.63± 1.3	1.25± 0.11	0.18	335
14l	6.61± 0.07	1.40± 0.06	0.30	345
14m	1.71± 0.14	1.46± 0.13	0.88	384

Table 25: Filtering activity purine derivatives

VI.3.2.2. Antioxidant activity

All the synthesized purines were evaluated for their *in vitro* antioxidant activity by DPPH and FRAP assays (paragraph V.1.2.2). The results are expressed respectively in IC₅₀ value ($\mu\text{g/mL}$) and $\mu\text{molT/g}$, and summarized in **Table 26**. Antioxidant activity varies with substitution of the number and the position of the -OH on the phenyl ring. The hydroxyl group in position 6 of the purine ring is very important: when not present the activity considerably decreases. Compounds with two hydroxyl groups on the phenyl ring and a hydroxyl in position 6 of the imidazopyrimidine ring (**14g**, **14h**, **14e**) showed the highest potency in the DPPH assay and the best result is obtained with **14h**, while compounds with only one -OH on the phenyl ring were moderately potent (**14b**, **14c**, **14d**). In agreement with these results we could confirm that the feature responsible of the increase in antioxidant activity is the presence of an additional -OH group on the phenyl ring. Of interest, when the OH-group of the phenyl ring of **14d** is substituted by a methoxy (compound **14e**) activity increased but, however, when the same replacement is applied at position 4 the activity decreased (i.e. **14h** vs **14i**). This is difficult to explain but certainly related to the presence of the OH-group in the *para*-position. The poor antioxidant capacity of **14k**, **14i**, **14l** confirms the importance of the OH-group in position 6 of the imidazopyrimidine ring. The mono phenolic compounds **14b**, **14d** have the -OH at the *ortho* and *para*-position and are more active. The *para* position is favored because the *ortho* -OH moiety can establish a hydrogen bond between the nitrogen of the purine ring and the -OH phenyl ring. This hypothesis is confirmed by the result obtained with **14g**, **14h**. In both DPPH and FRAP assays, compounds with methoxy moieties in the *para*

position of the phenyl ring (compound **14e**) give better results, comparable to that of molecules with a hydroxyl at the same position (compound **14d**). Considering FRAP assay, the molecule with a better antioxidant profile is **14h**, bearing two hydroxyl groups in positions 3 and 4 of the phenyl ring, then followed by **14g** and **14e**.

Compound	DPPH IC50 (µg/ml)	FRAP µmolT/g
14b	83.42 ± 3.09	520.01 ± 8.74
14c	154.07 ± 2.54	363.45 ± 0.53
14d	46.90 ± 0.23	2680.00 ± 0.96
14e	24.09 ± 0.98	3537.078 ± 1.52
14g	8.59 ± 0.67	3810.10 ± 0.38
14h	15.60 ± 0.30	7557.50 ± 0.69
14i	98.16 ± 1.64	2002.46 ± 0.84
14j	N.D. ^[a]	N.D. ^[a]
14k	63.88 ± 2.31	384.11 ± 4.55
14l	775.12 ± 8.48	45.99 ± 2.22
14m	133.11 ± 4.01	479.92 ± 0.38

^[a] not detected

Table 26: Antioxidant activity of the compounds. Each value was obtained from three different experiments (mean ± SE).

VI.3.2.3. Antifungal activity

Synthesized compounds were investigated for their antifungal activities against six dermatophytes responsible for the most common dermatomycoses: *Microsporum gypseum*, *Arthroderma cajetani*, *Trichophyton mentagrophytes*, *Epidermophyton floccosum*, *Trichophyton tonsurans* and *Microsporum canis*. Inhibition of the dermatophytes was evaluated daily by measuring the colony diameter at each disk (**Table 27**). All the tested compounds showed inhibitory activities toward the six species of fungi. Compounds **14c** and **14d** at the concentration of 100 µg/mL were active against *A. cajetani*, *T. mentagrophytes* and *M. canis*. Compound **14l** at 100 µg/ml displayed moderate activity against *T. mentagrophytes*, *T. tonsurans* and *M. canis*. Compounds **14m** and **14i** showed activity against *E. floccosum*.

Compound concentrations should deserve special attention because of the poor solubility in the medium for many of the compounds. Indeed **14b**, **14d**, **14e**, **14g**, **14h**, **14j** and **14m** at a concentration of 100 µg/ml plunged into the plates, therefore only the next lower concentration could be taken into consideration.

Entry	[] µg/mL	<i>M.</i> <i>gypseum</i>	<i>A.</i> <i>cajetani</i>	<i>T.</i> <i>mentagrophytes</i>	<i>E.</i> <i>floccosum</i>	<i>T.</i> <i>tonsurans</i>	<i>M.</i> <i>canis</i>
14b	20	1.69± 0.01	6.67± 0.36	+	2.63± 0.02	+	+
	100	5.08± 0.18	0.74± 0.03	+	5.26± 0.34	14.71± 0.01	+
14c	20	+	12.10± 0.20	7.33± 0.11	0.00± 0.17	+	1.26± 0.11
	100	2.65± 0.09	16.94± 1.31	28.00± 1.56	2.86± 0.55	0.00± 0.39	11.32± 0.53
14d	20	1.71± 0.02	4.92± 0.34	1.69± 0.01	+	+	6.86± 0.26
	100	4.27± 0.11	21.31± 0.99	23.73± 0.08	+	2.82± 0.06	18.29± 0.49
14e	20	5.71± 0.29	+	+	+	8.70± 1.55	10.57± 0.15
	100	12.4± 0.33	+	2.08± 0.16	+	17.39± 2.56	17.07± 1.80
14g	20	+	+	+	+	+	1.72± 0.05
	100	2.20± 0.18	+	0.73± 0.01	+	7.94± 1.62	6.03± 0.02
14h	20	2.65± 0.14	2.88± 0.54	+	+	6.33± 1.45	2.5± 0.08
	100	6.19± 0.26	5.04± 0.37	+	+	12.66± 2.05	3.75± 0.34
14i	20	4.35± 0.36	9.78± 1.45	0.97± 0.05	15.22± 1.09	+	2.48± 0.18
	100	7.61± 0.04	13.04± 1.86	1.94± 0.04	19.57± 0.06	9.76± 0.41	4.13± 0.60
14j	20	+	8.24± 0.45	+	14.52± 1.61	+	+
	100	0.00± 0.45	15.29± 2.45	5.51± 1.23	16.29± 1.33	3.51± 0.09	2.21± 0.06
14k	20	4.63± 0.17	7.81± 0.23	3.65± 1.58	+	+	+
	100	6.48± 0.27	7.81± 1.26	+	+	2.70± 0.02	+
14l	20	4.67± 0.41	+	3.51± 0.04	0.00± 0.23	5.26± 1.01	2.19± 0.11
	100	16.82± 0.15	+	24.56± 0.89	4.55± 1.67	15.79± 1.22	22.63± 0.18
14m	20	0.00± 0.19	+	+	0.00± 0.03	10.00± 0.34	+
	100	4.30± 0.65	+	+	23.91± 1.98	17.50± 3.05	4.42± 1.05

+ the compound stimulates the growth of the fungus

[] concentration

Table 27: Percent growth inhibition of dermatophytes treated with the substituted purine derivatives at 20 or 100 µg/mL. Each value is the mean of three measurements.

VI.3.2.4. Antiproliferative activity

Antiproliferative activity was determined for five cancerous cell lines: murine leukemia (L1210), human CD₄⁺ T-lymphoma (CEM), human cervix carcinoma (HeLa), human pancreatic (Mia Paca-2) and human endothelial (HMEC-1) cells (**Table 28**). Compound **14e** displayed good activity against all the assayed cell lines, in particular L1210, CEM and Mia Paca-2. Thus, -OCH₃ in *para* position of the phenyl group seems important for the antiproliferative activity. Compounds **14g**, **14h**, **14i**, **14k** and **14l** showed slight inhibitory activity on HMEC-1. However, compound **14h** is also active against L1210. Compound **14m** showed a lower activity against all the assayed cell lines, likely due to the lack of -OH in position 6 of imidazopyrimine ring. None of the compounds were cytotoxic against primary human embryonic lung fibroblast cell cultures (**Table 28**).

Compound	IC ₅₀ ^a (μ M)					MIC ^b (μ M)
	L1210	CEM	HeLa	Mia-Paca-2	HMEC-1	HEL
14b	148 \pm 0	112 \pm 1	240 \pm 13	126 \pm 6	142 \pm 78	> 100
14c	\geq 250	176 \pm 20	\geq 250	\geq 250	\geq 250	> 100
14d	194 \pm 80	118 \pm 4	\geq 250	135 \pm 6	108 \pm 2	> 100
14e	30 \pm 11	23 \pm 6	58 \pm 0	34 \pm 29	55 \pm 31	100
14g	155 \pm 108	\geq 250	> 250	> 250	92 \pm 13	> 100
14h	18 \pm 5	106 \pm 2	192 \pm 82	106 \pm 5	38 \pm 28	> 100
14i	143 \pm 17	152 \pm 48	> 250	177 \pm 43	92 \pm 10	> 100
14j	\geq 250	\geq 250	\geq 250	184 \pm 94	119 \pm 23	> 100
14k	214 \pm 50	214 \pm 50	193 \pm 13	160 \pm 47	45 \pm 6	> 100
14l	185 \pm 47	109 \pm 24	156 \pm 2	132 \pm 11	93 \pm 19	> 100
14m	> 250	> 250	> 250	> 250	> 250	> 100

^a 50% Inhibitory concentration or compound concentration required to inhibit cell proliferation by 50%. Five-fold dilutions of the test compounds starting with 250 μ M as highest concentration were tested.

^b Minimal inhibitory concentration or compound concentration required to cause a microscopically visible alteration of human embryonic lung fibroblast (HEL) cell morphology.

Table 28: *Inhibitory effects of substituted purine derivatives on the proliferation of L1210, CEM, HeLa, Mia Paca-2 and HMEC-1 cells*

VII: Stability studies

Stability of all synthesized compounds (benzimidazole, benzothiazole and imidazopyrimidine) was studied in DMSO, MeOH and/or H₂O at a concentration of 0.0015% by HPLC. Study conditions included room temperature and accelerated aging at 40°C. Benzimidazole derivatives and 2-arylbenzothiazoles were studied in MeOH while 2,6-disubstitutedbenzothiazoles were studied in DMSO and H₂O. Imidazopyrimidine were studied in DMSO.

All compounds showed good stability, either in DMSO, MeOH and/or H₂O with the exception of the compound **11f**, which in one month showed a degradation of 50% (**data not shown**). However, the compounds stored at room temperature are more stable than those stored in the oven at 40 ° C.

VIII. Conclusion

Compound libraries were carried out using PBSA as lead compound. Since isosteric modification is the main strategy used in Medicinal Chemistry for development of innovation drug from commercial drug, we have exploited it in order to design desiderate compounds. In fact, classical and non-classical isosteres modifications were applied on PBSA to obtain benzimidazole, benzothiazole and imidazopyrimidine derivatives.

Nine benzimidazole derivatives were obtained by isosteric replacement of phenyl present in position 2 of PBSA with 5-membered ring (furan, thiophene and pyrrole) and replacement of $-\text{SO}_3\text{H}$ by $-\text{COOH}$ and $-\text{H}$. These novel series of compounds were synthesized through the condensation reaction between diamine and aldehyde derivatives in the presence of sodium bisulfite as catalyst. All compounds were obtained in good yield and their structures were characterized by the IR and UV spectroscopy, ^1H and ^{13}C NMR and mass spectroscopy. According to the design of multifunctional compounds and the biological activities of benzimidazole derivatives described in the literature, synthesized benzimidazoles were evaluated for their antioxidant, UV-filter, antifungal and antiproliferative activities.

Regarding the antifungal activity, compounds **DE31**, **DE35** and **DE37** exhibited good antifungal activity against *M. gypseum*, *M. canis*, *T. mentagrophytes*, *T. tonsurans* and *E. floccosum* with IC_{50} values in the range of 0.97– 3.80 $\mu\text{g}/\text{mL}$. Nevertheless, compound **DE 35** showed the best activity with IC_{50} range of 0.97-1.53 $\mu\text{g}/\text{mL}$. This compound is characterized by the presence of pyrrole in position 2 of the benzimidazole ring and devoid functional group in position 5. In addition, compounds **DE 38** and **DE 40** exhibited good activity against *Candida albicans* with $\text{MIC} = 16 \mu\text{g}/\text{mL}$.

Considering UV-filtering capacity, compounds **DE 31**, **DE 35** and **DE 37** showed good UVB-filter compared to PBSA, and the best photoprotective compound was **DE 37** bearing furan in position 2 of the benzimidazole ring and without substitution in position 6. However, all synthesized compounds had $\lambda_c < 370 \text{ nm}$, therefore none of these compounds has demonstrated a broad spectrum profile.

As regards antioxidant activity, compounds **DE 35** and **DE 37** showed good antioxidant activity; however according to DPPH test only **DE 35** endowed antioxidant activity, which could be due to the fact that the pyrrole group has a hydrogen donor which confers on the molecule the ability to trap the DPPH radical. According to FRAP test, both **DE 35** and **DE 37** had good antioxidant activity and the best had **DE 37**.

Finally, regarding the antiproliferative activity, compounds **DE35** displayed good activity against SK-Mel 5 (human melanoma cells) with $IC_{50} = 9.7 \mu M$.

Taken together all performed biological test, the best multifunctional molecule was **DE 35**, which well showed a wide range as UV-filter, antioxidant, antifungal and antiproliferative activities. Compound **DE 37** also displayed good UV-filter, antioxidant and antifungal activities. Therefore, this series of benzimidazoles has a very interesting biological activity; they could be useful for developing novel multifunctional molecules for the treatment of multifactorial diseases. Compound **DE 35** is a potential candidate in the development of drugs in case of cutaneous neoplastic diseases, in particular melanoma.

Thirty benzothiazole derivatives were carried out by an isosteric modification of the benzoimidazole nucleus (PBSA) with the benzothiazole nucleus, replacement of phenyl ring with (poly)phenol and substitution of $-SO_3H$ with $-SO_2NH_2$, $-COOH$ and $-H$. Compounds were synthesized via the condensation reaction between 2-aminothiophenols and benzaldehyde derivatives using sodium hydrosulfite and obtained compounds were investigated for *in vitro* UV-filter capacity, antioxidant, antifungal and antiproliferative activities.

Regarding UV-filter capacity, compounds **4g**, **4h**, **4k**, **11d**, **11g**, **11o** and **11r** could be considered as broad-spectrum and UVA-filter compounds since their $\lambda_c \geq 370$ nm and the UVA-PF value of each compound was greater than 1/3 of its SPF value. Compounds **4d** and **4j** were the potential candidates for UVB protection.

According to antifungal activity, compound **4h** showed the highest activity against all five dermatophytes, in particular against *Microsporum gypseum*, *Trichophyton tonsurans* and *Epidermophyton floccosum* with range IC_{50} of 11.63 - 43.31 $\mu g/mL$. This compound is more active against *E. floccosum* with $IC_{50} = 11.63 \mu g/mL$. Significant activity was also observed for compounds **4f** and **4g** against *Microsporum gypseum* and *Epidermophyton floccosum*. Moreover compounds **4f** and **4k** were more effective against *candida albicans* with MIC = 4 and 8 $\mu g/mL$ respectively.

Molecules with good antioxidant profile were compounds of classes **F** and **H**, characterized respectively by the presence of two hydroxyl groups in positions 3,4 and 2,5- of the phenyl ring. The best was compound **4g** according to DPPH test, whereas according to FRAP, the best was **11h**.

With regard to the antiproliferative activity, compounds **4g** and **4k** are the best candidates since they exhibited against both CEM and SK-Mel 5 tumor cells line. While compounds **4e**, **11n** and **11o** were respectively 15, 18 and 5 fold more selective toward Mia-Paca-2

cells. Furthermore, since hERG potassium channels are over-expressed in many types of human tumors and significantly increasing proliferation, tumor cell invasion and metastasis, they are potential therapeutic targets for cancer treatment. This therapy can be performed using hERG channel blockers. In this work, the QPatch assay with automated patch clamp system was used to evaluate the blockade of hERG potassium channels expressed in HEK293 cells. **4g** reduced hERG channels to 60.32% with pIC₅₀ equal to 5.32 (IC₅₀ = 4.79 μM), therefore it could be a potential candidate for blocking hERG potassium channels.

Considering the biological tests evaluated, compound **4g** and **4k** could be potential candidates for the design of multifunctional drugs by virtue of their diverse biological activities. In addition, benzothiazole derivatives might have possible application as drugs for the treatment of neoplastic diseases such as childhood leukemia, pancreatic cancer and melanoma.

Thirteen imidazopyrimidine derivatives were obtained through isosteric modification of benzene (benzimidazole ring of PBSA) with pyrimidine and replacement of phenyl ring with (poly)phenol. Desiderate compounds were synthesized via condensation reaction of 6-hydroxy-4,5-diaminopyrimidine hemisulfate or 4,5-diaminopyrimidine with the corresponding benzaldehydes under free solvent and free catalyst. According to the results of in vitro photoprotection, compounds **14g**, **14j** and **14m** could be defined as the best candidates since they provided a broad spectrum profile. However **14k** and **14l** showed good protection against UVB.

Regarding antioxidant activity, Compounds **14e**, **14g**, **14d** and **14h** showed good antioxidant activity. The particularity of these compounds is the presence of electron or hydrogen donor group (-OCH₃, -OH) in position *orto* or *para* of the phenyl ring. Interestingly, compound **14e** with -OCH₃ in the *para* position of the phenyl ring gave better results comparable to **14d** bearing -OH at the same position.

In terms of antifungal activity, compounds **14c** and **14d** at the concentration of 100 μg/mL were slight active against *A. cajetani*, *T. mentagrophytes* and *M. canis*, while compound **14l** at 100 μg/mL displayed moderate activity against *T. mentagrophytes*, *T. tonsurans* and *M. canis*. Finally, compounds **14m** and **14i** showed slight activity against *E. floccosum*.

As regards antiproliferative activities, Compound **14e** displayed activity against all the assayed cell lines, in particular L1210, CEM and Mia-Pa-2 cells line. Thus, -OCH₃ in *para* position of the phenyl group seems important for the antiproliferative activity. However,

compound **14h** exhibited good active against L1210 and HMEC-1 and compounds **14g**, **14i**, **14k** and **14l** showed slight inhibitory activity on HMEC-1.

Taken together all biological tests, the best multifunctional molecule was **14g**, which well performed as wide range UV filter, antioxidant and antiproliferative activity.

In summary, isosteric modifications in PBSA have led to benzimidazole, benzothiazole and purine derivatives with important biological tests. They are promising candidates in the development of UV radiation-protective molecules in case of skin cancer such as melanoma or in the development of prescription drugs in cases of childhood cancer and pancreatic cancer. Therefore, these classes of compounds can have both cosmetic and pharmaceutical applications. To confirm this proposal, studies will be carried out to verify the safety, the pharmacodynamic and pharmacokinetic profile.

IX. Experimentalsection

IX.1. General information

Reagents and solvents were purchased from Sigma-Aldrich and Carlo Erba Reagenti (Italia) and without further purification. Analytical TLC was performed on silica gel plates (Macherey-Nagel Poligram SIL G/UV254 0.20 mm) and visualized by exposure to ultraviolet light (254 nm) and /or used 1% solution of KMnO₄. Column chromatography was performed using silica gel Macherey-Nagel 60M 230400 mesh. ¹H-NMR and ¹³C-NMR were registered on VXR-200 Varian spectrometer and Mercury Plus- at room temperature. Chemical shifts are measured with respect to tetramethylsilane and relative to residual solvent peaks as an internal standard set to D₂O and (CD₃)₂SO and are expressed in parts per million (ppm). The following abbreviations are used to indicate signal multiplicity: s (singlet), d (doublet), t (triplet), q (quartet), m (multiplet), brs (broad singlet) and dd (doublet of doublets). Molecular weights of the compounds were determined by ESI (Micromass ZMD 2000), and the values are expressed as [MH]⁺. UV spectrophotometric analyses were carried out on a UV-VIS spectrophotometer (Shimadzu UV-2600) or on a Life Science UV/VIS spectrophotometer (Beckman Coulter™, DU@530, Single Cell Module). Stability of compounds was determined by HPLC analysis performed using an Agilent 1100 Series HPLC System equipped with a G1315A DAD, autosampler and with a Phenomenex Synergi Hydro-RP C18 80Å column (4.6 × 150 mm, 4 μm).

IX.2. Synthetic Procedures

IX.2.1. Synthesis of Benzimidazole derivatives

3,4-Diamino-benzenesulfonic acid, sulfate salt (I)

To 0.5 g (4.62 mmoles) of o-phenylenediamine were added 3 mL of 96% sulfuric acid at 0 ° C under stirring, then the solution was refluxed for 24 hours. The reaction mixture was cooled and then cold water was added to obtain a precipitate. The mixture was filtered and washed with methanol to obtain 0.62 g of white powder, 46% yield

¹H NMR (400MHz, DMSO-d₆): δ(ppm) 6.80 (s,1H),6.60(d, 1H),6.54(t, 1H). ¹³C-NMR (400MHz, DMSO-d₆): 140.03, 138.39, 135.04, 118.22, 117.01.ESI-M [M+H]⁺: calcdforC₆H₁₀N₂O₇S₂, 2885.99; found286.27.

General method for the synthesis of benzimidazole derivatives

Synthesis of 2-substitutedbenzimidazoles

To a solution mixture of 3 mmol of **I** and 4 mmol of aldehyde in ethanol (3ml), 6 mmol of sodium bisulfite were added under stirring. The reaction mixture was heated at 80°C under reflux for 24 hours. The solvent was then evaporated under vacuo and the solid was treated with HCl 2N. The suspension was filtered and the solid was washed with ethanol to afford desired product.

2-(thiophen-2-yl)benzimidazole (DE 31): yield 72%; yellow solid; m.p. > 250°C. ¹H NMR (400MHz, DMSO-d₆): δ (ppm) 7.98-7.72 (d, 4H), 7.24 (t, 2H), 7.00(t, 1H). ¹³C-NMR (400MHz, DMSO-d₆): 145.33, 142.71, 140.11, 139.67, 128.07, 127.23, 126.61, 122.00, 114.25. ESI-M [M+H]⁺: calcd for C₁₁H₈N₂S, 200.04; found 200.11.

2-(1H-pyrrol-2-yl)benzimidazole (DE 35): yield 55%; yellow solid; m.p. > 250°C. ¹H NMR (400MHz, DMSO-d₆): δ (ppm) 7.84 (d, 2H), 7.47 (t, 2H), 7.01 (d, 1H), 6.65 (d, 1H), 6.33(t, 1H). ¹³C-NMR (400MHz, DMSO-d₆): 154.34, 134.04, 120.89, 119.30, 113.45, 110.11, 105.86. ESI-M [M+H]⁺: calcd for C₁₁H₉N₃, 183.08; found 183.12.

2-(furan-2-yl)benzimidazole (DE 37): yield 60%; yellow solid; m.p. > 250°C. ¹H NMR (400MHz, DMSO-d₆): δ (ppm) 8.10-7.90 (d, 3H), 7.19 (t, 2H), 7.09 (d, 1H), 6.70 (t, 1H). ¹³C-NMR (400MHz, DMSO-d₆): 154.04, 141.45, 140.76, 139.11, 123.45, 115.09, 112.86, 107.23. ESI-M [M+H]⁺: calcd for C₁₁H₈N₂O, 184.06; found 184.21.

Synthesis of 2-substitutedbenzimidazole-5-carboxylicacids

To a solution mixture of 3 mmol of **II** and 4 mmol of aldehyde in ethanol (3ml), 6 mmol of sodium bisulfite were added under stirring. The reaction mixture was heated at 80°C under reflux for 24 hours. The solvent was then evaporated under vacuo and the solid was treated with HCl 2N. The suspension was filtered and the solid was washed with ethanol to afford desired product.

2-(1H-pyrrol-2-yl)benzimidazole -5-carboxylicacid (DE 36): yield 51%; yellow solid; m.p. > 250°C. ¹H NMR (400MHz, DMSO-d₆): δ(ppm) 11.23 (br, COOH), 8.14(s, 1H), 8.00 (dd, 1H), 7.80 (d, 1H), 6.77(d, 1H), 6.50 (d, 1H), 6.43 (t, 1H). ¹³C-NMR (400MHz, DMSO-d₆): 166.00, 155.68, 146.91, 138.56, 128.87, 126.88, 120.55, 116.31, 111.75, 107.70. ESI-M [M+H]⁺: calcd for C₁₂H₉N₃O₂, 227.07; found 227.32.

2-(furan-2-yl)benzimidazole -5-carboxylic acid (DE 38): yield 49%; yellow solid; m.p. > 250°C. ¹H NMR (400 MHz, DMSO-d₆): δ (ppm) 11.19 (br, COOH), 8.30 (s, 1H), 8.16 (d, 1H), 8.06 (dd, 1H), 7.89 (d, 1H), 7.76 (d, 1H), 6.50 (t, 1H). ¹³C-NMR (400 MHz, DMSO-d₆): 166.73, 154.02, 145.55, 142.03, 139.40, 138.00, 126.62, 120.13, 115.74, 113.11, 106.85. ESI-M [M+H]⁺: calcd for C₁₂H₈N₂O₃, 228.05; found 228.14.

2-(thiophen-2-yl)benzimidazole -5-carboxylic acid (DE 40): yield 69%; yellow solid; m.p. > 250°C. ¹H NMR (400 MHz, DMSO-d₆): δ (ppm) 11.26 (br, COOH), 8.25 (s, 1H), 8.02 (dd, 1H), 7.82 (d, 1H), 7.75 (d, 1H), 7.50 (d, 1H), 7.01 (t, 1H). ¹³C-NMR (400 MHz, DMSO-d₆): 166.07, 146.76, 141.86, 138.62, 129.11, 118.65, 114.04, 113.29. ESI-M [M+H]⁺: calcd for C₁₂H₈N₂O₂S₂, 244.03; found 244.26.

Synthesis of 2-substituted benzimidazole-5-sulfonic acid

To a solution mixture of 3 mmol of **IV** and 4 mmol of aldehyde in ethanol (3 ml), 6 mmol of sodium bisulfite were added under stirring. The reaction mixture was heated at 80°C under reflux for 24 hours. The solvent was then evaporated under vacuo and the solid was treated with HCl 2N. The suspension was filtered and the solid was washed with ethanol to afford desired product.

2-(1H-pyrrol-2-yl)benzimidazole -5-sulfonic acid (DE 64): yield 56%; Yellow solid; m.p. > 250°C. ¹H NMR (400 MHz, DMSO-d₆): δ (ppm) 8.99 (s, 1H), 7.79 (m, 2H), 6.80 (d, 1H), 6.55 (d, 1H), 6.10 (t, 1H). ¹³C-NMR (400 MHz, DMSO-d₆): 154.33, 140.51, 138.71, 121.65, 117.82, 111.80, 106.02. ESI-M [M+H]⁺: calcd for C₁₁H₉N₃O₃S, 263.04; found 263.17.

2-(thiophen-2-yl)benzimidazole -5-sulfonic acid (DE 66): yield 69%; yellow solid; m.p. > 250°C. ¹H NMR (400 MHz, DMSO-d₆): δ (ppm) 8.00 (s, 1H), 7.80 (d, 1H), 7.60 (d, 1H), 7.50 (d, 2H), 7.20 (t, 1H). ¹³C-NMR (400 MHz, DMSO-d₆): 145.45, 143.42, 141.67, 140.39, 128.00, 121.88, 116.43, 113.09. ESI-M [M+H]⁺: calcd for C₁₁H₈N₂O₄S₂, 280.00; found 280.18.

2-(furan-2-yl)benzimidazole -5-sulfonic acid (DE 68): yield 40%; yellow solid; m.p. > 250°C. ¹H NMR (400 MHz, DMSO-d₆): δ (ppm) 8.14-8.00 (m, 2H), 7.55 (m, 2H), 7.11 (d, 1H), 6.60 (t, 1H). ¹³C-NMR (400 MHz, DMSO-d₆): 154.01, 145.69, 142.54, 140.63,

138.48, 121.00, 117.19, 111.89, 106.09. ESI-M $[M+H]^+$: calcd for $C_{11}H_8N_2O_4S$, 264.02; found 264.22.

IX.2.2. Synthesis of Benzothiazole derivatives

General Method for the Synthesis of 2-arylbenzothiazoles unsubstituted on the benzothiazole ring

To a solution of 2-aminothiophenol (3.2 mmol) and aldehyde (3.2 mmol) in ethanol (3.5mL) at room temperature was added solution of sodium hydrosulfite (2 eq. in 3 mL H_2O). The mixture was heated at reflux for 12 h. After cooling to room temperature, the solution was concentrated in vacuo. The residue was treated with HCl 2N and filtered to obtain the crude solid, which was recrystallized from appropriate solvent.

2-phenylbenzothiazole (4a): yield 60%; white solid; mp 98–99°C. IR (KBr) cm^{-1} : 3446.68, 1589.75, 1474.34, 1316.39, 1217.18, 756.85. 1H NMR (400MHz, DMSO- d_6): δ (ppm) 8.10-8.01 (dd,2H),7.98 (dd, 2H), 7.56 (t, 2H), 7.42 (m, 2H), 7.33(t, 1H). ^{13}C -NMR (400MHz, DMSO- d_6): 169.45, 154.4, 143.65, 133.32, 131.87, 130.32, 129.00, 126.76, 124.54, 123.67 and 120.09.ESI-M $[M+H]^+$: calcd for $C_{13}H_9NS$, 211.05; found 211.20.

2-(2-hydroxyphenyl)benzothiazole (4b): yield 80%; yellow solid; mp 125-126.4 °C. IR (KBr) cm^{-1} : 3000.52, 1589.13, 1479.79, 1315.15, 1214.40, 724.70. 1H NMR (400MHz, DMSO- d_6): δ (ppm) 11.65(1H br OH), 8.21-8.18 (2H,m), 8.07 (1H,d), 7.58-7.39 (3H, m), 7.15-7.01 (2H, m). ESI-MS $[M+H]^+$: calcd for $C_{13}H_9NOS$, 228.04; found 228.17.

2-(3-hydroxyphenyl)benzothiazole (4c): yield 71%; yellow solid; mp 158-159 °C. IR (KBr) cm^{-1} : 3251.25, 1597.99, 1453.57, 1317.08, 1231.33, 759.01. 1H NMR (400MHz, DMSO- d_6): δ (ppm) 9.93(1H br OH), 8.19 (1H,d), 8.08 (1H,d), 7.60-7.39 (5H, m), 6.99 (1H, dd). ESI-MS $[M+H]^+$: calcd for $C_{13}H_9NOS$, 228.04; found 227.97

2-(4-hydroxyphenyl)-benzothiazole (4d): yield 78%; yellow solid; mp 224-225 °C. IR (KBr) cm^{-1} : 3200.52, 1603.51, 1424.65, 1283.49, 754.39. 1H NMR (400MHz, DMSO- d_6): δ (ppm)10.22(1H br OH), 8.08 (1H,d), 7.98 (1H,d), 7.96 (2H, dd), 7.38-7.56 (2H, m), 6.91 (2H, dd). ESI-MS $[M+H]^+$: calcd for $C_{13}H_9NOS$, 228,04; found 228.18.

2-(4-methoxyphenyl)-benzothiazole (4e): yield 82%; white solid; m.p. 118–119 °C. IR (KBr) cm^{-1} : 2995.99, 2835.91, 1589.13, 1433.59, 1224.41, 1170.73, 751.73. 1H NMR

(400MHz, DMSO-d₆): δ (ppm) 8.17- 7.98 (4H, m), 7.46-7.38 (2H,t), 7.17 (2H,dd), 3.92(3H, s). ESI-MS [M+H]⁺: calcd for C₁₄H₁₁NOS, 241.06; found 241.27.

2-(2,4-dihydroxyphenyl)-benzothiazole (4f): yield 68%; yellow solid; m.p. 212–213 °C. IR (KBr) cm⁻¹: 3446.68, 1599.75, 1474.34, 1217.18, 756.85. ¹H NMR (400MHz, DMSO-d₆): δ (ppm) 8.18-8.01 (2H, dd), 7.56-7.46 (3H,m), 6.42 (1H,d), 6.33(1H, s). ESI-MS [M+H]⁺: calcd for C₁₃H₉NO₂S, 243.04; found 243.11.

2-(3,4-dihydroxyphenyl)-benzothiazole (4h):yield 70%; yellow solid; m.p. 216–217 °C. IR (KBr) cm⁻¹: 3488.58, 2916.83, 1599.09, 1474.34, 1260.50, 754.05. ¹H NMR (400MHz, DMSO-d₆): δ (ppm) 8.12-7.98 (2H, dd), 7.56 (2H,m), 7.41 (2H,m), 6.88(1H, d). ESI-MS [M+H]⁺: calcd for C₁₃H₉NO₂S, 243.04; found 243.29.

2-(3-hydroxy-4-methoxyphenyl)-benzothiazole (4i):yield 65%; white solid; m.p. 184–185°C. IR (KBr) cm⁻¹: 3252.29, 1597.41, 1474.34, 1122.71, 763.91. ¹H NMR (400MHz, DMSO-d₆): δ (ppm) 9.49 (1H, brs, OH), 8.08 (1H, d), 7.98 (1H, d), 7.56-7.46 (3H, m), 7.40 (1H, t), 7.01(1H, d). ESI-MS [M+H]⁺: calcd for C₁₄H₁₁NO₂S, 257.05; found 257.09.

2-(2,5-dihydroxyphenyl)-benzothiazole (4g): yield 58%; yellow solid; m.p. 220–221°C. IR (KBr) cm⁻¹: 3332.79, 1579.75, 1495.95, 1197.20, 756.53. ¹H NMR (400MHz, DMSO-d₆): δ (ppm) 8.17-8.01 (2H,dd), 7.59-7.38 (3H,m), 6.98-6.82 (2H,d). ESI-MS [M+H]⁺: calcd for C₁₃H₉NO₂S, 243.04; found 243.14.

2-(3,5-dihydroxyphenyl)-benzothiazole (4j): yield 58%; yellow solid; m.p. 225–226°C. IR (KBr) cm⁻¹: 3068.72, 1606.88, 1438.28, 1147.93, 755.64. ¹H NMR (400MHz, DMSO-d₆): δ (ppm) 10.01-10.22(2H, br, OH), 8.05 (1H, d), 7.96 (1H, d), 7.38-7.56 (2H, m), 6.98 (2H, d), 6.29 (1H, s). ESI-MS [M+H]⁺: calcd for C₁₃H₉NO₂S, 243.04; found 243.29.

2-(2,4,5-trihydroxyphenyl)-benzothiazole (4k): yield 51%; grey solid; m.p. 225–226°C. IR (KBr) cm⁻¹: 3068.80, 1603.17, 1437.76, 1150.33, 756.09. ¹H NMR (400MHz, DMSO-d₆): δ (ppm) 8.10 (2H, d), 8.00 (1H, d), 7.50-7.53 (2H, m), 6.98 (1H, s), 6.29 (1H, s). ESI-MS [M+H]⁺: calcd for C₁₃H₉NO₃S, 259.03; found 259.18.

2-aminobenzothiazole-5-carboxylic acid hydrochloride (6): to a solution of para-aminobenzoic acid (6.85 g, 0.050 mol) and potassium thiocyanate (5.28 g, 0.054 mol) in

methanol (25 mL), bromine (1.28 ml, 0.025 mol) was added with stirring below -5 °C during the addition. After the addition, the mixture was left under stirring for 2 hours at the same temperature. The precipitated was collected by filtration and washed with water. The solid obtained was suspended in HCl 1 N (20 mL), refluxed for 2 hours and filtered hot. To the filtrate, was added concentrated HCl (18.5 mL), and the mixture was stored in the refrigerator to provide a white solid, which were collected by filtration and dried under vacuum to give 9.05g as a white powder with a yield of 78%

IR (KBr) cm^{-1} : 33020.34, 1701.86, 1630.23, 1602.64. ^1H NMR (400MHz, DMSO- d_6): δ (ppm) 8.21 (1H, d), 7.84 (1H, dd), 6.79 (1H, d). ESI-MS $[\text{M}+\text{H}]^+$: calcd for $\text{C}_8\text{H}_6\text{N}_2\text{O}_2\text{S}$, 194.01, found 194.18.

4-amino-3-mercaptobenzoic acidhydrochloride (7): a solution of KOH (3.95 g of KOH in 5.8 ml of H_2O) was added to the 2-amino-benzothiazole-6-carboxylic acid hydrochloride (3 g, 0.013 mol), the mixture was refluxed for 8 hours. After cooling, the solution was filtered and to the filtrate, concentrated HCl was added dropwise at -5 ° C then, placed in the refrigerator overnight. The precipitated solids were collected by filtration and the product was washed with H_2O and subsequently dried and purified by recrystallization in EtOH to obtain 0.81 g (0.0039 moles) of the desired compound (7) as a white solid, with a yield of 30%.

IR (KBr) cm^{-1} : 3361.98, 1710.65, 1592.42. ^1H NMR (400MHz, DMSO- d_6): δ (ppm) 7.8 (1H, d), 7.38(1H, dd), 6.63 (1H, d). ESI-MS $[\text{M}+\text{H}]^+$: calcd for $\text{C}_7\text{H}_7\text{NO}_2\text{S}$, 169.02; found 169.23.

2-aminobenzothiazole-6-sulfonamide (9): 4-amino-benzenesulfonamide (5.00g, 0.029 mol) and potassium thiocyanate (5.64g, 0.058 mol) were dissolved in glacial acetic acid (45 mL). The mixture was stirred at room temperature for 20 minutes and then a bromine solution (1.49 mL 0.029 mol) in glacial acetic acid (5 mL) was added with a dropping funnel. After the addition, the mixture was kept under stirring at room temperature for 24 h. The precipitated solids were collected by filtration and obtained solid was dissolved in H_2O . NH_3 30% was added to the solution to bring the solution up to a pH6-9 and placed in the refrigerator overnight. The precipitated solids were collected by filtration and the product was washed with H_2O . The white product was dried and recrystallized in EtOH to obtain 3.01g of 9 as a white solid, with a yield of 45%. ^1H NMR (400MHz, DMSO- d_6): δ (ppm) δ 8.23 (1H, d), 7.96 (1H, dd), 6.83 (1H, d). ESI-MS $[\text{M}+\text{H}]^+$: calcd for $\text{C}_7\text{H}_7\text{N}_3\text{O}_2\text{S}_2$, 229.00; found 229.09.

bis(2-amino-4-benzenesulfonamide) disulfide (10): To the 2-amino-benzotiazole-6-sulfonamide (3g, 0.013 mol), a KOH solution (3.95 g of KOH in 5.8 ml of H₂O) was added, which was subsequently refluxed for 8 hours. After cooling, 35% HCl was added at -5 ° C until PH = 8. The mixture was placed in refrigerator overnight and then filtered. The solid product was washed with H₂O and subsequently dried and recrystallized in EtOH to obtain 1.10g (0.0054 mol) of **10** as a yellow solid, with a yield of 32%. ¹H NMR (400MHz, DMSO-d₆): δ (ppm 7.59 (1H, d, H₆), 7.39(1H, m), 7.28 (2H, br), 6.75(1H, m), 6.26 (2H,br). ESI-MS [M+H]⁺: calcd for C₁₂H₁₄N₄O₄S₄, 405.99; found 406.45.

General method for the synthesis of 2-arylbenzothiazoles substituted on the benzothiazole ring

To a solution of 4-amino-3-mercaptobenzoic acid (2.9 mmol) or bis(2-amino-4-benzenesulfonamide) disulfide (5.8 mmol) and 2-hydroxybenzaldehyde in ethanol (10 mL) at room temperature was added solution of sodium hydrosulfite (1 eq. in 5 mL H₂O). The mixture was heated at reflux for 36h. After cooling to room temperature, the solution was concentrated in vacuo. The residue was treated with HCl 2N and filtered to obtain the crude solid, which was recrystallized in EtOH/H₂O

2-(2-hydroxyphenyl)benzothiazole-5-carboxylic acid (11b): yield 71%; yellow solid; m.p. >250 °C. IR (KBr) cm⁻¹: 3111.61, 1677.78, 1590.62, 1481.81, 1217.68, 1167.09, 739.94. ¹H NMR (400MHz, DMSO-d₆) δ (pmm) 11.80 (1H, br, COOH), 8.78 (1H, d.), 8.24(1H, dd), 8.07 (2H,m), 7.45(1H, t) 7.17(1H,m) 7.02 (1H,m). ESI-MS [M+H]⁺: calcd for C₁₄H₉NO₃S, 271.03; found 271.24.

2-(3-hydroxyphenyl)benzothiazole-5-carboxylic acid (11c): yield 55%; yellow solid; m.p. >250°C. IR (KBr) cm⁻¹: 3110.61, 1676.63, 1582.62, 1481.60, 1217.55, 1142.38, 769.51. ¹H NMR (400MHz, DMSO-d₆): δ (ppm) 10.46 (1H, br), 8.62 (1H, d), 8.07 (2H, dd), 7.63 (2H, m), 7.33 (2H, m), 6.98 (1H, m). ESI-MS [M+H]⁺: calcd for C₁₄H₉NO₃S, 271.03; found 272.31.

2-(4-hydroxyphenyl)benzothiazole-5-carboxylic acid (11d): yield 67%; yellow solid; m.p. >250 °C. IR (KBr) cm⁻¹: 3259.12, 1680.90, 1587.38, 1418.42, 1240.15, 1166.98, 770.51. ¹H NMR (400MHz, DMSO-d₆): δ (ppm) 10.29 (1H, br), 8.68 (1H, d), 8.05 (2H, d), 7.98 (2H, dd), 6.92 (2H, dd). ESI-MS [M+H]⁺: calcd for C₁₄H₉NO₃S, 271.03; found 271.20.

2-(4-methoxyphenyl)benzothiazole-5-carboxylic acid (11e): yield 82%; yellow solid; m.p. >250 °C. IR (KBr) cm^{-1} : 2980.83, 1682.95, 1592.82, 1480.19, 1263.22, 1085.38, 711.96. ^1H NMR (400MHz, DMSO- d_6): δ (ppm) 9.87 (1H, br), 8.75 (1H, d), 8.17 (3H, m), 7.87 (1H, dd), 7.44 (2H, m), 3.82 (3H, s). ESI-MS $[\text{M}+\text{H}]^+$: calcd for $\text{C}_{15}\text{H}_{11}\text{NO}_3\text{S}$, 285.05; found 286.17.

2-(2,4-dihydroxyphenyl)benzothiazole-5-carboxylic acid (11f): yield 53%; yellow solid; m.p. >250 °C. IR (KBr) cm^{-1} : 3351.24, 1674.14, 1577.94, 1481.51, 1216.83, 1090.15, 779.85. ^1H NMR (400MHz, DMSO- d_6): δ (ppm) 10.22 (1H, br), 8.79 (1H, d), 7.99 (2H, m), 7.79 (1H, d), 6.58 (1H, dd), 6.39 (1H, d). ESI-MS $[\text{M}+\text{H}]^+$: calcd for $\text{C}_{14}\text{H}_9\text{NO}_4\text{S}$, 287.03; found 287.30.

2-(2,5-dihydroxyphenyl)benzothiazole-5-carboxylic acid (11g): yield 75%; yellow solid; m.p. >250 °C. IR (KBr) cm^{-1} : 3440.72, 2533.32, 1676.84, 1596.86, 1493.62, 1288.45, 1180.40, 780.50. ^1H NMR (400MHz, DMSO- d_6): δ (ppm) 13.05 (1H, br), 8.71 (1H, d), 8.04 (2H, m), 7.67 (1H, s), 6.87 (2H, m). ESI-MS $[\text{M}+\text{H}]^+$: calcd for $\text{C}_{14}\text{H}_9\text{NO}_4\text{S}$, 287.03; found 281.23.

2-(3,4-dihydroxyphenyl)benzothiazole-5-carboxylic acid (11h): yield 69%; yellow solid; m.p. >250 °C. IR (KBr) cm^{-1} : 3487.36, 1681.79, 1594.07, 1417.66, 1274.73, 1180.79, 770.33. ^1H NMR (400MHz, DMSO- d_6): δ (ppm) 12.45 (1H, br), 8.79 (1H, d), 8.27 (1H, d), 8.07 (1H, dd), 7.44 (1H, m), 7.17 (1H, dd), 7.01 (1H, t). ESI-MS $[\text{M}+\text{H}]^+$: calcd for $\text{C}_{14}\text{H}_9\text{NO}_4\text{S}$, 287.03; found 287.23.

2-(3-methoxy-4-hydroxyphenyl)benzothiazole-5-carboxylic acid (11i): yield 69%; yellow solid; m.p. >250 °C. IR (KBr) cm^{-1} : 3547.61, 2956.41, 1702.89, 1587.42, 1477.57, 1217.18, 1142.38, 769.51. ^1H NMR (400MHz, DMSO- d_6): δ (ppm) 13.11 (1H, br), 8.82 (1H, d), 8.35 (1H, d), 8.01 (1H, dd), 7.19 (1H, m), 7.16 (1H, dd), 6.89 (1H, t), 3.84 (3H, s). ESI-MS $[\text{M}+\text{H}]^+$: calcd for $\text{C}_{15}\text{H}_{11}\text{NO}_4\text{S}$, 301.04; found 301.19.

2-(3,5-dihydroxyphenyl)benzothiazole-5-carboxylic acid (11j): yield 59%; yellow solid; m.p. >250 °C. IR (KBr) cm^{-1} : 3481.41, 1681.03, 1589.78, 1423.22, 1270.12, 1182.90, 772.76. ^1H NMR (400MHz, DMSO- d_6): δ (ppm) 11.78 (1H, br), 8.84 (1H, d), 8.18 (1H, d), 8.11 (1H, dd), 6.95 (2H, d), 6.25 (1H, s). ESI-MS $[\text{M}+\text{H}]^+$: calcd for $\text{C}_{14}\text{H}_9\text{NO}_4\text{S}$, 287.03; found 287.12.

2-(2,4,5-trihydroxyphenyl)benzothiazole-5-carboxylic acid (11k): yield 63%; grey solid; m.p. >250 °C. IR (KBr) cm^{-1} : 3498.01, 1689.67, 1611.54, 1454.98, 1277.45, 1186.04, 775.34. ^1H NMR (400MHz, DMSO- d_6): δ (ppm) 11.24 (1H, br), 8.90 (1H, d), 8.23(1H, d), 8.07 (1H, dd), 6.96 (1H, s), 6.19 (1H, s). ESI-MS $[\text{M}+\text{H}]^+$: calcd for $\text{C}_{14}\text{H}_9\text{NO}_5\text{S}$, 303.02; found 303.23.

2-(2-hydroxyphenyl)benzothiazole-5-sulfonamide (11m): yield 78%; yellow solid; m.p. >250 °C. IR (KBr) cm^{-1} : 3315.96, 3242.71, 1584.16, 1483.69, 1312.74, 1151.54, 745.97. ^1H NMR (400MHz, DMSO- d_6): δ 8.62(1H, d), 8.38 (1H, d), 8.19 (1H, d), 7.98 (1H, dd), 7.45 (2H,br), 7.18-7.01(3H,m). ESI-MS $[\text{M}+\text{H}]^+$: calcd for $\text{C}_{13}\text{H}_{10}\text{N}_2\text{O}_3\text{S}_2$, 306.01; found 306.19.

2-(3-hydroxyphenyl)benzothiazole-5-sulfonamide (11n): yield 78%; yellow solid; m.p. >250 °C. IR (KBr) cm^{-1} : 3312.90, 3206.34, 1584.64, 1461.60, 1300.81, 1290.43, 1152.38, 779.97. ^1H NMR (400MHz, DMSO- d_6): δ (ppm) 8.63(1H, d), 8.21 (1H, d), 7.98 (1H, dd), 7.59 (1H, dd), 7.34 (2H,br,) 7.33(2H,m), 6.91 (1H,d). ESI-MS $[\text{M}+\text{H}]^+$: calcd for $\text{C}_{13}\text{H}_{10}\text{N}_2\text{O}_3\text{S}_2$, 306.01; found 306.22.

2-(4-hydroxyphenyl)benzothiazole-5-sulfonamide (11o): yield 84%; yellow solid; m.p. > 250 °C. IR (KBr) cm^{-1} : 3337.23, 3230.15, 1605.65, 1478.29, 1303.03, 1273.04, 1147.75, 832.77. ^1H NMR (400MHz, DMSO- d_6): δ (ppm) 8.59(1H, d), 8.11 (1H, d), 7.97 (3H, m), 7.44 (2H, br), 7.44 (3H,m). ESI-MS $[\text{M}+\text{H}]^+$: calcd for $\text{C}_{13}\text{H}_{10}\text{N}_2\text{O}_3\text{S}_2$, 306.01; found 306.12.

2-(4-methoxyphenyl)benzothiazole-5-sulfonamide (11p): yield 80%; yellow solid; m.p. > 250 °C. IR (KBr) cm^{-1} : 3329.36, 3258.18, 1605.40, 1480.21, 1303.99, 1261.21, 1165.22, 829.89. ^1H NMR (400MHz, DMSO- d_6): δ (ppm) 8.59(1H, d), 8.17 (1H, d), 8.09 (2H, dd), 7.97 (1H, dd), 7.43(2H, br), 7.18 (2H,m), 3.83(3H, s). ESI-MS $[\text{M}+\text{H}]^+$: calcd for $\text{C}_{14}\text{H}_{12}\text{N}_2\text{O}_3\text{S}_2$, 320.03; found 321.23.

2-(2,4-dihydroxyphenyl)benzothiazole-5-sulfonamide (11q): yield 74%; yellow solid; m.p. > 250 °C. IR (KBr) cm^{-1} : 3338.39, 3230.09, 1592.61, 1474.59, 1340.05, 1296.68, 1150.53, 807.53. ^1H NMR (400MHz, DMSO- d_6): δ (ppm) 8.49(1H, d), 8.09 (2H, m), 7.87 (1H, d), 7.42 (2H, br), 6.51(2H,m). ESI-MS $[\text{M}+\text{H}]^+$: calcd for $\text{C}_{13}\text{H}_{10}\text{N}_2\text{O}_4\text{S}_2$, 322.01; found 322.34.

2-(2,5-dihydroxyphenyl)benzothiazole-5-sulfonamide (11r): yield 55%; yellow solid; m.p. > 250 °C. IR (KBr) cm^{-1} : 3347.86, 3263.09, 1601.59, 1496.48, 1342.38, 1215.45, 1155.52, 765.54. ^1H NMR (400MHz, DMSO- d_6): δ (ppm) 8.60 (1H, d), 8.19 (1H, d), 7.98(1H, dd), 7.64 (1H, d), 7.42(2H,br), 6.98- 6.83 (2H,m). ESI-MS $[\text{M}+\text{H}]^+$: calcd for $\text{C}_{13}\text{H}_{10}\text{N}_2\text{O}_4\text{S}_2$, 322.01; found 322.19.

2-(3,4-dihydroxyphenyl)benzothiazole-5-sulfonamide (11s): yield 69%; yellow solid; m.p. > 250 °C. IR (KBr) cm^{-1} : 3498.98, 3307.06, 1602.96, 1490.80, 1335.69, 1279.30, 1145.20, 825.21. ^1H NMR (400MHz, DMSO- d_6): δ (ppm) 8.42 (1H, d), 8.19 (1H, d), 7.98(1H, dd), 7.41 (2H,br),7.16 (2H, m), 6.83 (1H,dd). ESI-MS $[\text{M}+\text{H}]^+$: calcd for $\text{C}_{13}\text{H}_{10}\text{N}_2\text{O}_4\text{S}_2$, 322.01; found 322.46.

2-(3-hydroxy-4-methoxyphenyl)benzothiazole-5-sulfonamide (11t): yield 78%; yellow solid; m.p. > 250 °C. IR (KBr) cm^{-1} : 3329.36, 2957.66, 1605.40, 1486.52, 1313.43, 1270.78, 1169.89, 826.44. ^1H NMR (400MHz, DMSO- d_6): δ (ppm) 8.64 (1H, d), 8.24 (1H, d), 7.94(1H, dd), 7.45 (2H,br),7.25 (1H, dd), 7.20 (1H, d), 6.89 (1H, d), 3.86 (3H, s). ESI-MS $[\text{M}+\text{H}]^+$: calcd for $\text{C}_{14}\text{H}_{12}\text{N}_2\text{O}_4\text{S}_2$, 336.02; found 336.38.

2-(3,5-dihydroxyphenyl)benzothiazole-5-sulfonamide (11u): yield 63%; yellow solid; m.p. > 250 °C. IR (KBr) cm^{-1} : 3499.67, 3312.08, 1623.34, 1492.21, 1338.23, 1278.89, 1144.63, 826.10. ^1H NMR (400MHz, DMSO- d_6): δ (ppm) 8.51 (1H, d), 8.22 (1H, d), 7.96(1H,dd), 7.44 (2H,br),7.16 (2H, d), 6.82 (1H, s). ESI-MS $[\text{M}+\text{H}]^+$: calcd for $\text{C}_{13}\text{H}_{10}\text{N}_2\text{O}_4\text{S}_2$, 322.01; found 322.34.

2-(2,4,5-trihydroxyphenyl)benzothiazole-5-sulfonamide (11v): yield 51%; grey solid; m.p. > 250 °C. IR (KBr) cm^{-1} : 3350.33, 3264.78, 1609.54, 1495.78, 1341.92, 1216.34, 1157.43, 766.76. ^1H NMR (400MHz, DMSO- d_6): δ (ppm) 8.45 (1H, d), 8.12 (1H, d), 7.93(1H, dd), 7.64, 7.47(2H, br), 6.83 (1H, s), 6.36 (1H, s). ESI-MS $[\text{M}+\text{H}]^+$: calcd for $\text{C}_{13}\text{H}_{10}\text{N}_2\text{O}_5\text{S}_2$, 338.00; found 338.18.

IX.2.3. Synthesis of imidazopyrimidine derivatives

General procedure for the synthesis of purine derivatives

In a round-bottomed-flask, 0.52 g (1.48 mmol) of pyrimidines (**12** or **13**) and 1.48mmol of the corresponding benzaldehyde were mixed. Under free solvent and vigorous stirring, the mixture was heat using oil bath for 6 h. Caution should be made to the high temperature,

the round-bottomed-flask was equipped with a condenser. During this time, the temperature was increased by small intervals until the maximum desired temperature value is reached (200°C). The residue was then cooled at room temperature, dissolved in HCl 2N, concentrated with vacuum. Purification was effected by column chromatography or recrystallization from an appropriate solvent to afford the desired products.

8-(phenyl)-7H-purine (14a): recrystallization with AcOEt/ MeOH, 71.97% yield, grey solid; m.p. = 260°C. IR (KBr) cm^{-1} : 3300-2305(N-H, C₂-H of purine ring, C-H of aromatic ring), 1688.46 (N₃-C₄), 1604.51 (C₄=C₅), 1572.55 (N₇=C₈or C₈=N₉), 1503.47(C=C-Arom), 1187.99 (N₁-C₂). ¹H-NMR (400MHz, DMSO-d₆): δ (ppm) 8.96 (1H, s), 8.46(1H, s), 8.01 (2H, dd), 7.69 (2H, m), 7.22 (1H, t). ¹³C-NMR (400 MHz, DMSO-d₆): δ (ppm) 164.09 (C₂=N), 161.43(C₈=N), 159.11 (C₆-), 152.28 (C₄=C₅), 137.50 (C₄=C₅), 130.60 (C₈-C-Ar), 131.10 (C_{para}-Ar), 128.41 (C_{meta}-Ar), 126.56 (C_{ortho}-Ar). ESI-MS [M+H]⁺: calcd for C₁₁H₈N₄, 196.07; found 196.10.

8-(2-hydroxyphenyl)-7H-purin-6-ol (14b): recrystallization with AcOEt/ MeOH, 53.49% yield, grey solid; m.p. = 260-265 °C (dec.). IR (KBr) cm^{-1} : 3300-2305(N-H, O-H, C₂-H of purine ring, O-H C-H of aromatic ring), 1688.46 (N₃-C₄), 1604.51 (C₄=C₅), 1572.55 (N₇=C₈or C₈=N₉), 1503.47(C=C-Arom), 1294.94 (C₆-O), 1240.69 (O-Ar), 1187.99 (N₁-C₂). ¹H-NMR (400MHz, DMSO-d₆): δ (ppm) 8.02 (1H, s), 7.98(2H, d), 6.80 (2H, d). ¹³C-NMR (400 MHz, DMSO-d₆): δ (ppm) 171.9 (C₆-O), 161.7(C₈=N), 160.6 (Ar-C-O), 152.3 (C₄=C₅), 148.9 (C₂=N), 137.7 (C₄=C₅), 127.0 (C₈-C-Ar), 130.3 (C_{ortho}-Ar), 114.8 (C_{meta}-Ar). ESI-MS [M+H]⁺: calcd for C₁₁H₈N₄O₂, 228.06; found 228.03.

8-(3-hydroxyphenyl)-7H-purin-6-ol (14c): recrystallization with AcOEt/ MeOH, 78% yield, grey solid; m.p. > 240°C (dec.) (KBr) cm^{-1} : 3300-2305(N-H, O-H, C₂-H of purine ring, O-H C-H of aromatic ring), 1689.69 (N₃-C₄), 1604.41 (C₄=C₅), 1575.65 (N₇=C₈or C₈=N₉), 1503.60 (C=C-Arom), 1294.76 (C₆-O), 1242.14 (O-Ar), 1188.19 (N₁-C₂). ¹H-NMR (400MHz, DMSO-d₆): δ (ppm) 8.18 (1H, s), 7.46(1H, d), 7.44 (1H, s), 7.06 (2H, m). ¹³C-NMR (400 MHz, DMSO-d₆): δ (ppm) 171.9 (C₆-O), 161.7(C₈=N), 160.6 (Ar-C-O), 152.3 (C₄=C₅), 148.9 (C₂=N), 137.7 (C₄=C₅), 127.0 (C₈-C-Ar), 130.3 (C_{ortho}-Ar), 114.8 (C_{meta}-Ar). ESI-MS [M+H]⁺: calcd for C₁₁H₈N₄O₂, 228.06; found 228.05

8-(4-hydroxyphenyl)-7H-purin-6-ol (14d): recrystallization with AcOEt/ MeOH, 73% yield, grey solid; m.p. >250°C. IR (KBr) cm^{-1} : 3300-2305(N-H, O-H, C₂-H of purine ring,

O-H C-H of aromatic ring), 1688.08 (N₃-C₄), 1604.56 (C₄=C₅), 1560.65 (N₇=C₈or C₈=N₉), 1505.68(C=C-Arom), 1365.84 (C₆-O), 1240.30 (O-Ar), 1186.95 (N₁-C₂).¹H-NMR (400MHz, DMSO-d₆): δ(ppm) 8.02 (1H, s), 7.98(2H, d), 6.80 (2H, d).¹³C-NMR (400 MHz, DMSO-d₆): δ(ppm) 171.9 (C₆-O), 161.7(C₈=N), 160.6 (Ar-C-O), 152.3 (C₄=C₅), 148.9 (C₂=N), 137.7 (C₄=C₅), 127.0 (C₈-C-Ar), 130.3 (C_{ortho}-Ar), 114.8 (C_{meta}-Ar).ESI-MS [M+H]⁺: calcd for C₁₁H₈N₄O₂, 228.06; found 228.18.

8-(4-methoxyphenyl)-7H-purin-6-ol (14e): the residue was washed with H₂O, The solution was filtered and solid part was washed again with MeOH to obtain 0.29 g of yellow solid **7** with a yield of 81%; m.p. > 250 (°C)dec.IR (KBr) cm⁻¹: 3400-2250 (N-H, O-H, C₂-H of purine ring, O-H C-H of aromatic ring), 1682.60 (N₃-C₄), 1603.47 (C₄=C₅), 1520.05 (N₇=C₈or C₈=N₉), 1500.27(C=C-Arom), 1296.12 (C₆-O), 1243.46 (C-O-Ar), 1187.37 (N₁-C₂).¹H-NMR (400MHz, D₂O): δ(ppm) 8.30 (1H, s), 8.00(2H, d), 7.02 (2H, d), 3.90 (3H, s).¹³C-NMR (400 MHz, D₂O): δ (ppm) 163.11 (C₄=C₅), 161.67(C₈=N), 159.53 (C_{para} -O), 146.27 (C₂=N), 145.93 (C₆-O), 129.45 (C_{ortho}-Ar), 128.55 (C₄=C₅), 117.90 (C₈-C-Ar), 114.98 (C_{meta}-Ar), 54.94 (CH₃-O). ESI-MS [M+H]⁺: calcd for C₁₂H₁₀N₄O₂, 243.08; found 243.15.

8-(2,5-dihydroxyphenyl)-7H-purin-6-ol (14g): recrystallization with AcOEt /MeOH, 75% yield, brown solid; m.p = 240-245 °C (dec.). IR (KBr) cm⁻¹: 3400-2250 (N-H, O-H, C₂-H of purine ring, O-H C-H of aromatic ring), 1687.42 (N₃-C₄), 1604.42 (C₄=C₅), 1582.25 (N₇=C₈or C₈=N₉), 1503.68(C=C-Arom), 1294.82 (C₆-O), 1242.95 (C-O-Ar), 1187.95 (N₁-C₂).¹H-NMR (400MHz, DMSO-d₆): δ(ppm) 9.07 (1H, s), 8.06(1H, d), 6.82 (2H, s).¹³C-NMR (400 MHz, DMSO-d₆): δ(ppm) 171.9 (C₆-O), 161.7(C₈=N), 160.6 (Ar-C-O), 152.3 (C₄=C₅), 148.9 (C₂=N), 137.7 (C₄=C₅), 127.0 (C₈-C-Ar), 130.3 (C_{ortho}-Ar), 114.8 (C_{meta}-Ar), 55.8 (CH₃-O).ESI-MS[M+H]⁺: calcd for C₁₁H₈N₄O₃, 244.06; found 244.39.

8-(3,4-dihydroxyphenyl)-7H-purin-6-ol (14h): recrystallization with AcOEt/ MeOH, and DCM, 75 % yield, grey solid; m.p>250°C.IR (KBr) cm⁻¹: 3300-2305(N-H, O-H, C₂-H of purine ring, O-H C-H of aromatic ring), 1689.46 (N₃-C₄), 1604.83 (C₄=C₅), 1504.93 (C=C-Arom), 1294.84 (C₆-O), 1243.42 (O-Ar), 1187.21 (N₁-C₂).¹H-NMR (400MHz, DMSO-d₆): δ(ppm)8.05 (1H, s), 7.59(2H, d), 6.88 (2H, d).¹³C-NMR (400 MHz, DMSO-d₆): δ(ppm) 171.9 (C₆-O), 161.7(C₈=N), 160.6 (Ar-C-O), 152.3 (C₄=C₅), 148.9 (C₂=N), 137.7 (C₄=C₅), 127.0 (C₈-C-Ar), 130.3 (C_{ortho}-Ar), 114.8 (C_{meta}-Ar), 55.8 (CH₃-O).ESI-MS [M+H]⁺:calcd for C₁₁H₈N₄O₃, 244.06; found 245.38.

8-(3-hydroxy-4-methoxyphenyl)-7H-purin-6-ol (14i): recrystallization with AcOEt / MeOH and EtO₂/DCM, 83% yield, grey solid; m.p. = 180-185 °C. IR (KBr) cm⁻¹: 3400-2250 (N-H, O-H, C₂-H of purine ring, O-H C-H of aromatic ring), 1688.08 (N₃-C₄), 1604.48 (C₄=C₅), 1720.15 (N₇=C₈ or C₈=N₉), 1503.77 (C=C-Arom), 1294.74 (C₆-O), 1241.63 (C-O-Ar), 1188.22 (N₁-C₂). ¹H-NMR (400MHz, DMSO-d₆): δ(ppm) 8.25 (1H, s), 7.50(1H, d), 7.20 (1H, s), 6.85 (1H, d) 3.90 (3H, s). ¹³C-NMR (400 MHz, DMSO-d₆): δ(ppm) 171.9 (C₆-O), 161.7(C₈=N), 160.6 (Ar-C-O), 152.3 (C₄=C₅), 148.9 (C₂=N), 137.7 (C₄=C₅), 127.0 (C₈-C-Ar), 130.3 (C_{ortho}-Ar), 114.8 (C_{meta}-Ar), 55.8 (CH₃-O). ESI-MS [M+H]⁺: calcd for C₁₂H₁₀N₄O₃, 258.08; found 258.37.

8-(3,5-dihydroxyphenyl)-7H-purin-6-ol (14j): chromatography with AcOEt/ MeOH, 1/5, 54% yield, grey solid; m.p. >250°C. IR (KBr) cm⁻¹: 3300-2305 (N-H, O-H, C₂-H of purine ring, O-H C-H of aromatic ring), 1688.75 (N₃-C₄), 1604.49 (C₄=C₅), 1502.71 (C=C-Arom), 1294.87 (C₆-O), 1241.44 (O-Ar), 1188.12 (N₁-C₂). ¹H-NMR (400MHz, DMSO-d₆): δ(ppm) 8.15 (1H, s), 6.53(2H, s), 6.03 (1H, s). ¹³C-NMR (400 MHz, DMSO-d₆): δ(ppm) 171.9 (C₆-O), 161.7(C₈=N), 160.6 (Ar-C-O), 152.3 (C₄=C₅), 148.9 (C₂=N), 137.7 (C₄=C₅), 127.0 (C₈-C-Ar), 130.3 (C_{ortho}-Ar), 114.8 (C_{meta}-Ar), 55.8 (CH₃-O). ESI-MS [M+H]⁺: calcd for C₁₁H₈N₄O₃, 244.06; found 244.08.

8-(4-hydroxyphenyl)-7H-purine (14k): recrystallization with H₂O/ DCM, 60% yield, brown solid; m.p > 250°C. IR (KBr) cm⁻¹: 3400-2250 (N-H, O-H, C₂-H of purine ring, O-H C-H of aromatic ring), 1682.67 (N₃-C₄), 1604.85 (C₄=C₅), 1560.05 (N₇=C₈ or C₈=N₉), 1504.81 (C=C-Arom), 1294.93 (C₆-O), 1242.99 (C-O-Ar), 1187.33 (N₁-C₂). ¹H-NMR (400MHz, DMSO-d₆): δ(ppm) 9.00 (1H, s), 8.90(1H, s), 7.90 (2H, d), 6.92 (2H, d). ¹³C-NMR (400 MHz, DMSO-d₆): δ(ppm) 162.01 (C₄=C₅), 160.98 (C₈=N), 158.89 (C_{para}-O), 146.92 (C₂=N), 134.83 (C₆), 129.89 (C_{ortho}-Ar), 128.42 (C₄=C₅), 117.12 (C₈-C-Ar), 115.76 (C_{meta}-Ar). ESI-MS [M+H]⁺: calcd for C₁₁H₈N₄O, 212.07; found 212.31.

8-(4-methoxyphenyl)-7H-purine (14l): recrystallization with H₂O/ DCM. 80% yield, amorphous solid. IR (KBr) cm⁻¹: 3400-2250 (N-H, O-H, C₂-H of purine ring, O-H C-H of aromatic ring), 1689.46 (N₃-C₄), 1604.83 (C₄=C₅), 1504.93 (C=C-Arom), 1294.84 (C₆-O), 1243.42 (C-O-Ar), 1187.21 (N₁-C₂). ¹H-NMR (400MHz, DMSO-d₆): δ(ppm) 8.96 (1H, s), 8.94(2H, d), 7.90 (2H, d), 6.92 (2H, d), 3.90 (3H, s). ¹³C-NMR (400 MHz, DMSO-d₆): δ(ppm) 163.11 (C₄=C₅), 161.67(C₈=N), 159.53 (C_{para}-O), 146.27 (C₂=N), 133.93 (C₆),

130.00 (C_{ortho}-Ar), 128.55 (C_{4=C₅}), 117.90 (C_{8-C}-Ar), 114.61 (C_{meta}-Ar), 55.46 (CH₃-O). ESI-MS [M+H]⁺: calcd for C₁₂H₁₀N₄O, 226.08; found 226.18.

8-(2,5-dihydroxyphenyl)-7H-purine (14m): Chromatography with AcOEt/ MeOH, 2/5, 51% yield, grey solid: m.p. > 250°C. IR (KBr) cm⁻¹: 3300-2305 (N-H, O-H, C₂-H of purine ring, O-H C-H of aromatic ring), 1687.36 (N₃-C₄), 1604.87 (C₄=C₅), 1504.51 (C=C-Arom), 1294.87 (C₆-O), 1236.31 (O-Ar), 1188.44 (N₁-C₂). ¹H-NMR (400MHz, DMSO-d₆): δ (ppm) 9.07 (1H, s), 8.06 (1H, d), 6.82 (2H, s). ¹³C-NMR (400 MHz, DMSO-d₆): δ (ppm) 171.9 (C₆-O), 161.7 (C₈=N), 160.6 (Ar-C-O), 152.3 (C₄=C₅), 148.9 (C₂=N), 137.7 (C₄=C₅), 127.0 (C_{8-C}-Ar), 130.3 (C_{ortho}-Ar), 114.8 (C_{meta}-Ar), 55.8 (CH₃-O). ESI-MS [M+H]⁺: calcd for C₁₁H₈N₄O₂, 228.06; found 228.16.

IX.3. Protocols for the evaluation of the biological activity

IX.3.1. Antioxidant Activity Assays

IX.3.1.1. Free radical Scavenging Activity on DPPH.

The methanolic solution of DPPH (1.5 mL) was added to 0.750 mL of tested sample solutions (methanol + DMSO v/v) at different concentrations (1, 0.5, 0.25, 0.125 and 0.0625 mg/mL). The samples were kept in the dark at room temperature. After 30 min, the absorbance values were measured using a Life-Science UV-VIS spectrophotometer (*Beckman Coulter*TM, DU@530, Single Cell Module) at fixed wavelength of 517 nm. Blank sample was prepared adding methanol to DPPH solution. The percentage of the DPPH radical scavenging is calculated using **Equation 5**.

Equation 5: DPPH radical-scavenging capacity (%) = $[1 - (A_1 - A_2) / A_0] \times 100\%$

Where A₀ was the absorbance of the control (without sample), A₁ was the absorbance in the presence of the sample, and A₂ was the absorbance without DPPH.

Then, linear regression plots are carried out for calculating the effective concentration of the sample required to scavenge 50% of DPPH free radicals.

IX.3.1.2. Ferric Reducing Antioxidant Power (FRAP) assay

FRAP assay is based on the reduction of ferric ions (Fe³⁺) to ferrous ions (Fe²⁺) in the presence of TPTZ (2,4,6-tripyridyl-striazine). This reaction is monitored by measuring the change in absorbance at 593 nm after 10 minutes of incubation in the dark at 37°C. The analysis reagent was freshly prepared by mixing the following solutions in the reported ratio 10/1/1 (v:v:v): i) 0.1 M acetate buffer pH 3.6, ii) TPTZ 10 mmol/L in 40 mmol/L HCl,

iii) ferric chloride 20 mmol/L. 1.9 mL of FRAP reagent was mixed with 0.1 mL of sample proper diluted or solvent when blank was performed. FRAP values are obtained by comparing the absorbance change at 593 nm in sample solution with the absorbance of the blank reaction, using a UV-VIS spectrophotometer. Because Trolox was used to effect the calibration curves, the antioxidant activity was expressed in $\mu\text{MolT/g}$.

IX.3.2. Photoprotection assay

IX.3.2.1. Evaluation of filtering parameters of compounds in solution

Absorbance of synthesized compounds were measured between 290-400 nm using a 1 cm quartz cell at intervals of one 1 nm using a UV-Vis Spectrophotometer (SHIMADZU UV-2600 240 V). Test compounds were dissolved in dimethylsulfoxide at the concentration of 0.0015 (± 0.0005) % and the absorbance at wavelength λ is related to the transmittance $T(\lambda)$ by the **Equation 1**

$$\text{Equation 1: } A(\lambda) = -\text{Log}[T(\lambda)]$$

Where $T(\lambda)$ is the fraction of incident irradiance transmitted by the sample.

Then, Filtering parameters were calculated by applying **Equation 2**, **Equation 3** and **Equation 4** described below.

IX.3.2.2. *In vitro* evaluation of filtering parameters of cream formulation

Synthesized compounds were included at the concentration of 1% in cosmetic formulation oil-in-water (O/W).

INCI: aqua, glycerin, Euxyl PE 9010, Xanthan gum, cetareth-12, cetareth-20, Stearic acid, Butylhydroxytoluene, Myritol, PEG-7 glycerylcocoate and sodium solution 10%.

32.5 mg of each compound formulation were spread onto $5 \times 5 \text{ cm}^2$ PMMA plates (WW5 PMMA plates have been purchased from Schonberg GmbH; Munich, Germany) in small droplets of approximately equal mass evenly distributed over the rough surface of the plate. For each product, three plates were prepared. In order to facilitate the formation of a standard stabilized sunscreen film, the plate was placed in a dark for 15-30 minutes and then it was inserted into the instrument for measurement. The measure of UV transmittance was carried out from 290 to 400 nm on 5 different sites of each plate. The blank was prepared using a plate covered with 32.5 mg of glycerin, because of its non-fluorescence and UV transparency.

Moreover, values of *in vitro* SPF, UVA-PF and Critical Wavelength were calculated according to **Equation 2**, **Equation 3** and **Equation 4** respectively using SPF Calculator Software (SPF Calculator Software (version 2.1), Shimadzu, Milan (Italy)).

$$\text{Equation 2: } \text{SPF}_{\text{in vitro}} = \frac{\int_{\lambda=290\text{nm}}^{\lambda=400\text{nm}} E(\lambda) \times I(\lambda) \times d\lambda}{\int_{\lambda=290\text{nm}}^{\lambda=400\text{nm}} E(\lambda) \times I(\lambda) \times 10^{-A_0(\lambda)} \times d\lambda}$$

Where $E(\lambda)$ is the erythema action spectrum, $I(\lambda)$ is the spectral irradiance of the UV source, $A_0(\lambda)$ is the monochromatic absorbance of the test sample before UV exposure, and $d\lambda$ is the wavelength step (1 nm)

$$\text{Equation 3: } \text{UVAPF} = \frac{\int_{\lambda=290\text{nm}}^{\lambda=400\text{nm}} P(\lambda) \times I(\lambda) \times d\lambda}{\int_{\lambda=290\text{nm}}^{\lambda=400\text{nm}} P(\lambda) \times I(\lambda) \times 10^{-A(\lambda) \times C} \times d\lambda}$$

Where $P(\lambda)$ is the persistent pigment darkening (PPD) action spectrum. C is the coefficient of adjustment. $A(\lambda)$ is the mean monochromatic absorbance of the test product layer after UV exposure.

The wavelength at which the summed absorbance reaches 90% of total absorbance is defined as the critical wavelength. Therefore $T(\lambda)$ were converted into absorbance values $A(\lambda)$ following **Equation 4** and final Critical Wavelength is:

$$\text{Equation 4: } \int_{290\text{nm}}^{\lambda_c} A\lambda \times d\lambda = 0.9 \int_{290\text{nm}}^{400\text{nm}} A\lambda \times d\lambda$$

Where $A(\lambda)$: monochromatic absorbance calculated from transmittance at wavelength λ

IX.3.3. Study of photostability

Each UV-filter incorporated in an oil-in-water (O/W) emulsion were spread on PMMA plate and irradiated with a solar simulator applying different UVA-dose equivalent to an effective erythemal radiant exposure of 100 J/m^2 . The spectral transmittance of thin film of sunscreen was measured before and after sunlight exposure from 290 to 400 nm. The residual percentages of SPF *in vitro* (% SPF_{eff}) and UVA-PF (% $\text{UVA-PF}_{\text{eff}}$) were calculated according to **Equations 7** and **8** respectively. In fact, a filter is considered photostable if % SPF_{eff} and % $\text{UVA-PF}_{\text{eff}}$ are more than or equal to 80.

$$\text{Equation 7: } \% \text{SPF}_{\text{eff}} = \text{in vitro SPF}_{\text{after}} / \text{in vitro SPF}_{\text{before}} \times 100$$

$$\text{Equation 8: } \% \text{UVA} - \text{PF}_{\text{eff}} = \text{UVA-PF}_{\text{after}} / \text{UVA-PF}_{\text{before}} \times 100$$

IX.3.4. Stability study by HPLC analysis

HPLC analysis was performed using an Agilent 1100 Series HPLC System equipped with a G1315A DAD, and with a Hydro-RP C18Synergi 80 Å column (4.6 x 150 mm, 4 µm) from Phenomenex, kept at 25 °C during all the time of the analysis. The mobilephase consisted of solvent A (water 0.01 M H₃PO₄) and solvent B (acetonitrile0.01 M H₃PO₄). The determination of all compounds solutions was carried out in isocratic condition, between A: 60-90%, B: 40-10%. Separation was monitored at λ_{max} of the each molecule; the flow rate was 1.0 mL/min. The sample solutions were filtered by a 0.45-µm filter, before injection (HPLC filters were purchased from Scharlab S.L., Barcelona, Spain).

Synthesized compounds were in DMSO, MeOH and/or H₂O at a concentration of 0.0015% and their stability were studied by HPLC. Study conditions included room temperature and accelerated aging at 40°C. Benzimidazole derivatives and 2-arylbenthiazoles were studied in MeOH while purine and 2,6-disubstitutedbenthiazoles were studied in DMSO and H₂O.

IX.3.5. Antifungal activity

IX.3.5.1. Anti-dermatophytes activity

Microorganisms

The dermatophytes used were *Epidermophytonfloccosum* var. floccosum (Netherlands) CBS 358.93 strain;*Trichophyton tonsurans* (Netherlands) CBS 483.76 strain; *Trichophytonmentagrophytes* (Netherlands) CBS 160.66 strain; *Microsporumcanis* (Iran) CBS 131110strain; and*Microsporumgypseum* (Iran) CBS 130948 strain.All dermatophytes were maintained at 4°C as agar slants on Sabouraud dextrose agar (SDA; Sigma-Aldrich SRL, Milano, Italy).

Growth inhibition

In vitro antifungal activity against five dermatophytes (*Microsporum gypseum*, *Microsporum canis*, *Trichophyton mentagrophytes*, *Trichophyton tonsurans* and*Epidermophyton floccosum*) was evaluated using plate growth rate method.Each compound was dissolved in dimethylsulfoxide (DMSO). The DMSO concentration in the final solution adjusted to 0.1%was added to the sterile culture medium (SDA) at 45°C. The final concentration of the medium was 100 µg/ mL for the first preliminary study and then changed for the evaluation of IC₅₀. The mixture was homogenized and transferred to a sterile Petridish to solidify.Controls were also prepared with equivalent concentrations

(0.1% v/v) of DMSO. Inoculums were previously obtained by transplanting mycelium disks cut from the periphery of a single mother cultures, incubated on thin sheets of cellophane delicately extended on the agar plates and placed at 26°C until the appearance of some characters that show how the fungus grew. According to the poisoned-food technique, inoculums were then transferred to analyzed Petridish and incubated under growth conditions. Antifungal activity was determined by measuring the diameter of the inhibition zone for seven days. Percentages of growth inhibition were calculated by comparing mean value of diameters of the mycelia in test plates with that of untreated control plates following the **Equation 6**. The percent inhibition of growth was determined as the average of three different experiments.

Equation 6: $I = [(C - T)/C] 100\%$.

Where, I is the growth inhibition rate (%), C is the extended diameter of the circle mycelium of the control (mm), and T is the exyended diameter of the circle during testing (mm).

IX.3.5.1. Anti-*Candida albicans* activity

Stock solutions were prepared by dissolving the compounds in DMSO at a concentration of 12.80 mg/mL. Minimal inhibitory concentration (MIC) of the synthesized agents was performed by broth microdilution method. RPMI 1640 was buffered with 0.165 M MOPS, solution was agitated and brought to PH 6.9 with a 1N NaOH solution. The solution was filtered with a 8µm filter using a sterilized syringe and stocked in fridge. Just before setting up the assay, further dilute of stock solutions was dilute in 1:10 RPMI.

Fungal suspension was prepared by suspending a *Candida albicans* (ATCC 10231) aliquot in 5 ml of sterilized water. The solution is well mixed and the density at 600 nm of the microorganisms is measure so that the absorbance is between 0.08 and 0.1 corresponding to the standard 0.5 McFarland i.e. 1×10^6 to 5×10^5 cells per mL. Fungal suspension was added to the medium culture such that the final optical density at 600 nm will be 10^3 cells per mL.

The last lane is the control plate containing 198 µL of nutrient broth + 2 µl of DMSO. In the penultimate lane, 180 µL of fungal suspension without any test material +20µL nutrient broth 10% (v/v) DMSO using as uninhibited fungal growth control. A volume of 40 µL of test material in 1:10 (DMSO: RPMI) was pipetted into the first lane of the plate. To all other wells 20 µL of nutrient broth. Serial dilutions were performed using a multichannel pipette such that each well had 20 µL of the test material in serially descending

concentrations. First 10 rows were complete with 180 μL of fungal suspension ($5 \cdot 10^3$ cfu/mL) was added to each well to achieve a concentration of $5 \cdot 10^2$ cfu/mL. Plate was covered and placed into an incubator to 26°C and allow growth for 24 h.

The MIC value was defined as the lowest concentration of test compounds that resulted in a culture with turbidity less than or equal to 80% inhibition when compared with the growth of the control.

IX.3.6. Antiproliferative activity

Cell lines

Human cervical carcinoma (HeLa) and human CD_4^+T -lymphoblast (CEM) cells were obtained from ATCC (Middlesex, UK). Human pancreatic carcinoma (Mia-Paca 2) cells were kindly provided by Prof. Anna Karlsson (Karolinska Institute, Stockholm, Sweden). All cell lines were grown in Dulbecco's modified Eagle's medium (DMEM; Gibco, Carlsbad, CA, USA), supplemented with 10% fetal bovine serum (FBS, Gibco), 0.01M HEPES (Gibco) and 1 mM sodium pyruvate (Gibco) in a humidified 5% CO_2 incubator at 37°C .

Cell proliferation

Suspension of CEM cells were seeded in 96-well microtiter plates at 60,000 cells/well in the presence of different concentrations of the compounds. The cells were allowed to proliferate for 48 h or 72 h, respectively, and then counted in a Coulter counter. The 50% inhibitory concentration (IC_{50}) was defined as the compound concentration required to reduce cell proliferation by 50%. HeLa and Mia-Paca2 cells were seeded in 96-well plates at 15,000 cells/well in the presence of different concentrations of the compounds. After 4 days of incubation, the cells were trypsinized and counted in a Coulter counter).

IC_{50} Determination

The compounds were dissolved in DMSO at 20 mM (stock solution) and kept in the refrigerator until use. Then, compound dilutions were made in cell culture medium, and serial compound concentrations were tested starting at 100 μM as the highest concentration. The DMSO concentration, present at the highest compound concentration was 0.5% that is at a concentration that did not affect the tumour cell proliferation. The IC_{50} values were calculated using **Equation 10**.

Equation 10: $C1 - [50 - N1\%/N2\% - N1\%] - (C1 - C2)$

Wherein C1 is the compound concentration that inhibits cell proliferation more than 50%; C2 is the compound concentration that inhibits cell proliferation less than 50%; N1% represents the cell number (in percent of control in the absence of compound) obtained in the presence of C1 and N2% represents the cell number (in percent of control in the absence of compound) obtained in the presence of C2.

IX.3.7. HERG expressed in HEK

Cell line

Electrophysiology study was performed using HEK293 cells stably transfected with hERG cDNA.

Reagents and solutions

Test substances were formulated in 0.1% DMSO. Stock solutions were diluted in extracellular solution plus 0.05% Pluronic F-68 (Sigma), to final perfusion concentrations, which were 0.1, 1 and 10 μ M. In positive control group, 0.003-0.03-0.3 μ M E-4031 (Tocris) was assessed as a test compound.

The composition of the extracellular solution was (in mM): NaCl 137; KCl 4; CaCl₂ 1.8; MgCl₂ 1; D-glucose 10; N 2 hydroxyethylpiperazine-N'-2-ethanesulfonic acid (HEPES) 10; pH 7.4 with 1 M NaOH.

The intracellular solution composition was (in mM): KCl 130; MgCl₂ 1.0; Ethylene glycol-bis(β -aminoethyl ether)-N,N,N',N'-tetraacetic acid (EGTA) 5; MgATP 5; HEPES 10; pH 7.2 with 1 M KOH. The intracellular solution was filtered through a 0.2 μ m polycarbonate membrane filter upon formulation.

All reagents were purchased from Sigma-Aldrich.

Voltage protocol

The voltage protocol used to evaluate the effect of test substances on hERG channel current was as follows: step from -80 mV to -50 mV for 200 ms, +20 mV for 4.8 s, step to -50 mV for 5 s then step to the holding potential of -80 mV. The step from -80 mV to the test command (+20 mV) results in an outward current (i.e. current flows out of the cell) and the step from the test command (+20 mV) to -50 mV results in the tail current. The

pulse pattern was repeated continuously at 15 sec intervals from a holding potential of -80 mV.

The voltage protocol was run and recorded continuously during the experiment. The stability of recording was assessed through initial wash with extracellular solution alone. The vehicle was then applied for 3 min followed by the test substance. The test substance was applied in triplicate to ensure adequate mixing. The standard combined exposure time was 5 min. Each substance was tested in at least 2 cells for every concentration. All experiments were performed at ambient temperature.

Data analysis

Data acquisition and analyses were performed using the QPatch Assay software. The average of current amplitude values recorded from 4 sequential voltage pulses were used to calculate for each cell the effect of the test substance by calculating the residual current (% control) compared with vehicle pre-treatment and the % of inhibition (**Equation 9**).

The normalized data were plotted against the concentration of compound. The $-\text{Log}$ of concentrations of compounds required to decrease current by 50% (pIC_{50}) were determined by fitting the data to a Hill equation with $n \geq 2$

Equation 9: $I/I_0 = 1/[1 + ([C]/\text{IC}_{50})^{nH}]$, with $\text{pIC}_{50} = -\log \text{IC}_{50}$

Where I_0 and I are the current amplitudes measured in the absence and presence of test compound, respectively, $[C]$ is the concentration of compound in the external solution and nH is the Hill coefficient.

X. References

- [1] Valko, M., Rhodes, C. J., Moncol, J.; Izakovic, M.; Mazur, M. Free radicals, metals and antioxidants in oxidative stress-induced cancer. *Chem. Biol. Interact.*, **2006**, *160*, 1-40
- [2] Lennon, S. V, Martin S. J.; Cotter, T. G. Dose-dependent induction of apoptosis in humantumour cell lines by widely diverging stimuli. *Cell. Prolif.* **1991**, *24*, 203-14.
- [3] Jacob, R.A. The integrated antioxidant system. *Nutrition Research.***1995**, *15*, 755-66.
- [4] Giles, G. I.; Jacob, C. Reactive sulfur species: an emerging concept in oxidative stress. *Biol. Chem.* **2002**, *383*, 375-88.
- [5] Ivo, J.; Dragana, N.; Dimitrios, K.; Wallace, A. H.; Aristidis, M.T. Biological importance of reactive oxygen species in relation to difficulties of treating pathologies involving oxidative stress by exogenous antioxidants. *Food Chem. Toxicol.* **2013**, *61*, 240-247.
- [6] Geier, D. A.; Kern, J. K.; Garver, C. R.; Adams, J. B.; Audhya, T.; Nata, R.; Geier M. R. Biomarkers of environmental toxicity and susceptibility in autism. *J. Neurol. Sci.* **2009**,*280*, 101-8.
- [7] Cadenas, E.; Davies, K. J. A. Mitochondrial free radical generation, oxidative stress, and aging, *Free Rad. Biol. Med.* **2000**, *29*, 222-230.
- [8] Marnett, L. J. Lipid peroxidation - DNA damage by malondialdehyde. *Mut. Res.-Fund. Mol. Mech. Mutagen.* **1999**, *424*, 83-95.
- [9] Girotti, A. W. Lipid hydroperoxide generation, turnover and effectors action in biological systems. *J. Lipid. Res.*, **1998**, *39*, 1529-1542.
- [10] Zarkovic, N. 4-Hydroxynonenal as a bioactive marker of pathophysiological processes. *Mol. Aspects Med.* **2003**, *24*(4-5), 281-291.
- [11] Caliskan-Can,E.; Miser-Salihoglu,E.; Atalay, C.; Yalcintas-Arslan,U.; Simsek,B.; Yardim-Akaydin, S. DNA Damage and Lipid Peroxidation in Several Types of Cancer. *FABAD J. Pharm. Sci.* **2010**, *35*, 125-132.
- [12] Stadtman, E. R. Role of oxidant species in aging. *Curr. Med. Chem.* **2004**, *11*, 1105-1112.
- [13] Stadtman, E. R.; Moskovitz, J.; Levine, R. L. Oxidation of methionine residues of proteins: biological consequences. *Antioxid. Redox. Signal.* **2003**, *5*, 577-582.
- [14] Floyd, R.A.The role of 8-hydroxyguanine in carcinogenesis. *Carcinogenesis*, **1990**, *11*, 1447-1450.

- [15] Fraga, C. G.; Shigenaga, M. K.; Park, J.; Deagan, P.; Ames, B. N. Oxidative damage to DNA during aging – 8-hydroxy-2’deoxyguanosine in rat organ DNA and urine. *Proc. Natl. Acad. Sci.* **1990**, *87*, 4533-4537.
- [16] Sugimura, T. Cancer prevention: past, present, future. *Mutat. Res.* **1998**, *402*, 7-14.
- [17] Alexander, R.W. The Jeremiah metzger lecture. Pathogenesis of atherosclerosis: Redox as a unifying mechanism. *Trans. Am. Clin. Climatol. Assoc.* **2003**, *114*, 273-304.
- [18] Cai, H.; Harrison, D.G. Endothelial dysfunction in cardiovascular diseases: the role of oxidant stress. *Cir. Res.* **2000**, *87*, 840-844.
- [19] Albers, D. S.; Beal, M. F. Mitochondrial dysfunction and oxidative stress in aging and neurodegenerative disease, *J. Neural. Transm. Suppl.* **2000**, *59*, 133-154.
- [20] Sharma, P.; Dubey, R. S. Ascorbate peroxidase from rice seedlings: properties of enzyme isoforms, effects of stresses and protective roles of osmolytes. *Plant Sci.* **2004**, *167*, 541-550.
- [21] Meera, R.; Zazt, L. J. Skin delivery of vitamin E. *J. Cosmet. Sci.* **1999**, *50*, 249-27.
- [22] Breecher, G.R.; Khachik, F. Qualitative relationship of dietary and plasma carotenoids in human beings. *Ann. N. Y. Acad. Sci. USA.* **1992**, *669*, 320-321.
- [23] Fiedor J.; Fiedor L.; Haessner R.; Scheer H. Cyclic ednoperoxides of β -carotene, potential pro-oxidants, as products of chemical quenching of singlet oxygen. *Biochim. Biophys. Acta.* 2005, **1709**, 1-4.
- [24] El-Agamey, A.; Lowe, G. M.; McGarvey, D. J.; Mortensen, A.; Philip, D. M.; Truscott T. G.; Young, A.J. Carotenoid radical chemistry and antioxidant/pro-oxidant properties. *Arch. Biochem. Biophys.* **2004**, *430*, 37-48.
- [25] Cui, G.; Luk, S. C; Li, R. A.; Chan, K. K.; Lei, S. W.; Wang. L.; Shen. H.; Leung, G. P.; Lee, S. M. Cytoprotection of baicalein against oxidative stress-induced cardiomyocytes injury through the Nrf2/Keap1 pathway. *J. Cardio. Vasc. Pharmacol.* **2015**, *65*, 39-46
- [26] Dong, Q.; Chen, L., Lu. Q., Sharma, S.; Li, L.; Morimoto, S., Wang, G. Quercetin attenuates doxorubicin cardiotoxicity by modulating Bmi-1 expression. *Br. J. Pharmacol.* **2014**, *171*, 4440-4454.
- [27] Rani, N.; Bharti, S.; Manchanda, M.; Nag, T.C.; Ray, R.; Chauhan, S.S.; Kumari, S.; Arya D.S. Regulation of heat shock proteins 27 and 70, p-Akt/p-eNOS and MAPKs by naringin dampens myocardial injury and dysfunction in vivo after ischemia/reperfusion. *PLoS ONE.* **2013**, *8*:e82577.

- [28] Hsieh, S. R.; Hsu, C. S.; Lu, C. H.; Chen, W. C.; Chiu, C. H.; Liou, Y. M. Epigallocatechin-3-gallate-mediated cardioprotection by Akt/GSK-3 β /caveolin signalling in H9c2 rat cardiomyoblasts. *J. Biomed. Sci.* **2013**, 20:86.
- [29] Biswas, S.; Rahman, I. Chapter 33 – Dietary Bioactive Functional Polyphenols in Chronic Lung Diseases. *Bioactive Food as Dietary Interventions for Liver and Gastrointestinal Disease*, **2013**, 513–525.
- [30] Liu, B.; Zhang, J.; Liu, W.; Liu, N.; Fu, X.; Kwan, H.; Liu, S.; Liu, B.; Zhang, S.; Yu, Z.; Liu, S. Calycosin inhibits oxidative stress-induced cardiomyocyte apoptosis via activating estrogen receptor- α/β . *Bioorg. Med. Chem. Lett.* **2016**, 26, 181-185.
- [31] Louis, X. L.; Thandapilly, S. J.; Kalt, W.; Vinqvist-Tymchuk, M.; Aloud, B. M.; Raj, P.; Yu, L.; Le, H.; Netticadan, T. Blueberry polyphenols prevent cardiomyocyte death by preventing calpain activation and oxidative stress. *Food Funct.* **2014**, 5, 1785-1794.
- [32] Zhang, X.; Zhu, P.; Zhang, X.; Ma, Y.; Li, W.; Chen, J. M.; Guo, H. M.; Bucala, R.; Zhuang, J.; Li, J. Natural antioxidant-isoliquiritigenin ameliorates contractile dysfunction of hypoxic cardiomyocytes via AMPK signaling pathway. *Mediators Inflamm.* 2013, *2013*:390890.
- [33] Marzocchella, L.; Fantini, M.; Benvenuto, M.; Masuelli, L.; Tresoldi, I.; Modesti, A.; Bei, R. Dietary flavonoids: molecular mechanisms of action as anti-inflammatory agents. *Recent Pat. Inflamm. Allergy Drug Discov.* **2011**, 5, 200-220.
- [34] Ya, Liu¹.; Yi, Liu.; Hongfei, Chen.; Xu, Yao., Yan, Xiao.; Xianliang, Zeng.; Qutong, Zheng.; Yun, Wei.; Chen, Song.; Yinxiang, Zhang.; Peng, Zhu.; Juan, Wang.; Xing, Zheng. Synthetic Resveratrol Derivatives and Their Biological Activities: A Review. *Open Journal of Medicinal Chemistry*. **2015**, 5, 97-105.
- [35] Peterson, J.; Dwyer, J.; Adlercreutz, H.; Scalbert, A.; Jacques, P.; McCullough 5, M. L. Dietary lignans: physiology and potential for cardiovascular disease risk reduction. *Nutr Rev.* **2010**, 68, 571-603.
- [36] Yoder, Seth. C.; Lancaster, S. M.; Hullar, M. A.J.; Lampe, J.W. Chapter 7 – Gut Microbial Metabolism of Plant Lignans: Influence on Human Health. *Diet-Microbe Interactions in the Gut. Effects on Human Health and Disease.* **2015**, 103-117.
- [37] Ku, H.C.; Lee, S.Y.; Yang, K.C.; Kuo, Y.H.; Su, M.J. Modification of caffeic acid with pyrrolidine enhances antioxidant ability by activating AKT/HO-1 pathway in heart. *PLoS ONE* **2016**, 11, e0148545.

- [38] Li, L.; Pan, Q.; Han, W.; Liu, Z.; Li, L.; Hu, X. Schisandrin B prevents doxorubicin-induced cardiotoxicity via enhancing glutathione redox cycling. *Clin. Cancer Res.* **2007**, *13*, 6753-6760.
- [39] Movahed, A.; Yu, L.; Thandapilly, S.J.; Louis, X.L.; Netticadan, T. Resveratrol protects adult cardiomyocytes against oxidative stress mediated cell injury. *Arch. Biochem. Biophys.* **2012**, *527*, 74-80.
- [40] Rowland, F. S. Stratospheric ozone depletivo. *Phil. Trans. R. Soc. B.* **2006**, *361*, 769-90.
- [41] González, S.; Fernández-Lorente, M.; Gilaberte-Calzada, Y. The latest on skin photoprotection. *Clin. Dermatol.* **2008**, *26*, 614-626.
- [42] Wang, S. Q.; Balagula, Y.; Osterwalder, U. Photoprotection: a Review of the Current and Future Technologies. *Dermatol. Ther.* **2010**, *23*, 31-47.
- [43] Rigel, D. S.; Rigel, E. G.; Rigel, A. C. Effects of altitude and latitude on ambient UVB radiation. *J. Am. Acad. Dermatol.* **1999**, *40*, 114-116.
- [44] D'Orazio, J.; Jarrett, S.; Amaro-Ortiz, A.; Scott, T. UV Radiation and the Skin. *Int. J. Mol. Sci.* **2013**, *14*, 12222-12248.
- [45] Proksch, E.; Brandner J. M.; Jensen, J-M. The skin: an indispensable barrier. *Exp. Dermatol.* **2008**, *17*, 1063-1072.
- [46] Elias, P. M. Stratum corneum defensive functions: an integrated view. *J. Invest. Dermatol.* **2005**, *125*, 183-200.
- [47] Letai, A.; Coulombe, P. A.; McCormick, M. B.; Yu, Q-C.; Hutton, E.; Fuchs, E. Disease severity correlates with position of keratin point mutations in patients with epidermolysis bullosa simplex. *Proc. Natl. Acad. Sci. USA.* **1993**, *90*, 3197-3201.
- [48] Perry, P. K.; Cook-Bolden, F. E.; Rahman, Z.; Jones, E.; Taylor, S. C. Defining pseudofolliculitis barbae in 2001: a review of the literature and current trends. *J. Am. Acad. Dermatol.* **2002**, *46*, 113-119.
- [49] Hänel, K. H.; Cornelissen, C.; Lüscher, B.; Baron, J. M. Cytokines and the Skin Barrier. *Int. J. Mol. Sci.* **2013**, *14*, 6720-6745.
- [50] Simon, J. D.; Peles, D. N. Thered and the black. *Acc. Chem. Res.* **2010**, *43*, 1452-1460,
- [51] Prota, G. Melanins, melanogenesis and melanocytes: looking at their functional significance from the chemist's viewpoint. *Pigment Cell Res.* **2000**, *13*, 283-293.
- [52] Del Marmol, V.; Beermann, F. Tyrosinase and related proteins in mammalian pigmentation, *FEBS Lett.* **1996**, *381*, 165-168.

- [53] Kobayashi, T.; Urabe, K.; Winder, A.; JiinCnez-Cervantes, C.; Imokawa, G.; Brewington, T.; Solano, F.; Garcfa-Borr6n, J. C.; Hearing, V. J. Tyrosinase related protein 1 (TRP1) functions as a DHICA oxidase in melanin biosynthesis. *EMBO. J.* **1994**, *13*, 5818-5825.
- [54] Tsukamoto, K.; Jackson, I.; Urabe, K.; Montague, P.; Hearing, V. A second tyrosinase-related protein, TRP-2, is a melanogenic enzyme termed dopachrome tautomerase. *EMBO. J.* **1992**, *11*, 519-526.
- [55] Meredith, P.; Sarna, T. The physical and chemical properties of eumelanin. *Pigment Cell Res.* **2006**, *19*, 572-594.
- [56] Van Den, B. K.; Naeyaert, J. M; Lambert, J. The quest for the mechanism of melanin transfer. *Traffic.* **2006**, *7*, 769-78.
- [57] Cardinali, G.; Bolasco, G.; Aspite, N.; Lucania, G.; Lotti, L.V.; Torrissi, M. R.; Picardo, M. Melanosome transfer promoted by keratinocyte growth factor in light and dark skin-derived keratinocytes. *J. Invest. Dermatol.* **2008**, *128*, 558-567.
- [58] Imokawa, G. Autocrine and paracrine regulation of melanocytes in human skin and in pigmentary disorders. *Pigment Cell Res.* **2004**, *17*, 96-110.
- [59] Prota, G. Structure and biogenesis of pheomelanins, *Pigmentation: Its Genesis and Biologic Control*. Edited by V Riley. New York, Appleton-Century-Crofts, **1972**, 615-630
- [60] Kim, E.; Panzella, L.; Micillo, R.; Bentley, W. E.; Napolitano, A., Payne, G. F. Reverse Engineering Applied to Red Human Hair Pheomelanin Reveals Redox-Buffering as a Pro-Oxidant Mechanism. *Scientific Reports* **5**, **2015**,18447
- [61] Vavricka, C. J.; Christensen, B. M.; Li, J. Melanization in living organisms: a perspective of species evolution. *Protein Cell.* **2010**, *1*, 830-841.
- [62] Herberman, R.B.; Nunn, M. E.; Lavrin, D. H. Natural cytotoxic reactivity of mouse lymphoid cells against syngeneic and allogeneic tumors. I. Distribution of reactivity and specificity. *Int. J. Cancer.* **1975**, *16*, 216-229.
- [63] Blom, B.; Spits, H. Development of human lymphoid cells. *Annu. Rev. Immunol.* **2006**, *24*, 287-320.
- [64] Grim, M.; Halata, Z. Developmental origin of avian Merkel cell. *Anat. Embryol. (Berl).* **2000**, *202*, 401-410.
- [65] Lucarz, A.; Brand, G. Current considerations about Merkel cell. *Eur J. Cell Biol.* **2007**, *86*, 243-51.

- [66] Moll, I.; Roessler, M.; Brandner, J. M.; Eispiert, A-C.; Houdek, P.; Moll, R. Human Merkel cells – aspects of cell biology, distribution and functions. *Eur. J. Cell Biol.* **2005**, *84*, 259-271.
- [67] Dupasquier, M.; Stoitzner, P.; van Oudenaren, A.; Romani, N.; Leenen, P. J. Macrophages and Dendritic Cells Constitute a Major Subpopulation of Cells in the Mouse Dermis. *J. Invest. Dermatol.* **2004**, *123*, 876-879.
- [68] Kanitakis, J. Anatomy, histology and immunohistochemistry of normal human skin. *Eur. J. Dermatol.* **2002**, *12*, 309-401.
- [69] Horne, K. A.; Jahoda, A. B.; Oliver, R. F. Whisker growth induced by implantation of cultured vibrissa dermal papilla cells in the adult rat. *J. Embryol. Exp. Morphol.* **1986**, *97*, 111-124.
- [70] Matsumura, Y.; Ananthaswamy, H. N. Toxic effects of ultraviolet radiation on the skin. *Toxicol. Appl. Pharmacol.* **2004**, *195*, 298-308.
- [71] Longstreth, J.; De Gruijl, F.R.; Kripke, M.L.; Abseckd, S.; Arnold, F.; Slaper, H.I.; Velders, G.; Takizawa, Y.; van der Leun, J.C. Health risks. *J. Photochem. Photobiol. B: Biology.* **1998**, *46*, 20-39.
- [72] Brenner, M.; Hearing, V. J. The Protective Role of Melanin Against UV Damage in Human Skin. *Photochem. Photobiol.* **2008**, *84*, 539-549.
- [73] Adhami, V. M.; Syed, D. N.; Khan, N.; Afaq, F. Phytochemicals for prevention of solar ultraviolet radiation induced damages. *Photochem. Photobiol.* **2008**, *84*, 489-500.
- [74] Halliday, G.M.; Lyons, J.G. Inflammatory doses of UV may not be necessary for skin carcinogenesis. *Photochem. Photobiol.* **2008**, *84*, 272-283.
- [75] Diffey B.L. Solar ultraviolet radiation effects on biological system. *Phys. Med. Biol.* **1991**, *36*, 299-328.
- [76] Wlaschek, M.; Tancheva-Poor, I.; Naderi, L.; Ma, W.; Schneider, L. A.; Razi-Wolf, Z.; Schuller, J.; Scharffetter-Kochanek, K.; Solar UV. irradiation and dermal photoaging. *J. Photochem. Photobiol. B.* **2001**, *63*, 41-51.
- [77] Courdavault, S.; Baudouin, C.; Charveron, M.; Canguilhem, B.; Favier, A.; Cadet, J.; Douki T. Repair of the three main types of bipyrimidine DNA photoproducts in human keratinocytes exposed to UVB and UVA radiations. *DNA Repair (Amst).* **2005**, *4*, 836-44.
- [78] Wolber, R.; Schlenz, K.; Wakamatsu, K.; Smuda, C.; Nakanishi, Y.; Hearing, V. J.; Ito, S. Pigmentation effects of solar-simulated radiation as compared with UVA and UVB radiation. *Pigment Cell Melanoma Res.* **2008**, *21*, 487-491.

- [79] Nita, A.; Young, A. R. Review: Melanogenesis: a photoprotective response to DNA damage? *Mutat Res.* **2005**, *571*, 121-132.
- [80] Baker, S.J.; Fearon, E.R.; Nigro, J.M.; Hamilton, S.R.; Preisinger, A.C.; Jessup, J.M.; van Tuinen, P.; Ledbetter, D.H.; Barker, D.F.; Nakamura, Y.; White, R.; Vogelstein, B. Chromosome 17 deletions and p53 gene mutations in colorectal carcinomas. *Science.* **1989**, *244*, 217-221.
- [81] Vogan, K.; Bernstein, M.; Leclerc, J.M.; Brisson, L.; Brossard, J.; Brodeur, G.M.; Pelletier J.; Gros, P. Absence of p53 gene mutations in primary neuroblastomas. *Cancer Res.* **1993**, *53*, 5269-5273.
- [82] Siegel, R.; Naishadham, D.; Jemal, A. Cancer Statistics, 2013. *CA Cancer J. Clin.* **2013**, *63*, 11-30.
- [83] Kanavy, H. E.; Gerstenblith, M. R. Ultraviolet radiation and melanoma. *Semin. Cutan. Med. Surg.* **2011**, *30*, 222-228.
- [84] Takeuchi, H.; Ruenger, T. M. Longwave ultraviolet light (UVA) induces the aging-associated program. *J. Invest. Dermatol.* **2013**, *133*, 1857-1862.
- [85] Behar-Cohen, F.; Baillet, G.; de Agyavives, T.; Garcia, P. O.; Krutmann, J.; Peña-García, P.; Reme, C.; Wolffsohn, J. S. Ultraviolet damage to the eye revisited: eye-sun protection factor (E-SPF®), a new ultraviolet protection label for eyewear. *Clin Ophthalmol.* **2014**, *8*, 87-104.
- [86] Commission Européenne. Règlements (UE) n° 344/2013 de la commission du 4 Avril 2013 modifiant les annexes 2,3,5 et 6 du règlement (CE) n°1223/2009 du parlement européen et du conseil relatif aux produits cosmétiques, **2013**, p. 59.
- [87] Klimová, Z.; Hojerová, J.; Pažoureková, S. Current problems in the use of organic UV filters to protect skin from excessive sun exposure. *Acta Chimica Slovaca.* **2013**, *6*, 82-88.
- [88] Sunscreen drug products for over-the-counter human use, Final Monograph, Federal Register 64 27666, US Food and Drug Administration, Rockville, MD, **2000**.
- [89] Sambandan, D. R.; Ratner, D. Sunscreens: An overview and update"; *J. Am. Acad. Dermatol.* **2011**, *64*, 749-758.
- [90] Federal Register. Proposed rules: sunscreen drug products for over-the-counter human use. *Fed. Regist.* **1978**; *43*, 38250-38251.
- [91] Cole, C.; Shyr, T.; Ou-Yang, H.; Metal oxide sunscreens protect skin by absorption, not by reflection or scattering. *Photodermatol. Photoimmunol. Photomed.* **2016**, *32*, 5-10.

- [92] Manaia, E. B.; Kaminski, R. C. K.; Corrêa, M. A.; Chiavacci L. A. Inorganic UV filters *Braz. J. Pharm. Sci.* **2013**, *49*, 202-209.
- [93] Wang, S. Q.; Balagula, Y.; Osterwalder, U. Photoprotection: a Review of the Current and Future Technologies. *Dermatol. Ther.* **2010**, *23*, 31-47.
- [94] Carlile, M. J.; Watkinson, S. C.; *The Fungi*. Academic Press London. **1994**.
- [95] Baldauf, S. L.; Bhattacharya, D.; Cockrill, J.; Hugenholtz, P.; Pawlowski, J.; Simpson A.G.B. The Tree of Life: An Overview, Chapter 4 in *Assembling the Tree of Life*. Eds. Cracraft and Donoghue, Oxford University Press, USA. **2004**.
- [96] McLaughlin, D.; McLaughlin, E.; Lemke, P. (eds) *The Mycota VII (Part A)*. Springer-Verlag, Barr DJS. Chytridiomycota. Berlin. **2001**.
- [97] Longcore, J.; Pessier, A.; Nichols, D. *Batrachochytrium dendrobatidis* gen et. sp. nov., a chytrid pathogenic to amphibians. *Mycologia*. **1999**, *91*, 219-227.
- [98] Hawksworth, D.L. The magnitude of fungal diversity: the 1.5 million species estimate revisited. *Mycol. Res.* **2001**, *105*, 1422-1432.
- [99] Raven, P.H.; Evert, R.F.; Eichhorn, S.E. "Fungi". *Biology of plants* (7th ed.). W.H. Freeman. **2005**, p. 268-269
- [100] Schüßer, A.; Schwarzott, D.; Walker, C. A new fungal phylum, the Glomeromycota: phylogeny and evolution. *Mycol. Res.* **2001**, *105*, 1413-1421.
- [101] Opik, M.; Moora, M.; Zobel, M.; Saks, U.; Wheatley, R.; Wright, F.; Daniell, T. High diversity of arbuscular mycorrhizal fungi in a boreal herb-rich coniferous forest. *New Phytologist*. **2008**, *179*, 867-876.
- [102] Schüßer, A. *Glomus claroideum* forms an arbuscular mycorrhiza-like symbiosis with the hornwort *Anthoceros punctatus*. *Mycorrhiza*. **2000**, *10*, 15-21.
- [103] Hibbett, D. S.; Binder, M. Evolution of marine mushrooms. *Biol. Bull.* **2001**, *201*, 319-322.
- [104] Benjamin, D.R. *Mushrooms: poisons and panaceas*. W.H. Freeman and Company, New York. **1995**.
- [105] Bérdy, J. Bioactive microbial metabolites. A personal view. *J. Antibiot.* **2005**, *58*, 1-26.
- [106] Gertz, J.; Siggia, E. D.; Cohen, B. A. Analysis of combinatorial cis-regulation in synthetic and genomic promoters. *Nature*. **2009**, *457*, 215-218.
- [107] Brown, G. D.; Denning, D. W.; Levitz, S. M. Tackling human fungal infections. *Science*. **2012**, *336*, 647.
- [108] Sullivan, D.; Moran, G.; Coleman, D.; Kavanagh, K. (ed) *Fungal diseases of humans*. *Fungi: biology and applications*. Wiley, Chichester, UK. **2005**, p 171-190.

- [109] Roderick, Hay. Superficial fungal infections. *Medicine*. **2017**, *45*, 707-710.
- [110] Georg, L.K. Animals ringworm in public health. *Diagnosis and Nature, Bulletin*, **1959**, 57.
- [111] Luilma, A.G.; Sidrimb, J.J.C.; Domingos, T.M.; Cechinel, V.F.; Vietla, S.R. In vitro antifungal activity of dragon's blood from *Croton urucurana* against dermatophytes. *J. Ethnopharmacol.* **2005**, *97*, 409-412.
- [112] Chen, B.K.; Friedlander, S.F. Tinea capitis update: A continuing conflict with an old adversary. *Curr. Opin. Pediatr.* **2001**, *13*, 331-335.
- [113] Rippon, J.W. Host specificity in dermatophytoses. *Proceedings of the Eight Congress of the International Society for Human and Animal Mycology.* **1982**, 28-33.
- [114] Theodore, C.W.; Brian, G. O.; Yvonne, G.; Matthew, R. H. Generating and testing molecular hypotheses in the dermatophytes. *Eukaryotic Cell.* **2008**, *7*, 1238-1245.
- [115] Judith, A.W. Allergy and dermatophytes. *Clin. Microbiol. Rev.* **2005**, *18*, 30-43.
- [116] Odds, F. C. *Candida and candidiasis*. London: Bailliere Tindall; 1988
- [117] Velegraki, A.; Cafarchia, C.; Gaitanis, G.; Iatta, R.; Boekhout, T. *Malassezia* infections in humans and animals: pathophysiology, detection, and treatment. *PLoS. Pathog.* **2015**, *11*: e1004523.
- [118] Ravinder, K.;Megh, S. D.; Ritu, G.; Preena, B.; Richa, D. Spectrum of Opportunistic Fungal Infections in HIV/AIDS Patients in Tertiary Care Hospital in India. *Can. J. Infect. Dis. Med. Microbiol.* **2016**, *2016*, 7 pages.
- [119] Jain, S.; Singh, A. K.; Singh, R. P.; Bajaj, J. K.; Damle, A. S. Spectrum of opportunistic fungal infections in HIV-infected patients and their correlation with CD4+ counts in western India," *J. Med. Microbiol. Infect. Dis.* **2014**, *2*, 19-22.
- [120] Colombo, A. L.; De Almeida, J. J. N.; Slavin, M. A.; Chen, SC-A.; Sorrell, T. C. *Candida* and invasive mould diseases in nonneutropenic critically ill patients and patients with haematological cancer. *Lancet. Infect. Dis.* **2017**, *17*, e344-e356.
- [121] Sarici, G.; Cinar, S.; Armutcu, F.; Altinyazar, C.; Koca, R.; Tekin, N. S. Oxidative stress in *acne vulgaris*. *J. Eur. Acad. Dermatol. Venereol.* **2010**, *24*, 763-767.
- [122] Da Silva, D. A.; Day, A.; Ikeh, M.; Kos, I.; Achan, B.; Quinn, J. Oxidative Stress Responses in the Human Fungal Pathogen, *Candida albicans*. *Biomolecules.* **2015**, *5*, 142-165.
- [123] Sheehan, D. J.; Hitchcock, C. A.; Sibley, C. M. Current and emerging azole antifungal agents. *Clin. Microbiol. Rev.* **1999**, *12*, 40-79.

- [124] Sanati, H.; Belanger, P.; Fratti, R.; Ghannoum, M. A new triazole, voriconazole (UK-109,496), blocks sterol biosynthesis in *Candida albicans* and *Candida krusei*. *Antimicrob. Agents Chemother.* **1997**, *41*, 2492-2496.
- [125] Borelli, C.; Schaller, M.; Niewerth, M.; Nocker, K.; Baasner, B.; Berg, D.; Tiemann, R.; Tietjen, K.; Fugmann, B.; Lang-Fugmann, S.; Korting, H. C. Modes of action of the new arylguanidine abafungin beyond interference with ergosterol biosynthesis and in vitro activity against medically important fungi. *Chemotherapy.* **2008**, *54*, 245-59.
- [126] Lodish, H.; Berk, A.; Zipursky, S. L.; Matsudaira, P.; Baltimore, D.; Darnell, J.; Freeman W. H. (ed). Section 6.3 Viruses: Structure, Function, and Uses. *Molecular Cell Biology*, New York, 4th edition. **2000**.
- [127] Gelderblom, H. R.; Baron, S. (ed). Chapter 41 Structure and Classification of Viruses. Galveston (TX): University of Texas Medical Branch at Galveston. *Medical Microbiology*, 4th edition. **1996**.
- [128] Ubramanya, D.; Grivas, P. D. HPV and cervical cancer: updates on an established relationship. *Postgrad. Med. J.* **2008**, *120*, 7-13.
- [129] Dennehy PH (2015). "Rotavirus Infection: A Disease of the Past?". *Infectious Disease Clinics of North America*. 2015, 29 (4): 617–35
- [130] Ivanov, A. V.; Bartosch, B.; Isaguliant, M. G. Oxidative Stress in Infection and Consequent Disease. *Oxid. Med. Cell. Longev.* **2017**.
- [131] Patani, G. A.; LaVoie, E. J. Bioisosterism: A Rational Approach in Drug Design. *Chem. Rev.* **1996**, *96*, 3147-3176.
- [132] Wermuth C. G. Molecular variations based on isosteric replacements. *The Practice of Medicinal Chemistry*, Academic Press **1996**, pp 203-237
- [133] Gaikwad, P. L.; Gandhi, P. S.; Jagdale, D. M.; Kadam, V. J. The Use of Bioisosterism in Drug Design and Molecular Modification. *Am. J. Pharm. Tech. Res.* **2012**, *2*.
- [134] Alaqeel, S. I. Synthetic approaches to benzimidazoles from o-phenylenediamine: A literature review. *J. Saudi Chem. Soc.* **2017**, *21*, 229-237.
- [135] Diffey, B.L.; Robson, J. A new substrate to measure sunscreen protection factors throughout the ultraviolet spectrum. *J. Soc. Cosmet. Chem.* **1989**, *40*, 127-133.
- [136] SPF Calculator Software (version 2.1), Shimadzu, Milan (Italy).
- [137] US Food and Drug Administration, 21 CFR Parts 347 and 352, Sunscreen Drug Products for Over-the-Counter Human Use; Proposed Amendment of Final

- Monograph, Silver Spring, MD (USA), 2007, <https://www.fda.gov/OHRMS/DOCKETS/98fr/cd031.pdf> (accessed April 25, 2017).
- [138] Yadav, P. S.; Devprakash, D.; Senthilkumar, G. P. Benzothiazole: Different Methods of Synthesis and Diverse Biological Activities. *IJPSR*. **2011**, *3*, 01-07.
- [139] Jyotirling, R. M. Dhanaji, V. J.; Balaji, S. L.; Ramrao A. M. An efficient green protocol for the synthesis of 2-aryl substituted benzothiazoles. *Green Chem. Lett. Rev.* **2010**, *3*, 209-212.
- [140] Rajesh, S. K.; Uday, C. M. Synthesis of 2-Aryl and Coumarin Substituted Benzothiazole Derivatives. *J. Heterocyclic Chem.* **2006**, *43*, 1367-1369.
- [141] Firouz, M. M.; Ghasem, R. B.; Hossein, I.; Seyedeh, M. D. T. Facile and Efficient One-Pot Protocol for the Synthesis of Benzoxazole and Benzothiazole Derivatives using Molecular Iodine as Catalyst. *Synth. Commun.* **2006**, *36*, 2543-2548.
- [142] Hiroharu, M.; Nobuhiro, O.; Masahiko, M.; Hiroshi, S.; Katsuhito, M.; Noriaki, M.; Keiichiro, T.; Nobuaki, K.; Toshio A.; Yasuhisa, T.; Keiichi, Y.; Toshio, K. Antirheumatic Agents: Novel Methotrexate Derivatives Bearing a Benzoxazine or Benzothiazine Moiety. *J. Med. Chem.* **1997**, *40*, 105-111.
- [143] DEY, J.; DOGRA, S. K. Electronic absorption and fluorescence spectra of 2-phenyl-substituted benzothiazoles: study of excited-state proton transfer reactions. *Can. J. Chem.* **1991**, *69*, 1539-1547.
- [144] Garoli, D.; Pelizzo, M. G.; Bernardini, B.; Nicolosi, P.; Alaibac, M. Sunscreen tests: Correspondence between in vitro data and values reported by the manufacturers. *J. Dermatol. Sci.* **2008**, *52*, 193-204.
- [145] Farrelly, A. M.; Ro, S.; Callaghan, B. P.; Khoyi, M. A.; Fleming, N.; Horowitz, B.; Sanders, K. M.; Keef, K.D. Expression and function of KCNH2 (HERG) in the human jejunum. *Am. J. Physiol. Gastrointest. Liver Physiol.* **2003**, *284*, 883-895.
- [146] Wang, X. T.; Nagaba, Y.; Cross, H. S.; Wrba, F.; Zhang, L.; Guggino, S. E. The mRNA of L-type calcium channel elevated in colon cancer: Protein distribution in normal and cancerous colon. *Am. J. Pathol.* **2000**, *157*, 1549-1562.
- [147] Cherubini, A.; Taddei, G. L.; Crociani, O.; Paglierani, M.; Buccoliero, A. M.; Fontana, L.; Noci, I.; Borri, P.; Borrani, E.; Giachi, M.; Becchetti, A.; Rosati, B.; Wanke, E.; Olivotto, M.; Arcangeli, A. HERG potassium channels are more frequently expressed in human endometrial cancer as compared to non-cancerous endometrium. *Br. J. Cancer.* **2000**, *83*, 1722-1729.
- [148] Afrasiabi, E.; Hietamäki, M.; Viitanen, T.; Sukumaran, P.; Bergelin, N.; Törnquist, K. Expression and significance of HERG (KCNH2) potassium channels in the

regulation of MDA-MB-435 S melanoma cell proliferation and migration. *Cell Signal.* **2010**, *22*, 57-64.

- [149] Hu, Y.L.; Liu, X.; Lu, M. Synthesis and biological activity of novel 6-substituted purine derivatives. *J. Mex. Chem. Soc.* **2010**, *54*, 74-78.